In-line Ozonolysis coupled to Mass Spectrometry- A New Dimension of Structural Determination for Lipids

by

Chenxing Sun

A thesis submitted in partial fulfillment of the requirements for the degree of

Doctor of Philosophy

in

Food Science and Technology

Department of Agricultural, Food and Nutritional Science
University of Alberta

Abstract

The location of double bonds within unsaturated lipids can greatly affect their biological functions. Liquid chromatography coupled to mass spectrometry (LC/MS) has become a powerful tool for lipid separation and structural elucidation. However, the determination of double bond position remains challenging for both conventional MS and tandem MS (MS/MS) due to the lack of product ions arising from fragmentation at the double bonds. Ozone can specifically react with carbon-carbon double bonds, which generates ozonolysis products with predictable masses that could be used for the assignment of double bond positions. In this work, ozonolysis reaction coupled in-line with mass spectrometry (in-line O_3-MS) was developed for the unambiguous determination of double bond positions in unsaturated lipids. The in-line O_3 device was composed of a gas-permeable, liquid-impermeable Teflon tube passing through a glass chamber filled with the ozone gas. Unsaturated lipids in the mobile phase of LC passed through the semi-permeable tube where they rapidly reacted with the ozone that penetrated through the tubing wall. The ozonolysis products carried by the LC mobile phase were then detected by MS in real-time. The in-line O_3-MS method was successfully applied to mono- and poly-unsaturated fatty acid methyl ester (FAME), in which ozonolysis product aldehydes from the oxidative cleavage of each double bond were detected as protonated molecular ions under atmospheric pressure photo ionization (APPI) in positive ionization mode and used for the double bond localization. The in-line O_3-MS is compatible with LC separations which are required in the analyses of complex lipid mixtures. Silver

ion LC coupled to O_3-MS (Ag^+-LC/O_3-MS) was used for the identification of conjugated linoleic acid (CLA) isomers from various sources. The diagnostic ions of the aldehydes resulting from the ozonolysis of the conjugated double bonds were used to identify the positional isomers, while at the same time the geometry of the double bond (*cis* or *trans*) could be determined by the elution order in Ag^+-LC. The O_3-MS method was also expanded to double bond localization in phospholipids (PL). For complex PL extract, heart-cut two dimensional LC (2D-LC) using hydrophilic interaction liquid chromatography (HILIC) for PL class separation and C18 reverse phase LC for molecular species separation was achieved using a 10-port 2-position switching valve (HILIC×C18 LC). The PL species were firstly identified using electrospray ionization (ESI) in negative ionization mode with MS/MS analysis applied for the composition determination of the fatty acyl chains on the glycerol backbone. The ozonolysis device was then placed in-line between the 2D-LC and ESI source (HILIC×C18 LC/O_3-MS), and the ozonolysis product aldehydes allowed unambiguous assignment of double bond positions in both fatty acyl chains of PL. Compared to the previous methods used for double bond localization in lipids, no off-line derivatizations are needed and also the O_3-MS spectra are much simpler for interpretation. The in-line ozonolysis experiment can be easily incorporated into many existing LC/MS methods, and applied complementary with current lipidomic analysis. In conclusion, the LC/O_3-MS method can provide insight into the specific structure of lipid isomers and further reveal the complexity of the lipidome.

Preface

Part of Chapter 1 has been published as C. Sun and J.M. Curtis, "Locating double bonds in lipids - New approaches to the use of ozonolysis," *Lipid Technol.* 2013, *25*, 279-282. I was responsible for the literature review as well as the manuscript composition. Professor J.M. Curtis was the supervisory author and was involved with manuscript composition.

Chapter 2 of this thesis has been published as C. Sun, Y. Zhao and J.M. Curtis, "A study of the ozonolysis of model lipids by electrospray ionization mass spectrometry," *Rapid Commun. Mass Spectrom.* 2012, *26*, 921-930. I was responsible for performing the experiments, the data collection and analysis as well as the manuscript composition. Y. Zhao assisted with the data collection and contributed to manuscript edits. J.M. Curtis was the supervisory author and was involved with concept formation and manuscript composition.

Chapter 3 of this thesis has been published as C. Sun, Y. Zhao and J.M. Curtis, "The direct determination of double bond positions in lipid mixtures by liquid chromatography/ in-line ozonolysis- mass spectrometry," *Anal. Chim. Acta* 2013, *762*, 68-75. The in-line ozonolysis device referred to in Chapter 3 was designed by me with the assistance of Y. Zhao and J.M. Curtis. I was also responsible for performing the experiments, the data collection and analysis as well as the manuscript composition. Y. Zhao assisted with the data collection and contributed to manuscript edits. J.M. Curtis was the supervisory author and was involved with concept formation and manuscript composition.

Chapter 4 of this thesis has been published as C. Sun, B.A. Black, Y.

Zhao, M.G. Gänzle and J.M. Curtis, "The identification of conjugated linoleic acid (CLA) isomers by silver ion- liquid chromatography/in-line ozonolysis- mass spectrometry," *Anal. Chem.* 2013, *85*, 7345−7352. I was responsible for performing the experiments, the data collection and analysis as well as the manuscript composition. B.A. Black assisted with performance of experiments and contributed to manuscript edits. Y. Zhao assisted with the data collection and contributed to manuscript edits. Professor M.G. Gänzle and J.M. Curtis were the supervisory authors and were involved with manuscript composition.

Chapter 5 of this thesis has been accepted for publication as C. Sun, Y. Zhao and J.M. Curtis, "Elucidation of phosphatidylcholine isomers using two dimensional liquid chromatography coupled in-line with ozonolysis mass spectrometry," in *J. Chromatogr. A*. I was responsible for performing the experiments, the data collection and analysis as well as the manuscript composition. Y. Zhao assisted with the data collection and contributed to manuscript edits. J.M. Curtis was the supervisory author and was involved with concept formation and manuscript composition.

Chapter 6 of this thesis has been submitted for publication. I was responsible for performing the experiments, the data collection and analysis as well as the manuscript composition. Y. Zhao assisted with the data collection and contributed to manuscript edits. J.M. Curtis was the supervisory author and was involved with concept formation and manuscript composition.

Dedication

This work is dedicated to my husband Mike and my parents Fanxia and Heping,

for their endless love, encouragement and support.

Acknowledgements

I would like to express my special appreciation and thanks to my advisor Professor Jonathan M. Curtis for introducing me to the fascinating world of lipid research. I enjoyed all the excitement of the new discovery and also the hardship during my PhD study. I would like to thank you for encouraging my research and for allowing me to grow as a scientist. I would also like to thank Professor Andreas Schieber and Professor Frederick West for serving as my committee members.

I have had support and encouragement from my wonderful lab mates who are also lifelong friends with me now. I would like to offer my special thanks to Dr. Yuan-Yuan Zhao who always gave my constructive comments and warm encouragement. I also have benefited a great deal form all the stimulating discussions with Dr. Brenna Black, Dr. Tuan Nurul Sabiqah Tuan Anuar and Dr. Xiaohua Kong.

I own my deepest gratitude to my wonderful parents who have not only brought me up but also raised me as a strong and determined person. Mom and dad, thank you for the endless love and support. I am deeply grateful to my husband Mike who has always been there for me. With all these wonderful people around me, I feel I am truly lucky and blessed.

Table of Contents

List of Tables

List of Figures & Schemes

List of Abbreviations

GC	Gas chromatography
FA	Fatty acid
FAME	Fatty acid methyl ester
EI	Electron ionization
LC	Liquid chromatography
HPLC	High performance liquid chromatography
Ag^+-LC	Silver ion liquid chromatography
MS	Mass spectrometry
MS/MS	Tandem mass spectrometry
m/z	Mass to charge ratio
Q-TOF	Quadrupole time - of - flight mass spectrometer
CID	Collision induced dissociation
ESI	Electrospary ionization
APPI	Atmospheric pressure photo ionization
TIC	Total ion current chromatogram
XIC	Extracted ion chromatogram
O_3	Ozonolysis
OzESI-MS	Ozone electrospary ionization mass spectrometry
OzID-MS	Ozone induced dissociation mass spectrometry
O_3-MS	Ozonolysis coupled to mass spectrometry
CLA	Conjugated linoleic acid
PL	Phospholipids

GPL	Glycerolphospholipids
PC	Phosphatidylcholine
PE	Phosphatidylethanolamine
PI	Phosphatidylinositol
PS	Phosphatidylserine
SM	Sphingomyelin
t_R	Retention time
FIA	Flow Injection Analysis
APCI	Atmospheric pressure chemical ionization
NPLC	Normal phase liquid chromatography
RPLC	Reverse phase liquid chromatography
TAG	Triacylglycerol

CHAPTER 1

Introduction [1]

1.1. Structural Diversity of Lipids

Lipids play many important roles in cells such as energy storage, cell membrane components and signal transduction [1]. It is also known that lipid metabolism dysfunction is closely related to several diseases including cancers [2], Alzheimer [3] and cardiovascular diseases [4]. The wide ranges of biological functions in which lipids are involved fundamentally rely on the structural diversity present in lipid species. A recent study using modern mass spectrometry (MS) revealed that 150-450 phospholipids (PL) species existing in human plasma [5,6]. By some estimation, cellular lipids could be composed of tens of thousands of structurally distinctive species [7]. The structural elucidation of lipids is difficult due to the diversity of lipid species. Besides, the fact that unlike protein the lipid structures are unpredictable results in a huge analytical challenge.

Lipids have enormously diverse chemical structures that are classified into eight main categories: fatty acyls, sterol lipids, prenol lipids, saccharolipids, polyketides, spingolipids, glycerolipids and glycerophospholipids (GPL) [8]. Each class has its subclasses according to the classification system proposed by LIPID Metabolites and Pathways Strategy [9]. For example, GPL is composed of

---

[1] A version of this chapter has been published. Sun, C. and Curtis, J.M. *Lipid Technol.* 2013, *25*, 279-282.
Reprinted with permission.

a glycerol back bone with a radyl moiety at *sn*-1 position linked through acyl ester, alkyl ester or vinyl ester bonding; an acyl chain at *sn*-2 position; and a polar head group at *sn*-3 position through phosphodiester linkage. GPL can be divided into different classes depending on the type of head groups, for example, phosphatidylcholine (PC) phosphatidylethanolamine (PE) and phosphatidylinositol (PI). In addition to the different head groups, the two substituents in GPL can also have different chain lengths, number of double bonds and even the locations of these double bonds (**Figure 1-1**).

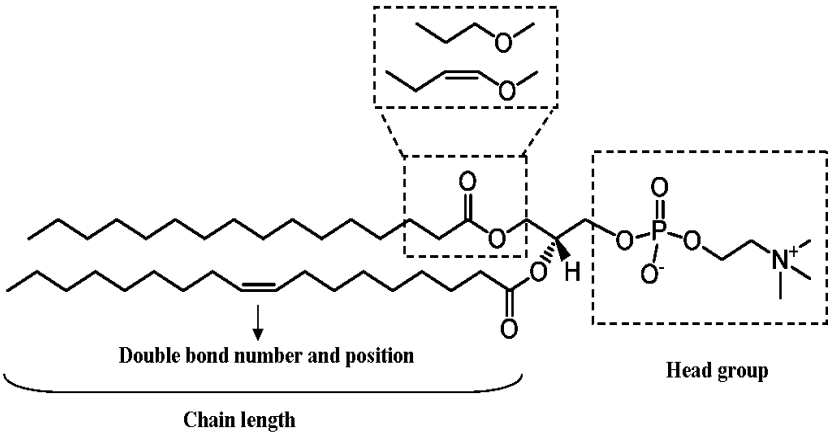

Figure 1-1. The structural diversity of lipids, demonstrated in the case of GPL (PC(16:0/18:1(*n*-*9*))).

Currently, mass spectrometry and tandem mass spectrometry (MS/MS) have become powerful tools for lipidomic analysis. Take PC(18:1(*n*-9)/18:1(*n*-9)) as an example, electrospray ionization (ESI) in positive ion mode-MS/MS analysis of PC(18:1(*n*-9)/18:1(*n*-9)) $[M+ H]^+$ ions resulted in the dominant product ions at *m/z* 184 representing phosphocholine ions. The MS/MS analysis under ESI in negative ion mode of PC(18:1(*n*-9)/18:1(*n*-9)) $[M+ HCOO]^-$ ions (ammonium

formate was added as a buffer in the mobile phase) yielded carboxylate anions at *m/z* 281 (**Figure 1-2b**), which corresponded to 18:1 fatty acyl chains as the two substituents. However, the determination of double bond position remains challenging for both conventional MS and MS/MS analysis, since these MS/MS spectra fail to provide any distinctive features indicative of double bond positions. For example, the ESI(-)-MS/MS spectra of the $[M+ HCOO]^-$ ions from PC(18:1(*n*-12)/18:1(*n*-12)) and PC(18:1(*n*-9)/18:1(*n*-9)) standards (**Figure 1-2**) are identical. The ambiguity of these two MS/MS spectra makes the identification of these PC isomers impossible.

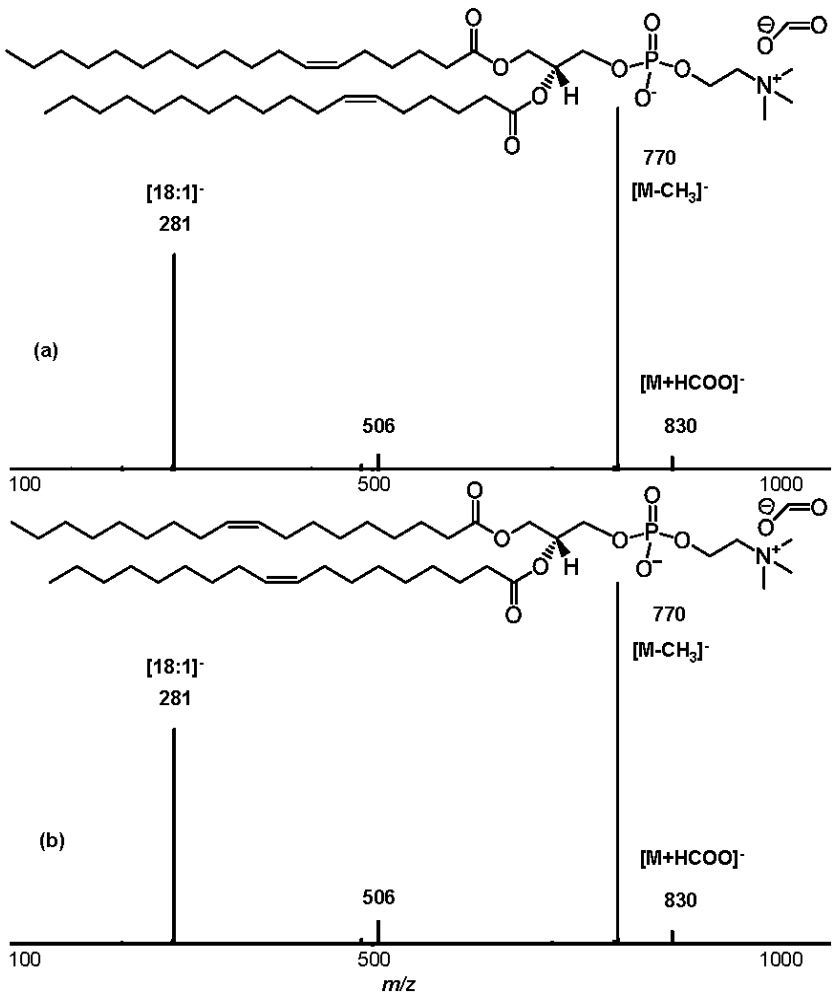

Figure 1-2. The ESI(-)- MS/MS spectra of (a) PC(18:1(*n*-12)/18:1(*n*-12)) and (b) PC(18:1(*n*-9)/18:1(*n*-9)) standards.

Although some of the lipid isomers are structurally different only in the positions of double bonds, these subtle structural isomers have drawn more and more interests with the progress of structure-function relationships studies of lipids. For instance, many studies have shown that both *n*-3 polyunsaturated fatty acid (PUFA) and *n*-6 PUFA can be released from PL by phospholipase A2 and subsequently converted into eicosanoids that are potent mediators of inflammation. Eicosanoids derived from *n*-6 PUFA such as arachidonic acid, are

pro-inflammatory, whereas eicosanoids derived from *n*-3 PUFA such as docosahexaenoic acid (DHA) have anti-inflammatory properties [10]. Another example is conjugated linoleic acid isomers, such as *cis*9,*trans*11-18:2 and *trans*10,*cis*12-18:2. It has been shown that only *trans*10,*cis*12-18:2 had effect on changing body composition by reducing the uptake of lipids into adipocytes, whereas *cis*9,*trans*11-18:2 appeared to enhance feed efficiency and growth in animal models [11,12]. In addition, the limitation of using MS to identify isomers with only double bonds located at different positions has been discussed in several critical reviews [13-15]. Therefore, it is important to develop a method that can be easily used for the accurate assignment of double bond positions in lipid, and also still takes advantage of the powerful structural elucidation ability of mass spectrometers.

1.2. Current Analytical Techniques for the Assignment of Double Bond Positions in Lipids

Gas chromatography coupled with flame ionization detection (GC/FID) is the most widely used method for fatty acid analysis by far. However, given the enormous numbers of possible isomeric forms of unsaturated fatty acids, obtaining authentic standards and proving sufficient chromatographic resolution to positively identify an unknown fatty acid methyl ester (FAME) by GC-FID is sometimes impractical. For this reason, fatty acids have been converted to derivatives, such as picolinyl esters and dimethyloxazolines (DMOX), which allows double bond positions to be inferred from fragment ions observed in the electron ionization mass spectra obtained in GC/EI-MS experiments [16,17]. In

some cases, the interpretation of these spectra is clear but in other cases, and especially for PUFA, some ambiguity remains. Under positive-ion chemical ionization (CI), it was reported that acetonitrile could go through self-reaction and form (1-methyleneimino)-1-ethenylium ions ($CH_2=C=N^+=CH_2$, *m/z* 54). The resulting ions then formed a charged covalent adduct across carbon-carbon double bonds in unsaturated FAME. Collision induced dissociation (CID) of these adduct ions $[M+54]^+$ resulted in two fragment ions formed by the cleavage of –C-C– bonds that are vinylic to each double bond. These fragment ions were diagnostic for the localization of double bonds [18-20]. In order to be compatible with GC/MS analysis, all the lipid samples have to be converted to molecules such as FAME that are volatile during GC analysis. While the derivatizaiton procedures are necessary for these analyses, the exact structures are lost during these derivatization procedures.

Although MS/MS analysis using high-energy CID can generate product ions from fatty acid $[M-H]^-$ ions for the determination of double bond positions [21], the low ionization efficiency and excessive fragmentation lead to difficulties in spectral interpretation. In addition, most MS/MS analysis is still overwhelmingly conducted under CID in the low-energy range (less than 100eV), which does not have the capacity of generating product ions arising from fragmentation at the double bonds. In order to enhance charge remote fragmentation during low-energy CID, metal adduct ions of fatty acids such as the di-lithium adduct ions $[M-H+2Li]^+$ have been used in MS/MS analysis [22,23]. Derivatization methods have also been developed to tackle this analysis challenge. The derivatization

agents such as N-(4-aminomethylphenyl) pyridinium (AMPP) react with carboxylic groups in fatty acids, generating a functional group that can localize the charge and hence enhance remote-site fragmentation during CID [24,25]. However, these methods still suffer from the difficulties of interpreting mass spectra due to the extensive fragmentation, and their application is also limited to fatty acid species.

Another approach is to use chemical derivatization to "label" double bonds prior to MS/MS analysis. For example, double bonds on fatty acyl chains were converted into di-hydroxy derivatives by off-line reactions with osmium tetroxide (OsO_4), and then the fragment ions in the ESI-MS/MS spectra of these derivatives can reveal the double bond positions [26]. This method has been applied to unsaturated fatty acids and phospholipids. However, OsO_4 also reacts slowly with other common organic functional groups resulting in the formation of byproducts, which could lower the efficiency of vicinal hydroxylation and further complicate mass spectra for double bond localization [27]. Recently, acetonitrile was used as an atmospheric pressure chemical ionization (APCI) reagent. Similar to positive-ion CI, the ions generated from the self-reaction of acetonitrile formed a charged covalent adduct across carbon-carbon double bonds. In this way, the double bond positions in triacylglycerol could be elucidated from the fragment ions generated from CID of these acetonitrile adduct ions [28]. Whether this approach can be applied to other lipids such as the PL for the determination of double bond positions is not clear.

In summary, off-line derivatization procedures are mostly required for existing methods that have been used for the determination of double bond positions. Furthermore, the unambiguous assignment of double bonds is still compromised by complex mass spectra due to extensive fragmentation. A possible solution to this problem is to react ozone with the unsaturated lipid which results in cleavage across the –C=C– double bond, generating ozonolysis products with predictable mass that can be used to identify the double bond positions [29,30]. Before describing how the ozonolysis reaction has been exploited as an analytical tool for double bond positional assignment, it is necessary to introduce the ozonolysis reaction mechanism.

1.3. Ozonolysis Reaction Mechanism

Ozone is an allotrope of oxygen with the chemical formula O_3, existing as a pale blue gas with distinctively pungent smell [31]. Ozone structure can be expressed as a resonance hybrid with a single bond on one side and double bond on the other resulting in an overall bond order of 1.5 [31]. Although ozone is much less stable than the diatomic allotrope O_2, it has much higher oxidizing strength than O_2 and can react with a variety of organic compounds [32]. As a strong oxidizing agent, ozone has been widely used in the treatment of water, wastewater [33] and also used as sanitization process in food industry [34]. In addition, ozone has proved to be highly useful in the chemical industry, such as in the manufacture of azelaic and pelargonic acids by the ozonolysis of oleic acid [35].

Ozonolysis is the reaction of ozone with alkene or alkyne at carbon-carbon double bonds or triple bonds. The mechanism of ozonolysis was intensely studied by organic chemists in the first half of the twentieth century. It was known that the ozonolysis products of carbon-carbon double bonds depend on the reaction conditions such as temperature and also other compounds that could join in the reaction, more detailed discussions can be found in the review authored by Bailey [36]. Currently, the 3-step mechanism proposed by Criegee is widely accepted [37]. Here, the ozonolysis of PC(16:0/18:1(*n-9*)) is used to illustrate the steps involved in the ozonolysis of one double bond (**Scheme 1-1**). In the first step, a molecule of ozone attacks the double bond resulting in the rapid formation of a so-called primary ozonide, a 1,2,3-trioxolane. These primary ozonides are usually unstable and readily decompose to give carbonyl compounds plus the zwitterions that are often known as Criegee intermediates. It can be seen in **Scheme 1-1** that ozonolysis of PC(16:0/18:1(*n-9*)) can result in the formation of two possible Criegee intermediate/aldehyde pairs. Criegee intermediates play important roles in the ozonolysis reaction since they can readily undergo further reactions. Then, in the absence of any participating solvent, the Criegee intermediates and either of the aldehydes can recombine to form secondary ozonides 1,2,4-trioxolanes that are relatively stable.

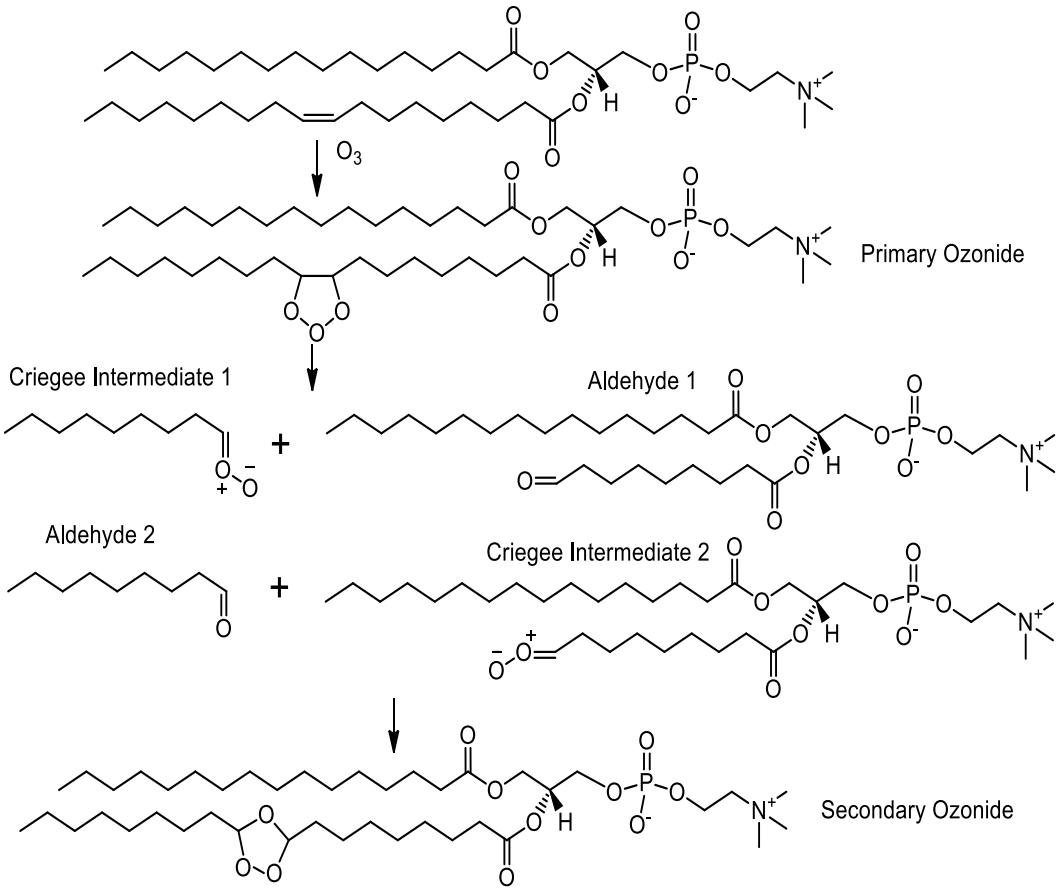

Scheme 1-1. Simplified ozonolysis reaction mechanism in the case of PC(16:0/18:1(*n-9*)).

As can be seen in **Scheme 1-1**, the ozonolysis products which include the aldehydes, Criegee intermediates and secondary ozonides, are all specific to the location of the initial double bond. In this example, ozonolysis of the *n*-9 double bond results in an aldehyde or Criegee intermediate with a 9-carbon chain length, or a secondary ozonide at the original double bond location. As shown below, if these ozonolysis products can be identified, then the location of the double bond in the starting lipid is also proven.

1.4. The Use of Ozonolysis for the Double Bond Localization

1.4.1. Off-line ozonolysis

Ozonolysis was used as an off-line reaction in the 1960s for the determination of double bond positions in FAME [29]. At this time, a solution of ozone in pentane at -70 ˚C was prepared by bubbling oxygen containing 2-3% ozone. The FAME standard in pentane was mixed with the ozone solution, resulting in the formation of ozonides that were then reduced to aldehydes by hydrogen in the presence of a catalyst. Reductive ozonolysis of a monounsaturated FAME resulted in the formation of both an aldehyde (similar to aldehyde 2 in **Scheme 1-1**) and an aldehyde-methyl ester (analogous to aldehyde 1 in **Scheme 1-1** but with methyl group replacing the substituted glycerol moiety) that could then be identified by gas chromatography (GC) through comparison of their retention times to those of standards. The chain lengths of these aldehydes indicated the position of the double bond along the monounsaturated FAME. Multiple double bond locations in polyunsaturated FAME could also be identified in a similar way. Although this technique was limited to use with individual FAME and the identification of products by retention time alone, it still showed great promise for using the ozonolysis reaction for the determination of double bond positions in unknowns.

More recently, Harrison and Murphy extended the use of ozonolysis as an off-line reaction for double bond localization in phospholipids by using electrospray mass spectrometry (ESI-MS) [30]. A PC sample was coated inside

of a glass capillary that was placed in a flow of ozone. The ozonized PC was dissolved in the electrospray mobile phase (methanol/ammonium acetate 85:15, v/v) and analyzed under positive ion ESI-MS. In this way, the relatively stable PC secondary ozonides were observed. Since secondary ozonides arise by the addition of O_3 to each double bond, a mass increment of 48 Da over the *m/z* for $[M+H]^+$ ions of the corresponding intact PC molecules was observed for each double bond present. MS/MS analysis of these PC ozonide ions following CID gave rise to fragment ions indicative of double bond positions in both mono- and polyunsaturated PC. In this study, the gas-liquid phase ozonolysis reaction was effectively carried out using a simple procedure, taking advantage of the high sensitivity and information content available from ESI-MS and MS/MS. Since ozonolysis was performed as an off-line reaction on individual GPL standards, this technique is not directly suitable for complicated lipid mixtures.

1.4.2. In-situ ozonolysis coupled to mass spectrometry (in-situ O_3-MS)

In-situ O_3-MS was first achieved by Blanksby et al who introduced ozone into nebuliser gas flow of the ESI source on a tandem quadrupole MS instrument (OzESI-MS) [38]. Unsaturated lipids reacted with ozone in the ionization source rather than performing ozonolysis off-line prior to MS analysis. In this way, the OzESI-MS technique achieved *in-situ* ozonolysis ie, within the mass spectrometer. Solutions of GPL, sphingomyelins and triacylglycerols were infused into an ESI source where ozone reacted with the double bonds of the ionized lipids. However, unlike off-line ozonolysis, the ions of stable ozonides were not observed. Instead, the oxidative cleavage product aldehydes, along with

α-methoxydroperoxides formed by the addition of methanol from the mobile phase to the Criegee intermediates, were observed and used to assign double bond positions. While OzESI-MS is applicable to individual lipids and simple lipid mixtures, it is less suited to the analysis of more complex lipid samples where overlapping mass spectra and potential ion suppression effects might occur.

In a further development from the same group, the ozone induced dissociation (OzID-MS) method was invented by introducing ozone vapor into a linear ion trap mass spectrometer [39]. In this experiment, lipid ions generated by ESI were mass-selected and held in the ion trap in the presence of ozone vapor for about 10s. The reaction between the gas phase lipid ions and ozone generated the expected aldehyde ions and the corresponding Criegee intermediates from each unsaturated site (See **Figure 1-3** for the example of PC(16:0/18:1(*n-9*))). These product ions were used for the direct assignment of double bond position in GPL and triacylglycerols. Since the ions of the targeted lipid could be isolated in the ion trap before ozonolysis, the OzID-MS method could be applied to more complex lipid mixtures. Published examples of the use of OzID-MS include the analysis of lipid extracts from a human lens, bovine kidney and olive oil [39]. However, since most of the lipid ions were trapped with ozone in the ion trap for 10s in order to generate enough product ions for the assignment of double bond position, improvements were needed in order to increase the sensitivity and speed. This was achieved by using the OzID-MS method in a tandem linear ion-trap mass spectrometer [40]. First, the *m/z* value for the lipid ions of interest were selected by MS1; these ions then reacted with the ozone vapor that was delivered

in continuous and stable flow into the collision cell; finally the ozonolysis product ions were analyzed for *m/z* and detected in MS2. This arrangement, with a spatial separation between the precursor ion selection and ozonolysis, can achieve fast analyses and high sensitivity as well as having potential compatibility with LC. Another possible advantage is that OzID and CID can be combined by applying a potential to the collision cell, although this results in the superimposition of OzID and CID product ions in the MS/MS spectrum. However, it should be noted that the OzID-MS method requires some modifications to the mass spectrometer to allow the introduction of ozone gas and that the introduction of an oxygen/ozone mixture into the vacuum system is potentially detrimental.

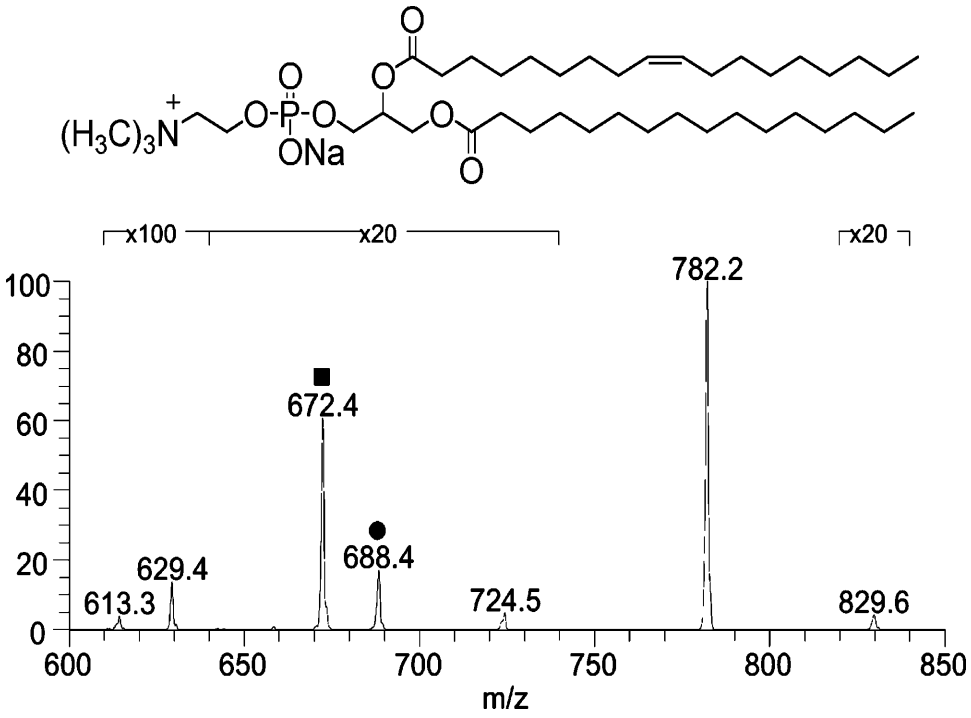

Figure 1-3. OzID spectrum of the [PC (16:0/18:1(*n-9*)) + Na]$^+$ ions under ESI (+). The pair of ions resulting from ozonolysis of the double bond are labeled with ■ and ●, indicating aldehyde and Criegee ions, respectively. From Reference [39] with permission of the American Chemical Society.

1.5. Hypothesis and Proposed Studies

The reaction of ozone with unsaturated lipids has been used with great success for the assignment of double bond positions as discussed above. Combining the ozonolysis reaction *in-situ* with modern mass spectrometry such as in the OzESI-MS and OzID-MS techniques, has been shown to simplify the elucidation of unsaturated lipid structures and help to reveal the diversity of lipids that exist in biological systems. However, there are undesirable instrumental modifications needed for *in-situ* ozonolysis mass spectrometry approach. In addition, the compatibility of OzID-MS technique with LC has not been proved either, which raises an issue for analyzing complex lipid mixtures.

Therefore, the hypothesis proposed in this thesis is that the assignment of double bond positions in unsaturated lipids can be achieved by using the ozonolysis reaction in-line with mass spectrometer, and this in-line ozonolysis device is also compatible with liquid chromatography (LC) separation. In order to test this hypothesis, the following studies were performed: (1) to investigate the off-line ozonolysis intermediates and products of lipid standards, (2) to develop a new approach of coupling ozonolysis reaction in-line with mass spectrometer (in-line O_3-MS) (prior to the ionization of MS), (3) to further develop the in-line O_3-MS method for the compatibility with LC, (4) to apply in-line O_3-MS method to different lipid species such as fatty acid methyl esters and phospholipids, (5) to demonstrate the applications of the LC/O_3-MS method for the unambiguous determination of double bond positions in complex agricultural and biological samples.

CHAPTER 2

A Study of the Ozonolysis of Model Lipids by Electrospray Ionization Mass Spectrometry [2]

2.1. Introduction

Recently, global interest in using renewable resources in place of fossil fuels for the production of energy, fine chemicals and polymers has greatly increased. Much research has focused on transforming vegetable oils, which are abundant and renewable in nature, into forms that are amenable to these applications [41]. Ozonolysis is one such transformation of vegetable oils that has shown potential in the manufacture of bio-based polymers and chemicals. Ozone, a very reactive oxidizing agent, can cleave the double bonds of the unsaturated triacylglycerides (TAG) found in vegetable oils. Ozonolysis has been used as one of the steps of making vegetable oil based polyols [42,43], these are polyhydroxyl compounds that are precursors used in polyurethane manufacture. However, formation of bio-based polyols by this pathway includes multiple steps, catalysts, and there are many challenges to producing high yields of polyols [44]. It is hoped that further elucidation of the products from the ozonolysis of vegetable oils will aid in the development of ozonolysis processes for the commercial production of bio-based polyols and other chemicals.

---

[2] A version of this chapter has been published. Sun, C., Zhao, Y. and Curtis, J.M. *Rapid Commun. Mass Spectrom.* 2012, *26*, 921-930.
Reprinted with permission.

The mechanism proposed by Criegee, describing the reaction of ozone with olefins is the widely accepted one [37]. **Scheme 2-1** is a simplified version showing the important intermediates and expected products for the ozonolysis of methyl oleate. The initial reaction occurs when an ozone molecule attacks the double bond and the primary ozonide forms. This high-energy primary ozonide can readily decompose into the Criegee intermediates 1 and 2, nonanal and 9-oxononanoic acid methyl ester. In the absence of any participating solvent, Criegee intermediates can recombine with nonanal and 9-oxononanoic acid methyl ester to form the secondary ozonide 1,2,4-trioxolanes, which include Compound 1, 2 and 3. The Criegee intermediates are very important intermediates of ozonolysis because they can readily undergo further reactions. In the liquid phase, 1,3- dipolar cycloaddition results in the formation of 1,2,4-trioxolanes. Step 3 in **Scheme 2-1** is an example of 1,3-dipolar cycloaddition between the Criegee intermediate 2 and nonanal.

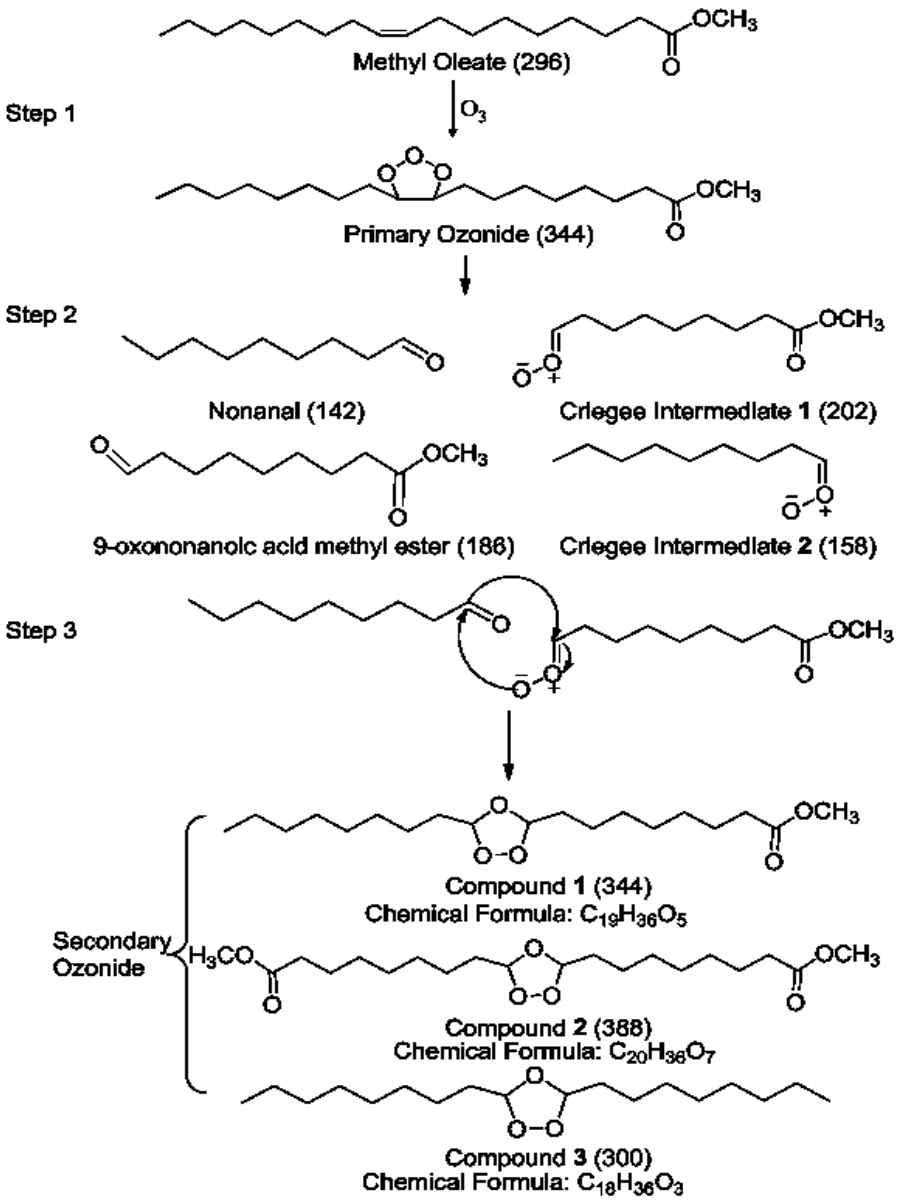

Scheme 2-1. Simplified version of ozonolysis mechanism based on Criegee theory in the specific case of methyl oleate. The nominal values of molecular weight are in the bracelet.

Several methods have been used for observation of both the intermediates and the products of the ozonolysis of free fatty acids and vegetable oils, including Fourier transform infrared (FTIR) spectroscopy and nuclear magnetic resonance

(NMR) spectroscopy. Soriano *et al.* used FTIR to follow the ozonolysis of sunflower oil; they observed the peaks in the IR spectrum that are characteristic of the formation of both aldehydes and ozonides [45]. Sega used ^{1}H NMR and ^{13}C NMR for analysis of sesame oil before and after ozonolysis to identify characteristic peaks that show the trend of ozonide formation and simultaneous decrease in double bonds. The relationship between the NMR signal and physico-chemical measurements, including peroxide value and viscosity, was also established [46]. Even though NMR can reveal lots of structural information, some of the spectral details can not be entirely assigned due to the complexity of spectrum, and a relatively large sample size is required for NMR analysis. The application of size exclusion chromatography (SEC) additionally revealed the formation of high molecular weight ozonolysis products, but very little structural information can be revealed [47]. Gas chromatography (GC) has also been widely used to analyze ozonolysis products, but its application is limited to the light fraction of the ozonolysis products that are suitable for GC analysis [48]. Methylation is commonly used to make the sample amenable to GC analysis, if the starting material is triglycerides or vegetable oils [49]. Ozonolysis of simple lipids has also been studied by mass spectrometry (MS), for example, the ozonolysis of methyl oleate was analyzed without any chromatographic separation using direct probe introduction into chemical ionization - mass spectrometry (CI-MS). This revealed the existence of secondary ozonides and NMR spectroscopy was used to further assign their structures [50]. Thornberry designed a coated-wall flow tube coupled to CI-MS to selectively monitor both

ozone loss and the production of volatile compounds when ozone reacted on a surface of oleic acid, linoleic acid and linolenic acid [51]. However, that work focused on gas-phase products and their experimental design more closely modeled ozone reactions on a particle surface than ozone reactions in a bulk solution. To our knowledge there has not to date been a report of a comprehensive liquid chromatography/ tandem mass spectrometry (LC-MS/MS) method for the identification of ozonolysis products from unsaturated lipids.

In this work, methyl oleate was selected as a simple model for unsaturated fatty acids, because it is an important component of many vegetable oils for which ozonolysis can only occur on one double bond. Similarly, triolein is selected as the simple model for unsaturated TAG, which is an abundant TAG in vegetable oils containing high amounts of oleic acid such as canola or sunflower oils. The overall objective of this study is to develop methods for the study of both the ozonolysis intermediates and products from the model lipids, methyl oleate and triolein. This was achieved using liquid chromatographic separation combined with quadrupole time - of - flight (Q-TOF) mass spectrometer, allowing both exact mass determination and MS/MS scans for structure identifications.

2.2. Experimental

2.2.1. Materials

Methyl oleate and triolein standard were purchased from Nu Chek Prep Inc. (Elysian, MN, USA). Hexanes, acetonitrile (ACN), isopropanol (IPA) and methanol (MeOH) were purchased from Fisher Scientific Company (Ottawa, ON,

Canada) and were of analytical grade. HPLC-grade ammonium acetate (≥99%) was supplied by Sigma (St. Louis, MO, USA). A solution of porcine renin substrate tetetradecapeptide at 10 pmol/ μL in acetonitrile/water (1:1, v/v) in a chemical standards kit was obtained from Applied Biosystems (Forster City, CA, USA). ESI-L low concentration tuning mix was purchased from Agilent Technologies Canada Inc. (Mississauga, ON, Canada).

2.2.2. Ozonolysis of methyl oleate and triolein

A mixture of 0.87 g lipid standards (methyl oleate or triolein) and 50 mL hexane was placed in 50 mL flask and the temperature of the flask was kept at 10 °C using Julabo F25 circulating chiller (Julabo USA Inc., Allentown, PA, USA). An ozone/oxygen mixture was introduced into the flask at a rate of 50 mL/min through a long stainless steel needle with an ozone concentration of approximately 0.4 g/m^3. Ozone was generated by passing dry oxygen as the feed gas through an Azcozon ozone generator coupled to a controller unit (RMU 16-16 and RMDC-32D, Azco Industries Limited, Langley, BC, Canada). During ozonolysis, 25 μL aliquots were taken from the reaction at 10, 15, 20, 30, 40, 50, 75, 90, 105, 120, 140, 160, 180, 210 and 240 min. The 25 μL aliquot was mixed with 75 μL hexane and immediately stored at -20 °C. The samples were diluted 100 times in hexane before any further analysis.

2.2.3. Liquid chromatography/ mass spectrometry (LC/MS)

LC/MS analysis was conducted on an Agilent 1200 series HPLC system (Agilent Technologies Inc, Palo Alto, CA, USA) coupled to a QSTAR Elite mass

spectrometer (Applied Biosystems/MDS Sciex, Concord, ON, Canada) using electrospray ionization (ESI) in positive ion mode. Analyst QS 2.0 software was employed for data acquisition and analysis. 2 μL of sample was injected for LC/MS analysis.

For the ozonolysis of methyl oleate, chromatographic analysis was performed on an Ascentis Si silica column (150 mm×2 mm i.d.) with a particle size of 3 μm (Sigma, St. Louis, MO, USA). The mobile phase A was hexane and B was IPA. The gradient was as follows: 0–4 min, 2% B; 4–10 min, 100% B; 10–14 min, 100% B; 14–20 min, 2% B. 40 mmol/L ammonia acetate in MeOH and IPA (3:1, v/v) was used as post-column flow at a rate of 25 μL/min. The mass spectra were acquired over the mass range of *m/z* 100 - 1,000. The ion source temperature was kept at 300°C. The other instrumental conditions were as follows: curtain gas 25; auxiliary gas 20; nebulizing gas 60. All the gas numbers are in arbitrary units, and nitrogen was used for all these gases. The ionspray voltage, declustering potential (DP), focus potential (FP), and DP2 were 5200 V, 35 V, 150 V and 10 V, respectively. For MS/MS analysis, collision induced dissociation (CID) at a collision energy of 28 eV and at a collision gas setting of 8 units was used.

For ozonolysis of triolein, chromatographic analysis was performed on an Ascentis C_{18} column (150 mm×2 mm i.d.) with a particle size of 3μm (Sigma, St. Louis, MO, USA). The mobile phase A consisted of ACN and B of IPA. The gradient was as follows: 0–0.1 min, 20% B; 0.1–25 min, 90% B; 25–27min, 90% B; 27–27.1 min, 90% B; 27.1-36 min, 20% B. The same ammonia acetate

solution was used as post -column flow at a flow rate of 20 μl/min. The mass spectra were acquired over the mass range of *m/z* 100 - 2,000. The ion source temperature was kept at 400°C. Other mass spectrometer conditions were the same as the conditions used for the ozonolysis of methyl oleate. MS/MS analysis used CID at a collision energy of 32 eV and a collision gas setting of 8 units.

All mass spectra were recorded using the high resolution TOF mass analyzer providing mass accuracies typically below 5 ppm over the range of *m/z* reported after calibration. The mass spectrometer was tuned by infusing porcine renin substrate tetetradecapeptide (m/z 879.9723, doubly charged ion and fragment ion at *m/z* 110.0713) at a resolution of above 10000 full width at half maximum (FWHM) in positive ion mode. This solution was also used for calibration of *m/z* 100-1,000; the Agilent ESI low concentration tuning mix was used for calibration of *m/z* 100-2,000.

2.2.4. Gas chromatography/mass spectrometry (GC/MS)

GC/MS analysis was only performed on the sample from the ozonolysis of methyl oleate. A 1 μL aliquot was analyzed using an Agilent 7890A gas chromatograph equipped with Agilent 5975C mass selective detector (MSD) (Agilent Technologies Inc, Palo Alto, CA, USA). An Rxi-5ms capillary column (30 m×0.25 mm i.d, 0.25 μm film thickness) (Restek Corporation, Bellefonte, PA, USA) was used. The helium flow was kept constant at 1 ml/min. The oven program was 40 °C for 3 min, then rising to 280 °C at a rate of 30 °C/min with a final hold at 280 °C for 2 min. Electron ionization was used at 70eV electron

energy and a mass scan range of *m/z* 35 - 500. An Agilent MSD Chem Station E.02.02.1431 was used for data analysis.

2.3. Results and Discussion

2.3.1. Identification of the products and the intermediates from the ozonolysis of methyl oleate

Lipids with double bonds on the fatty acyl chain can be oxidized with ozone. Due to the complexity of products and intermediates that could be formed by the ozonolysis of natural lipid mixtures, methyl oleate, which has only one double bond at the *n*-9 position, was instead studied as a model lipid compound. A sample of methyl oleate after 40 min of ozonolysis was introduced into the mass spectrometer by flow injection in positive ESI mode using a mobile phase of hexane and isopropanol (98:2, v/v) and with a post-column addition of 40mM ammonia acetate to aid ionization. The resulting mass spectrum is shown in **Figure 2-1**. The ions seen at *m/z* 362 and 406 are ammonium ion adducts of the Compounds 1 and 2 respectively (see **Scheme 2-1**), while ions at *m/z* 367 and 411 correspond to their sodium ion adducts and ions at *m/z* 383 and 427 are their potassium ion adducts. Furthermore, the elemental composition of ion at *m/z* 362.2898 was determined to be $[C_{19}H_{36}O_5 + NH_4]^+$ (Δ= -0.83 ppm), and that of *m/z* 406.2797 was determined to be $[C_{20}H_{36}O_7 + NH_4]^+$ (Δ=-0.49 ppm), consistent with the elemental compositions of Compounds 1 and 2 (**Scheme 2-1**).

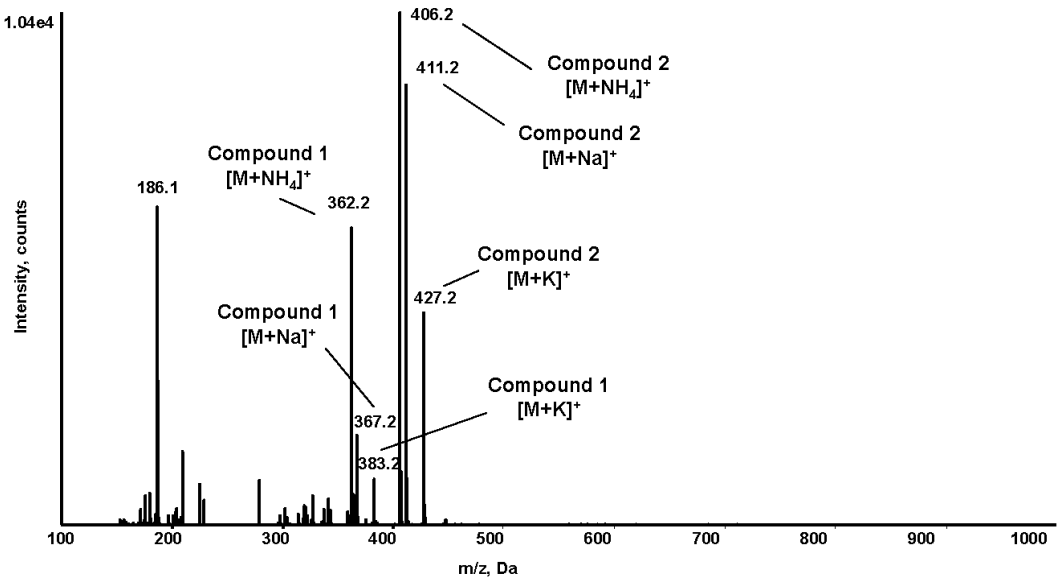

Figure 2-1. Flow injection ESI (+) mass spectrum of the products of the ozonolysis of methyl oleate for 40 min.

In order to confirm this identification, MS/MS spectra of the $[M+NH_4]^+$ ions of Compounds 1 and 2 at *m/z* 362 and 406 were obtained. As can be seen in **Figure 2-2**, the MS/MS spectra of ions at *m/z* 362 **(a1)** and 406 **(b)** are very similar, showing that ions at *m/z* 186 and 155 are the main product ions in both cases. The fragment ion at *m/z* 142 is only observed in the MS/MS spectrum of *m/z* 362; this fragmentation pathway is illustrated in the inset of **Figure 2-2(a1)**. The cleavage initially occurs at the peroxide bridge of trioxolane, and there can be either *ab* or *ac* cleavage. The result of *ac* cleavage is an aldehyde radical, which is the product ion at *m/z* 186. The other part of this cleavage is the Criegee intermediate 2, the ion of which is not seen in the MS/MS spectrum. However, this Criegee intermediate was observed in work of Thomas where methanol was present in the mobile phase, which reacts quickly with the Criegee intermediate to form a stable ion [38]. Apparently the ion at *m/z* 155 cannot directly form by this

route but rather is attributed to the cleavage of the ion *m/z* 186. Similarly, *ab* cleavage results in a product ion at *m/z* 142 of low intensity. Compound 2 is a symmetric trioxolane (**Scheme 2-1**), so its *ab* and *ac* cleavage of ion at *m/z* 406 produces the same product ion at *m/z* 186. The pattern of these product ions also agrees with Wu's results, even though in that work the trioxolane compounds were analyzed under chemical ionization conditions [50]. Hence, the accurate mass measurements and MS/MS spectra of the ions at *m/z* 362 and 406 support the conclusion that they are ammonium adducts of the secondary ozonides, Compounds 1 and 2 in **Scheme 2-1**.

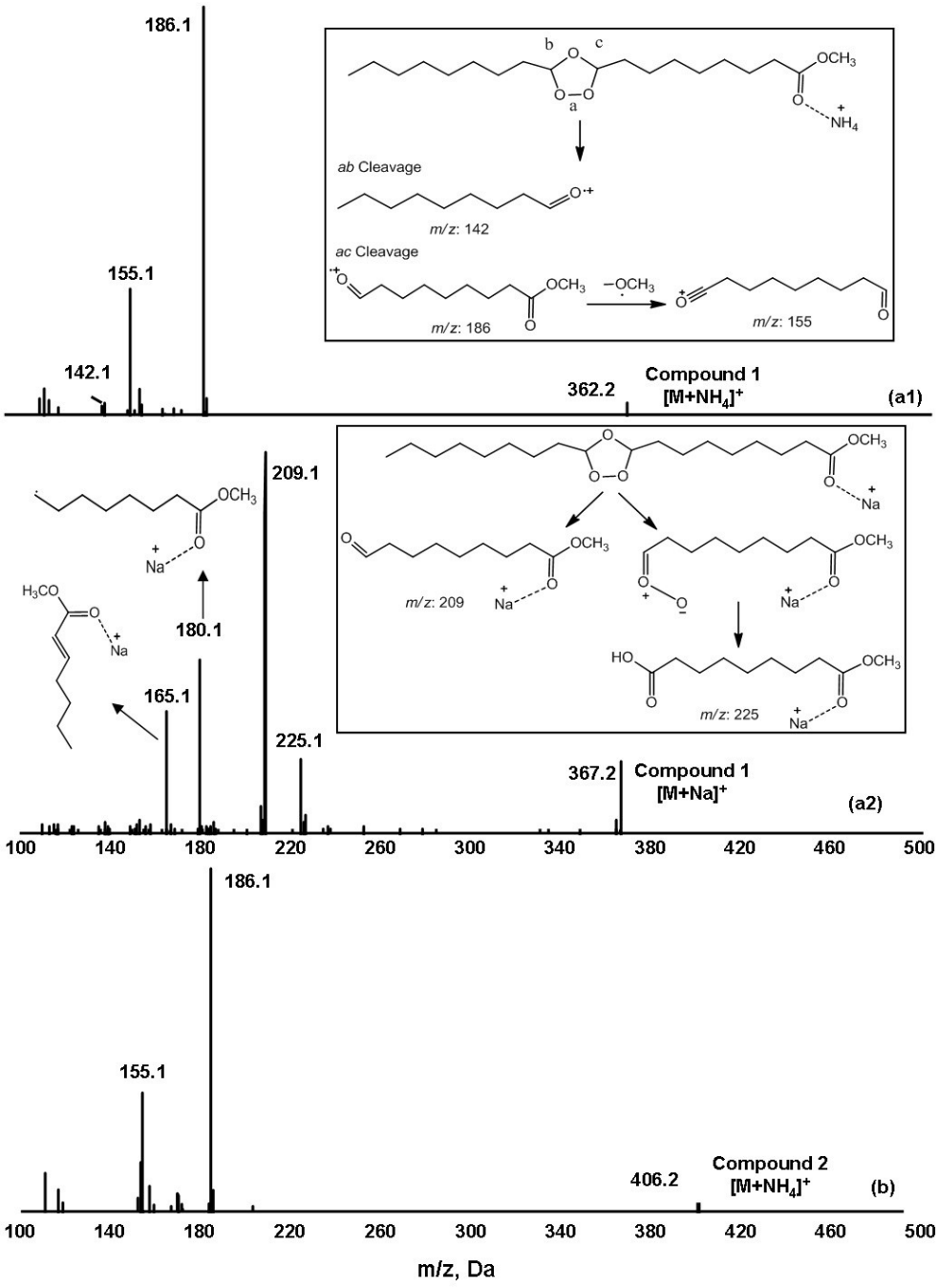

Figure 2-2. ESI (+) MS/MS spectra of the ions at (a1) *m/z* 362, (a2) *m/z* 367 and (b) *m/z* 406 of the products from the ozonolysis of methyl oleate for 40 min. The inset of (a1) is the fragmentation pathway of secondary ozonide Compound 1 (*m/z* 362). The inset of (a2) is the fragmentation pathway of secondary ozonide Compound 1 (*m/z* 367).

It is interesting to note that the fragment ions arising from the $[M+NH_4]^+$ ion of Compound 1 *m/z* 362 do not retain the ammonium adduct but instead are odd-electron species (**Figure 2-2(a1)**). For comparison, the MS/MS spectrum of the corresponding sodiated ion at *m/z* 367 $[M+Na]^+$ of Compound 1 shows that product ions are at *m/z* 225, 209, 180 and 165 (**Figure 2-2(a2)**), all of which retain the sodium ion. These product ions can be explained based on the trioxolane structure proposed for Compound 1 in **Figure 2-2**. For example, product ions at *m/z* 225 and 209 are formed by cleavage at the trioxolane group. This generates either the aldehyde ion at *m/z* 209 or the Criegee intermediate that can rearrange into the carboxylic acid observed at *m/z* 225. Other fragmentation due to cleavage of the hydrocarbon chain adjacent to the trioxolane group results in ions at *m/z* 180 and 165 (**Figure 2-2(a2)**). Hence, in contrast to the fragmentation observed for the $[M+NH_4]^+$ ion of Compound 1, the $[M+Na]^+$ ion of Compound 1 fragments in a manner that is closely analogous to that previously reported for trioxolane derivatives of other unsaturated lipids [30].

In order to confirm the existence of the secondary ozonides Compounds 1 and 2 as distinct species, normal phase-LC/MS was performed. The chromatogram in **Figure 2-3(a)** is the total ion current (TIC) trace for the separation of the products obtained following 40 min of ozonolysis of methyl oleate, using a silica column. The ions at *m/z* 362 and 406 are the base peaks of mass spectra eluting at 2.5 and 2.9 min, respectively. Since normal phase chromatography was used, the compound (*m/z* 406) eluting at 2.9 min is likely more polar than the compound (*m/z* 362) eluting at 2.5 min. This is consistent

with the structures of Compound 1 and 2 in **Scheme 2-1**, which show that Compound 2 has two ester groups compared to only one on Compound 1. Another dominant ion seen by flow injection (**Figure 2-1**) is the ion at *m/z* 186 which could either be the ammonium ion adduct of an intact compound or else an in-source fragment ion. Extracted ion chromatograms (XIC) of ion at *m/z* 362, 406 and 186 are shown in **Figure 2-3(b**). These indicate that the ion at *m/z* 186 has the same retention time as ion at *m/z* 362. Furthermore, the MS/MS spectrum of *m/z* 362 (**Figure 2-2(a1)**) has a major fragment ion at *m/z* 186. Based on this discussion, it appears to us that the ion at *m/z* 186 in the positive ion ESI spectrum shown in **Figure 2-1** is indeed a product ion of the secondary ozonide compound at *m/z* 362 rather than another unknown product from the ozonolysis of methyl oleate.

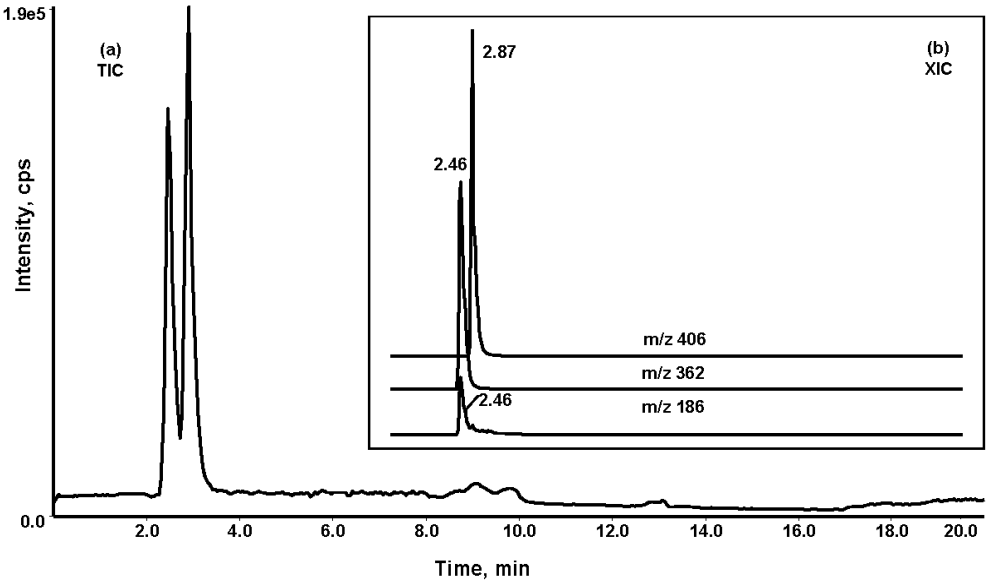

Figure 2-3. (a) Total ion current (TIC) chromatogram of products from the ozonolysis of methyl oleate for 40 min by LC/ ESI(+)-MS. (b) Extracted ion chromatograms (XIC) of the ions at *m/z* 362, 406 and 186.

It should be noted that the ion corresponding to intact methyl oleate is not observed under this experimental condition, even though methyl oleate was found to still exist in the sample based on GC/MS analysis. This is because methyl oleate is a neutral lipid, which does not ionize well by ESI as we have previously observed. Chemical derivatization, such as phosphonium labelling of these neutral lipids, has been shown to improve ionization under ESI [52]. On the other hand, we have obtained $[M+H]^+$ ions from methyl oleate using positive ion atmospheric pressure photo ionization (APPI) and atmospheric pressure chemical ionization (APCI) from the same ozonolysis sample. Methyl oleate has very low polarity, hence more easily ionized by APPI and APCI than by ESI. However, only fragment ions of secondary ozonides are observed using positive ion APCI and APPI. Overall, compared to APPI and APCI, ESI with post-column addition of ammonium ions was found to be a better choice of ionization method for the observation of ozonolysis products.

GC/MS results (**Figure 2-4**) indicate that nonanal, nonanoic acid and 9-oxononanoic acid methyl ester are the main volatile ozonolysis products. Nonanal and 9-oxononanoic acid methyl ester were seen to form at the beginning of ozonolysis whereas nonanoic acid is only observed by GC/MS in samples taken after 30 minutes of ozonolysis. Nonanoic acid can be formed either as a result of further oxidation of nonanal, which is abundant after ozonolysis starts, or via an internal rearrangement of the Criegee intermediate to form a more thermodynamically stable structure [53]. A mass balance between the reactants and volatile and involatile products formed during ozonolysis could not be

achieved in this study due to a constant loss of volatiles. Nevertheless, these qualitative observations by GC/MS are in agreement with the expected products indicated in **Scheme 2-1**.

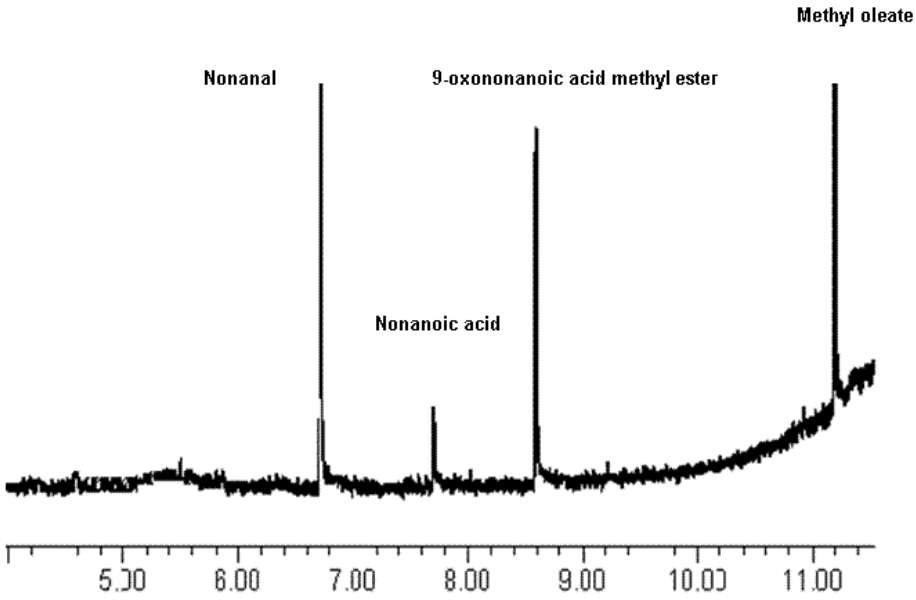

Figure 2-4. TIC of GC/EI-MS analysis of products from ozonolysis of methyl oleate for 30 min.

Ions of high *m/z* value (>500) were not observed in any of the mass spectra obtained following ozonolysis of methyl oleate for periods of up to 4 hours. Several researches have shown that Criegiee intermediates are able to react with other Criegee intermediates or acids to form oligomeric or polymeric compounds [54,55,56]. However, there are also reports showing that no oligomers are observed either in aerosol particles or in a bulk solution of oleic acid [57]. In the present study, both the presence of a large amount of an inert solvent (hexane) and the absence of the free carboxylic acid group in the methyl

oleate as starting material, likely minimize the probability oligomer formation through the Criegee intermediates and acids.

Ozonolysis has been used for determination of double bond position in unsaturated fatty acids and ester [30,38]. For example, a low temperature plasma (LTP) probe was recently used to for *in situ* ozonolysis [58]. The plasma containing ozone was directed at the sample and the resulting ions were sampled into a linear ion trap MS. For a fatty acid ester, only aldehyde oxidation products retaining the ester chain were observed in positive ion mode. In the case of a free fatty acid, only the aldehyde products from the oxidation of a double bond with retention of the carboxylic acid head group were observed in both positive and negative ion modes. The *m/z* values of these products can be used to assign the double bond location. However, in general the ozonolysis intermediates, such as, ozonides and diperoxides, were not observed. In contrast, in our study the ozonolysis products are present at low concentration in the solvent and the observation of ozonides besides 9-oxononanoic acid methyl ester is facile.

2.3.2. Identification of the products and intermediates from the ozonolysis of triolein

Identification of the major intermediates and products arising from the ozonolysis of methyl oleate should elucidate at least some of the basic principles and mechanisms important for ozonolysis in general. These can be extended in the interpretation of the ozonolyis products of a triolein standard. Investigation of TAG is more relevant to the vast majority of lipids in nature and triolein in

particular is the most abundant TAG found in canola oil. The triolein standard before and after ozonolysis for 60 min was analyzed using non-aqueous reverse phase (NARP) LC/MS as shown in **Figure 2-5**. The positive ion NARP- LC/MS chromatogram of triolein (**Figure 2-5(a)**) shows a single peak for a compound of *m/z* 902, consistent with the $[M+NH_4]^+$ ion of triolein. Following ozonolysis (**Figure 2-5(b)**), additional peaks appeared in the chromatogram and their molecular weight information is summarized in **Table 2-1**. It is evident from **Figure 2-5(b)** that three prominent groups of peaks appear at retention times of around 12, 15 and 19 min following ozonolysis. It was also observed that each of these groups is comprised of multiplets of isomeric compounds, mostly resolved by NARP chromatography.

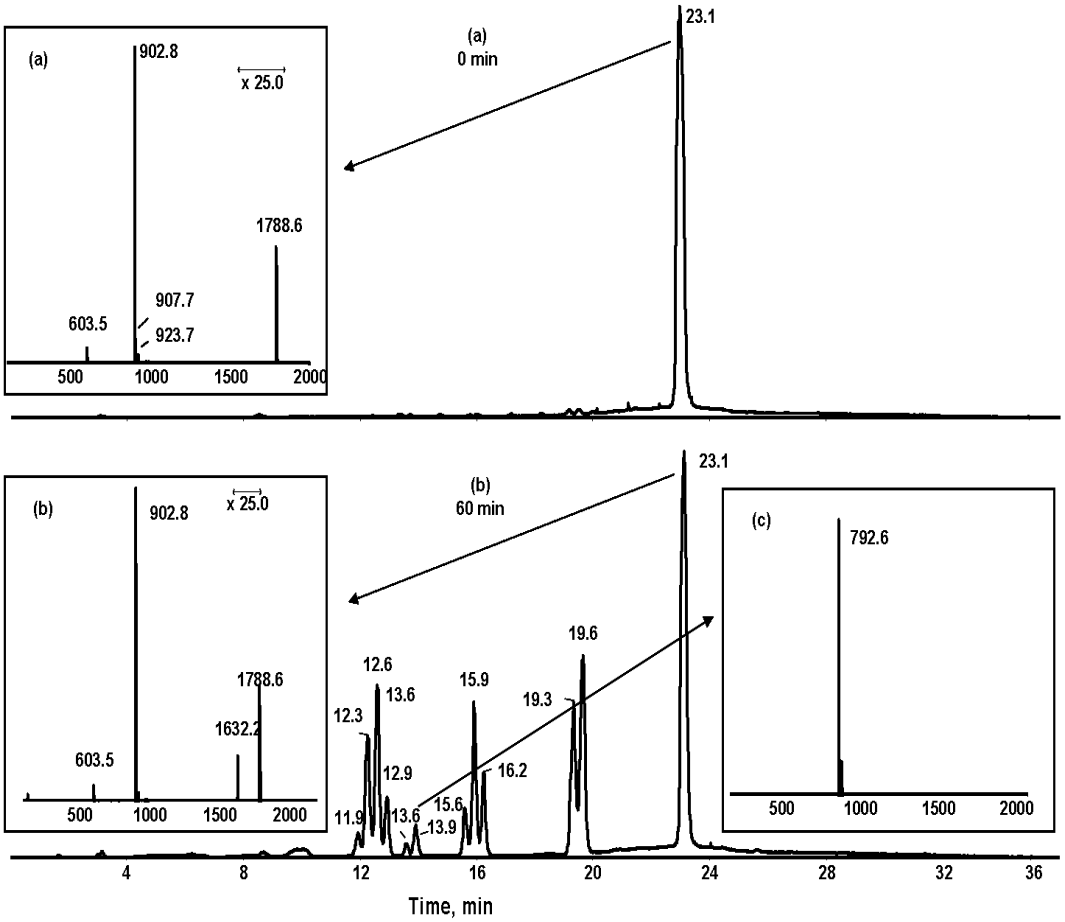

Figure 2-5. LC/ESI(+)-MS TIC chromatograms of (a) the triolein standard and (b) after 60 min of ozonolysis of triolein. Inset (a) is the mass spectrum of the triolein standard. Inset (b) is the mass spectrum after 60 min of ozonolysis of triolein averaged at retention time of 23.1 min. Inset (c) is the mass spectrum after 60 min of ozonlysis of triolein averaged at retention time of 13.6. The mass spectrum averaged at retention time of 13.9 min is the same as that at retention time of 13.6 min.

An ion of *m/z* 950 is the base peak in the mass spectra of compounds eluting at 19.3 and 19.6 min. This ion indicates the formation of mono-ozonide since the exact mass indicates that this ion contains an additional 3 oxygen atoms compared to the $[M+NH_4]^+$ ion of triolein (*m/z* 902). Since each fatty acyl chain

of triolein contains one double bond at the *n*-9 position and ozone can attack the double bond on either *sn*-1,3 or *sn*-2 fatty acyl chain, there can be two constitutional mono-ozonide isomers that differ in the location of trioxolane group. From a statistical consideration, the probability of forming an *sn*-1 or 3 isomer is twice that of forming *sn*-2 isomer. **Figure 2-5(b)** clearly shows the peak at 19.3 min is smaller, preceding a larger peak at 19.6 min; this indicates that peak at 19.3 min probably contains an *sn*-2 isomer. In order to confirm this and get more structural information, tandem mass spectrometry was performed on the ion at *m/z* 950 eluting at 19.6 and 19.3 min (**Figure 2-6(a1 and a2)**). It can be seen that the relative intensity of the product ion at *m/z* 603 is considerably greater in the former case. The ion at *m/z* 603 is the result of neutral loss of ammonia along with loss of a fatty acyl chain that contains a trioxolane group [($C_{57}H_{104}O_9$ + NH_4) - $C_{18}H_{34}O_5$ - NH_3]$^+$ (cleavage at position *a* or equivalent). An ESI study of the ammonium ion adducts of TAG positional isomers described by Byrdwell [59] demonstrates that the loss of a fatty acyl chain from either the *sn*-1 or the *sn*-3 positions is energetically favoured over the loss from the *sn*-2 position. Thus, it is expected that loss the fatty acyl chain containing the trioxolane group would be more facile at the *sn*-1 or 3 positions compared to that at the *sn*-2 position. Hence, the higher intensity of the fragment ion at *m/z* 603 of the compound eluting at 19.6 min compared to that eluting at 19.3 min suggests that the former has the trioxolane group at *sn*-1 or 3 positions whereas the latter is substituted at *sn*-2. This interpretation is also consistent with the above discussion concerning the abundance of these isomers.

Other product ions at *m/z* 493, 509 and 465 are also observed (**Figure2-6(a1 and a2)**). The loss of a fatty acyl chain and the cleavage of trioxolane group along with neutral loss of ammonia lead to the formation of ion at *m/z* 493 $[(C_{57}H_{104}O_9 + NH_4) - C_{18}H_{34}O_2 - C_9H_{18}O_2 - NH_3]^+$. This is shown as cleavage at position *b* and *c* in the inset of **Figure 2-6(a1)** for the illustrative example of an *sn*-1 mono-ozonide with loss of the *sn*-3 fatty acyl chain. Similarly, the fragment ion at *m/z* 509 $[(C_{57}H_{104}O_9 + NH_4) - C_{18}H_{34}O_2 - C_9H_{18}O - NH_3]^+$ results from cleavage at positions equivalent to *b* and *d*. Previously it has been proposed that fragmentation at the trioxolane group can cause the cleavage of the hydrocarbon chain adjacent to the trioxolane group [30]. For example, cleavage of the bond between *n*-8 and *n*-9 positions, which results in the formation of a product ion at *m/z* 465 $[(C_{57}H_{104}O_9 + NH_4) - C_{18}H_{34}O_2 - C_{10}H_{19}O_3 - NH_3]^+$ (cleavage at position *b* and *e* or equivalent).

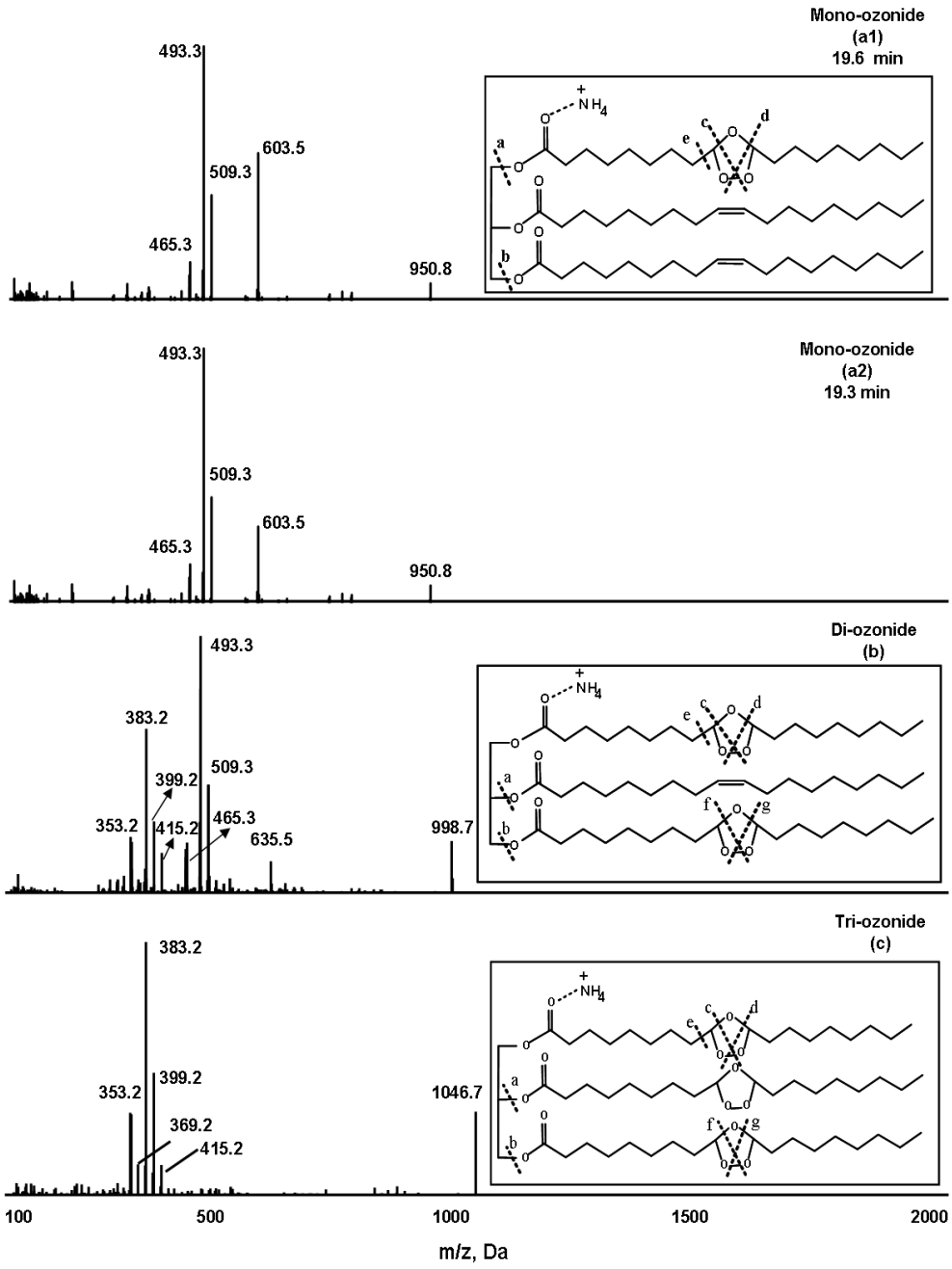

Figure 2-6. The MS/MS spectra of (a1) the mono-ozonide eluting at 19.6 min, (a2) the mono-ozonide eluting at 19.3 min, (b) the di-ozonides and (c) the tri-ozonides. The insets are examples of the proposed structures with letters indicating fragment positions. The structures given are examples of the possible isomeric structures and are not meant to imply unique structural assignments.

The peaks in the chromatogram at retention time of 15.6, 15.9 and 16.2 min (**Figure 2-5(b)**) were found to have the same $[M+NH_4]^+$ ion at *m/z* 998 as the base peak in each case. This indicates the formation of at least 3 isomeric forms of the di-ozonide. Since the di-ozonide has an additional oxygen-containing functional group with 3 more oxygens compared to the mono-ozonide, it has higher polarity and would be expected to elute earlier in NARP chromatography. This is consistent with the peak elution order seen in **Figure 2-5(b)**. The di-ozonide from triolein can exist as *sn*-1, 3 or *sn*-1, 2 positional isomers. In addition, each positional isomer can also have *cis/trans* geometric isomers [60], some of which maybe separated under the chromatographic conditions used here. Theoretically, there can be three *cis/trans* isomers of an *sn*-1, 3 di-ozonide plus three *cis/trans* isomers of an *sn*-1, 2 di-ozonide. However, in the present experiment a total of only three peaks are separated, so assignment of the exact isomeric structure of each peak is not yet possible.

The MS/MS spectrum of the di-ozonide $[M+NH_4]^+$ ion shows the same product ions at *m/z* 493 ($-NH_3$, cleavage at position *b* and *c*), *m/z* 509 ($-NH_3$, cleavage at position *b* and *d*) and *m/z* 465 ($-NH_3$, cleavage at position *b* and *e*) as was seen for the mono-ozonide. In addition, product ions at *m/z* 399 ($-NH_3$, cleavage at *a*, *c* and *g*), *m/z* 383 ($-NH_3$, cleavage at *a*, *c* and *f*) and *m/z* 415 ($-NH_3$, cleavage at *a*, *d* and *g*) (**Figure 2-6(b)**) are also observed. These come from the loss of one fatty acyl chain and the cleavage of both trioxolane groups, which results in aldehyde/aldehyde, aldehyde/carboxylic acid and carboxylic acid/carboxylic acid at the former two *n*-9 positions. The ion at *m/z* 635 is the

product ion from neutral loss of ammonia along with fragmentation at position *d* and *f*. The MS/MS spectra of the $[M+NH_4]^+$ ions (*m/z* 998) of the compounds eluting at 15.6, 15.9 and 16.2 min all contain the same product ions, but with differences in their intensity ratios. This probably arises due to the presence of positional and geometrical isomers but at this point there is no further data available for us to draw any conclusion on which isomers are present.

The mass spectra from the peaks at 11.9, 12.3, 12.6 and 12.9 min all have the ion at *m/z* 1046 as their base peak. Clearly the observation of the $[M+NH_4]^+$ ion at *m/z* 1046 demonstrates tri-ozonide formation. Since all of the double bonds have been ozonized, tri-ozonide can only exist as *cis/trans* geometric isomers, which is also the reason that there are four peaks instead of one peak shown between 11.0 and 13.0 min. **Figure 2-6(c)** is the MS/MS spectrum of a tri-ozonide $[M+NH_4]^+$ ion, which has product ions at *m/z* 399 ($-NH_3$, cleavage at *a*, *c* and *g*), *m/z* 383 ($-NH_3$, cleavage at *a*, *c* and *f*) and *m/z* 415 ($-NH_3$, cleavage at *a*, *d* and *g*) similar to the di-ozonide. Product ions at *m/z* 369 ($-NH_3$, cleavage at *a*, *e* and *g*) and *m/z* 353 ($-NH_3$, cleavage at *a*, *e* and *f*) are also observed. The other isomeric tri-ozonide MS/MS spectra differ only also in the relative intensities of the product ions.

Besides the formation of ozonides, the peaks at 13.6 and 13.9 min in **Figure 2-5(b)** show the presence of ozonolysis intermediates. Thus, the ion at *m/z* 792 is the base peak of the mass spectra of peaks at 13.6 and 13.9 min (**Figure 2-5**, Inset (c)). From the elemental composition (**Table 2-1**) and knowledge of the ozonolysis reaction pathway, this ion is likely the

decomposition product of a mono-ozonide with an aldehyde group at an *n*-9 position. Since this aldehyde can be present on *sn*-2 or *sn*-1 positions, two isomeric peaks are observed. Other intermediate ions such as *m/z* 888 and *m/z* 840 are also observed, which are the decomposition products of di-ozonides and tri-ozonides with an aldehyde group at *n*-9, respectively.

Table 2-1. Retention times, mass accuracy measurement and elemental composition of molecular ions of ozonolysis intermediates and products.

Compounds	Retention Time t_R (min)	Experimental *m/z*	Error (ppm)	Elemental Composition
Triolein	23.1	902.8211	4.4	$[C_{57}H_{104}O_6NH_4]^+$
Mono-ozonide	19.3, 19.6	950.8016	-1.6	$[C_{57}H_{104}O_9NH_4]^+$
Di-ozonide	15.6, 15.9, 16.2	998.7850	-1.6	$[C_{57}H_{104}O_{12}NH_4]^+$
Tri-ozonide	11.9, 12.3, 12.6,	1046.7717	0.4	$[C_{57}H_{104}O_{15}NH_4]^+$
Ozonolysis	13.6, 13.9	792.6704	-1.0	$[C_{48}H_{86}O_7NH_4]^+$
Intermediates	9.9, 10.0	840.6541	-2.1	$[C_{48}H_{86}O_{10}NH_4]^+$
	4.9, 6.3	888.6378	-3.3	$[C_{48}H_{86}O_{13}NH_4]^+$
	15.6, 15.9, 16.2	1776.2390	-3.8	$[C_{96}H_{172}O_{27}NH_4]^+$
	18.2, 18.4, 18.7	1728.2534	-4.5	$[C_{96}H_{172}O_{24}NH_4]^+$
Dimers	20.9	1680.2731	-1.9	$[C_{96}H_{172}O_{21}NH_4]^+$
	23.1	1632.2839	-4.7	$[C_{96}H_{172}O_{18}NH_4]^+$
	25.6	1584.3033	-2.2	$[C_{96}H_{172}O_{15}NH_4]^+$

In addition to the intermediates and products listed in **Table 2-1**, high molecular weight products were also formed. **Figure 2-7** shows the XIC over the range of *m/z* 1,000 to 2,000 from the reaction of triolein with ozone for 60, 105 and 120 min. At 60 min of ozonolysis, an ion at *m/z* 1776 appears with low intensity in the mass spectrum compared to the base peak at *m/z* 998, a di-ozonide

(**Figure 2-7**, Inset (a)). However, after 120 min of ozonolysis, peaks at similar retention times have mass spectra in which the ion at *m/z* 998 is absent whereas the ion at *m/z* 1776 is the base peak (**Figure 2-7**, Inset (b)). Hence, longer reaction times are resulting in the formation of higher amounts of high molecular weight products. The structure of ion at *m/z* 1776 is proposed in Inset (c) of **Figure 2-7**, which might be formed by the cyclo-additon of the ozonolysis intermediate having an aldehyde group at *n*-9 (*m/z* 888) with the corresponding Criegee intermediate. It should be noted that the ozonolysis intermediate with $[M+NH_4]^+$ ion at *m/z* 888 was also observed (**Table 2-1**). Although the dimer $[M+NH_4]^+$ ion at *m/z* 1776 has the same retention time as the di-ozonide $[M+NH_4]^+$ ion at *m/z* 998, it can be seen from **Figure 2-7** that the abundance of former ion is a function of ozonolysis time and is therefore unambiguously a reaction product and not formed in the ion source.

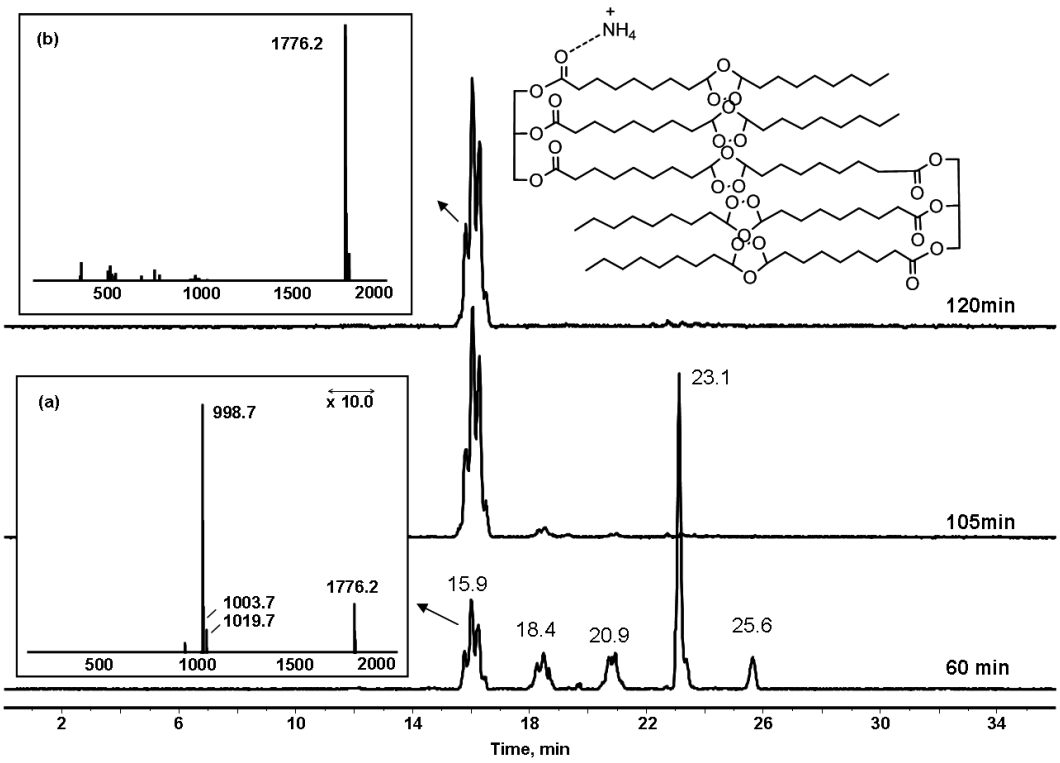

Figure 2-7. Extracted ion chromatograms of *m/z* 1,000-2,000 from LC/ESI(+)-MS runs of samples taken after the ozonolysis of triolein for 60, 105 and 120 min. The insets (a) and (b) are mass spectra averaged over retention times of 15.0-17.0 min for 60 and 120 min ozonolysis period samples, respectively. The inset (c) is the proposed structure of the dimer ion at *m/z* 1776.

The mass spectrum of the triolein standard (**Figure 2-5**, Inset (a)) and the mass spectra of peak at the same retention time (t_R 23.1 min) (**Figure 2-5**, Inset (b)) are very similar, except that ion at *m/z* 1632 is only observed after ozonolysis. Also, another three distinct groups of peaks are present at t_R 18.4 (*m/z* 1728), 20.9 (*m/z* 1680) and 25.6 min (*m/z* 1584) when the reaction time was 60 min (**Figure 2-7**). These four groups of peaks differ in molecular weight by 48 Da, ie. 3 oxygens (**Table 2-1**). This is because these high molecular weight products are formed by reactions between two ozonided triolein molecules. This occurs

through the linkage between an aldehyde group from one ozonided triolein molecule and a Criegee intermediate group from another ozonided triolein molecule. The ions at *m/z* 1728, 1680, 1632 and 1584 (t_R 18.4, 20.9, 23.1 and 25.6 min) have one, two, three, and four less trioxolane group(s) respectively, compared to the ion at *m/z* 1776. The elution order of these oxygen containing dimer products is consistent with their polarity so that the compounds containing more oxygen atoms are more polar and have shorter retention times. Also, by comparing the XIC of the range *m/z* 1000-2000 for the triolein ozonolysis products after 60, 105 and 120 min, it is clear that all of these dimers eventually convert to the compound of ion at *m/z* 1776, which is fully ozonided with no remaining double bonds. It is the first time that these dimers formed during ozonolysis of triolein are separated and observed under NARPLC/ESI- MS.

Based on the above study of the ozonolysis of methyl oelate and triolein, we can see that a variety of products are formed by ozonolysis of unsaturated lipids. These fall into three general categories: small volatile compounds such as aldehydes and acids; secondary ozonides including trioxolanes; and high molecular weight product dimers formed by reaction between ozonolysis intermediates.

2.4. Conclusions

LC-MS/MS has been used to observe ozonolysis intermediates and products of the model lipids methyl oleate and triolein. Secondary ozonide 1,2,4-trioxolanes from both methyl oleate and triolein can be observed as $[M+NH_4]^+$

ions under positive ESI when using post-column addition of ammonia acetate. Dimeric ozonolysis products from triolein were detected and separated by LC-MS. Accurate mass measurement and MS/MS provide information on the structure of secondary ozonides. LC-MS/MS gives a clear picture of the ozonolysis pathway for model lipids, providing the basis for understanding the ozonolysis of more complicated lipid mixtures such as vegetable oils. Future work will focus on applying this LC-MS/MS method to monitor the ozonolysis of plant oils, which will be useful in the synthesis of bio-based chemicals and polymers.

CHAPTER 3

The Direct Determination of Double Bond Positions in Lipid Mixtures by Liquid Chromatography/ In-line Ozonolysis- Mass Spectrometry [3]

3.1. Introduction

Lipids are a diverse class of molecules whose biological importance includes their function as energy reservoirs, as components of cell membranes and as signaling molecules [1]. The location and number of double bonds in fatty acids (FAs) regulate membrane fluidity and are critical to lipid metabolism and proper biological function [1,61].

Mass spectrometry (MS) has been used for lipid analysis almost since its invention and recent developments have allowed MS to become a powerful tool in many aspects of lipid elucidation, such as the new methods used in lipidomics [62-64]. However, the identification of double bond positions by conventional MS and tandem mass spectrometry (MS/MS) alone still remains a challenge. This is true for fragment ions arising from the widely used low-energy collision-induced dissociation (CID) processes that are not usually indicative of double bond positions [38]. Many strategies have been used to overcome this limitation of MS, as described in a recent review by Mitchell *et al*. on double bond

[3] A version of this chapter has been published. Sun, C., Zhao, Y. and Curtis, J.M. *Anal. Chim. Acta* 2013, *762*, 68-75.
Reprinted with permission.

localization methods [15]. An early approach used to elucidate double bond positions in underivatized FAs was to use MS/MS spectra to study charge-remote fragmentation (CRF). For example, high-energy CID of $[M-H]^-$ ions [21] and low-energy CID of di-lithium adduct ions $[M-H+2Li]^+$ of FAs and triacylglycerols [23,65] could give fragment ions that are characteristic of double bond positions. However, interpretation of these mass spectra was complicated due to the extensive fragmentation seen, especially for polyunsaturated FA (PUFA). Picolinyl ester and 4,4-dimethyloxazoline derivatives of FAs have also been used to insert a functional group that can localize charge and hence enhance remote-site fragmentation under electron ionization (EI) [16,17]. Recently, Yang *et al.* demonstrated the identification of FA isomers using conventional electrospray ionization (ESI)-MS/MS. The assignment of the first double bond from the methyl group end was based on the intensity distribution of fragment ions (loss of CO_2 or H_2O) from FA $[M-H]^-$ ions at different collision energies [66]. The localization of other remaining double bonds relied on the assumption that double bonds in PUFA are usually interrupted by a methylene group during biosynthesis. Clearly this method is not suitable for the determination of double bond positions in other FAs such as conjugated FAs or hydroxyl FAs, as stated by the author.

Another approach is to use chemical derivatization to "label" double bonds prior to MS/MS analysis. For example, double bonds on fatty acyl chains were converted into di-hydroxy derivatives by off-line reactions with OsO_4; ESI-MS/MS spectra of these derivatives can reveal the double bond positions [26].

MS/MS analyses of acetonitrile adducts of fatty acid methyl esters (FAME) formed during chemical ionization (CI) has also been used to characterize double bond positions [18-20]. Ozone has been used to react with double bonds either off-line or *in-situ*, producing fragment products of predictable mass, which can be used to identify double bond locations. For instance, in the work of Harrison *et al.*, CID of the ozonolysis products of unsaturated lipids formed off-line gave rise to fragment ions indicative of double bond positions [30]. Furthermore, *in-situ* ozonolysis was achieved by Thomas *et al.* by introducing ozone into the ESI source (OzESI-MS), so that ozonolysis occurred in the ionization source rather than off-line [38]. However, OzESI-MS is not directly applicable to complicated lipid samples. The same research group also developed the ozone-induced dissociation (OzID-MS) method by introducing ozone vapor into an ion trap mass spectrometer [39]. Each lipid component of interest was isolated in the ion trap before ozonolysis, providing the possibility for the analysis of more complex lipid mixtures. The OzID-MS method was also applied on a tandem linear ion-trap mass spectrometer, which provided spatial separation between the mass-selection of lipid ions, ozonolysis of these ions in the collision cell and mass analysis of ozonolysis products [40]. This arrangement allows for high speed analyses at high sensitivity, potentially compatible with on-line LC-MS analyses. However, specific mass spectrometers and instrumental modifications are needed for the OzID-MS method. In another report, the low temperature plasma (LTP) probe was used for *in-situ* ozonolysis under ambient temperature conditions [58]. In this work, FAs or fatty acid esters reacted with ozone generated by the LTP,

resulting in aldehydes retaining the carboxylic acid group (for FAs) or ester group (for fatty acid esters) which can be used to assign the double bond positions. Even though this method needs no instrumental modifications, the applicability to complex lipid samples is likely not as good as that from OzID-MS methods and the LTP is required.

The time-dependent oxidation of lipids at a catalytic nanostructured surface was described by Pávlasková *et al*.[67]. Using laser desorption ionization techniques, they observed aldehyde ions as oxidative cleavage products, as well as intact lipid molecular ions, after exposure to ambient air for 100 min. Time-dependent ambient ozonolysis has also been observed for unsaturated lipids deposited onto a silica thin layer chromatography (TLC) plate [68]. Desorption electrospray ionization (DESI)-MS was used to scan the plate in order to obtain mass spectra of ozonolysis products. An advantage of these ambient ozonolysis experiments is that an ozone generator is not required, making them accessible to many laboratories. However, TLC can only provide a limited degree of separation for complex lipid mixtures, ambient ozonolysis conditions will likely fluctuate and long exposure time is also needed prior to MS analysis.

In summary, the previous research has shown great promise, and some practical examples of using ozonolysis product ions for double bond localization. The OzID-MS method especially has the potential to allow double bond position determination even in lipid mixtures. Here we present a simple new approach to the direct determination of double bond positions by coupling ozonolysis reactions in-line with mass spectrometry (in-line O_3-MS) without the need for

instrumental modification. The in-line ozonolysis device used is a length of Teflon AF-2400 tubing, a highly microporous tubing with a high gas permeability [69]. The semi-permeable character of this tubing allows certain gases (including ozone), but not liquids, to cross from one side to the other [70]. Using this device we investigate the possibility of definitively assigning double bond positions in unsaturated FAME by O_3-MS under positive ion atmospheric pressure photoionization (APPI+). A key advantage of the proposed in-line ozonolysis reactor was expected to be the ability to directly couple HPLC separations to O_3-MS (LC/O_3-MS), giving rise to an additional dimension of information for the analysis of complex lipid extracts. In order to test this hypothesis, a sample of bovine fat known to contain a range of positional and *cis/trans* isomers of unsaturated FAME was analyzed by combined silver ion liquid chromatography / ozonolysis - mass spectrometry (Ag^+-LC/O_3-MS).

3.2. Experimental

3.2.1. Material

Analytical grade hexanes (HEX), acetonitrile (ACN), isopropanol (IPA) were purchased from Fisher Scientific Company (Ottawa, ON, Canada). All the fatty acid methyl ester (FAME) standards were purchased from Nu-Chek Prep Inc. (Elysian, MN, USA). A solution of porcine renin substrate tetetradecapeptide at 10 pmol/µl in acetonitrile/water (1:1, v/v) from a chemical standards kit (Applied Biosystems, Forster City, CA, USA) was used for the tuning and calibration of mass spectrometer. The Teflon AF-2400 tubing (0.020" OD,

0.010" ID) was purchased from Biogeneral Inc. (San Diego, CA, USA). NanoTight tubing sleeves (1/16" OD, 0.021" ID) and tubing nuts were purchased from IDEX Health & Science LLC (Oak Harbor, WA, USA). The total lipid of bovine adipose tissue was extracted into chloroform/methanol (2:1, v/v). The total lipid extract was dissolved in 1 mL of hexane and converted to FAME using 50 μL KOH (2M) in methanol at overnight room temperature [71,72]. FAME standard solutions were prepared in HEX/IPA (98:2, v/v) at a concentration of 200 mg/L.

3.2.2. In-line ozonolysis reaction apparatus

Ozone was generated by passing dry oxygen as the feed gas through a Nano ozone generator (Absolute Systems Inc., Edmonton, AB, Canada). The ozone concentration was measured by an ozone monitor (Model 454, Teledyne Technologies Inc., San Diego, CA, USA). The in-line ozonolysis reaction apparatus was composed of a 0.5 L Omnifit solvent bottle, a 3-valve bottle cap (Diba Industries Inc, Danbury, CT, USA) and the Teflon AF-2400 tubing. The solvent bottle was filled up with ozone and oxygen vapor by flushing the bottle under flow rate of 2.5 liter per minute (LPM) for 15s. Teflon AF-2400 tubing was inserted into the bottle through the cap valve and was surrounded by ozone. One end of the Teflon tubing was directly connected to the mass spectrometer APPI ion source; the other end was connected to the HPLC.

3.2.3. In-line O_3-MS analysis of FAME standards

An Agilent 1200 series HPLC system (Agilent Technologies Inc, Palo Alto, CA, USA) coupled to a hybrid quadrupole time - of - flight mass spectrometer (QSTAR Elite, Applied Biosystems/MDS Sciex, Concord, ON, Canada) was used to conduct the in-line O_3-MS analysis. 3 μL of the FAME working solution was delivered through the Teflon tubing by the LC pump with HEX/IPA (98:2, v/v) as the mobile phase at the flow rate of 0.2 mL/min. The FAME was oxidized by ozone gas that penetrated through the porous Teflon tubing, and the ozonoysis products were analyzed in real time by APPI/MS in the positive ion mode. NanoTight tubing sleeves and nuts were used to ensure leak-tight connections.

The mass spectrometer was tuned by infusing porcine renin substrate tetetradecapeptide (*m/z* 879.9723, doubly charged ion; *m/z* 110.0713, fragment ion) at a resolution of above 10000 full width at half maximum (FWHM) using ESI in positive ion mode. This solution was also used for calibration of mass range *m/z* 100-1,300. The APPI ion source temperature was kept at 375°C. The source region gas flows in arbitrary units assigned by the data system were as follows: curtain gas 25; auxiliary gas 10; nebulizing gas 50. In all cases, high purity nitrogen was the gas used. The ionspray voltage, declustering potential (DP), focus potential (FP), and DP2 were 1300 V, 35 V, 150 V and 10 V, respectively. Analyst QS 2.0 software was employed for data acquisition and analysis.

3.2.4. Ag^+-LC/O_3-MS analysis of a bovine fat sample

A ChromSpher 5 Lipids column of length 250mm, internal diameter 2mm and containing 5μm particles (Varian, Lake Forest, CA, USA) was the silver ion column used for the analysis. The sample injection amount was 3 μL and the flow rate was 0.2 mL/min. Mobile phase A consisted of IPA: ACN (100:0.1, v/v) and B of HEX: ACN (100:0.1, v/v). The gradient was as follows: 0-0.1 min, 99% B; 0.1–7 min, 99% B; 7–10min, 90% B; 10–13 min, 90% B. Addition of 0.1% ACN to each solvent helped to reduce equilibration time for the silver ion column whilst achieving adequate separation between FAME components with differing degrees of unsaturation. The end of the column was connected to the 10cm Teflon tubing by NanoTight tubing sleeves and nuts. Each FAME component eluting from the column was subjected to ozonolysis by passing through the in-line reaction apparatus before reaching the APPI ion source. MS conditions were as above.

3.3. Results and Discussion

3.3.1. Development of the in-line O_3-MS method

It has been shown that chemical reactions in solution can be monitored in real-time by means of various designs of microreactors connected in-line with atmospheric pressure ionization (API) MS. For reactions involving liquid reactants, a commercially available mixing tee can be easily connected to the ionization source via conventional LC tubing or a fused silica transfer capillary [73]. However, a mixing tee is not suitable for gas-liquid reactions because of the

poor mixing efficiency. In this research, this problem was overcome by using semi-permeable narrow-bore, thin-walled (0.020" OD, 0.010" ID) Teflon AF-2400 tubing as the in-line ozonolysis device. Ozone gas can pass freely through the wall of the tubing and react with the lipid solution that flows inside of the tubing. Furthermore, this Teflon AF-2400 tubing is directly suitable for in-line analysis because efficient ozonolysis of double bonds can occur in the tubing under common LC flow rates (0.2 mL/min was used here) due to the tubing's high surface-to-volume ratio. Thus, the semi-permeable character of the tubing and its compatibility with available LC fittings, makes in-line ozonolysis prior to the ion source possible without the need for modification to mass spectrometer [38-40]. Please see **Scheme 3-1** for LC/O_3-MS configuration.

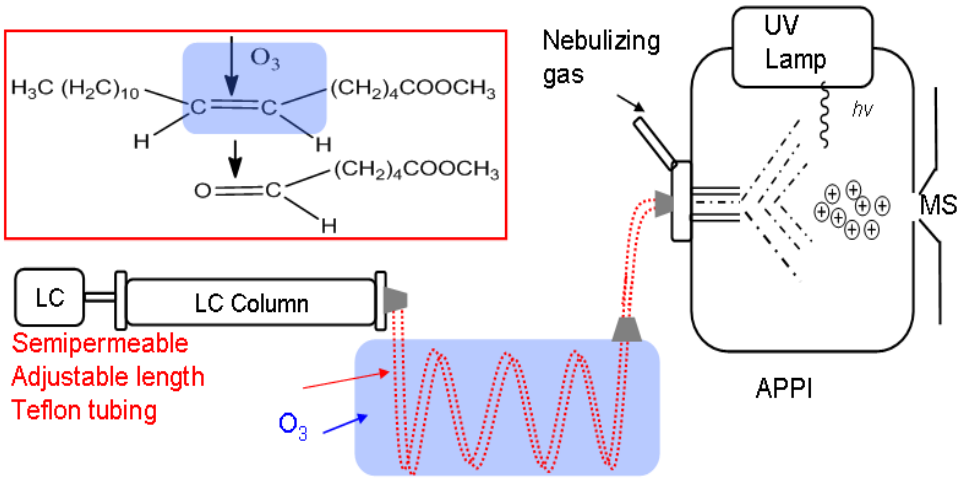

Scheme 3-1. The configuration of LC/O_3-MS with APPI as ionization source.

In this research, the parameters used to control the extent of the ozonolysis reaction are the tubing length (L) and the ozone concentration. **Figure 3-1** shows a set of experiments in which 2 µL of a solution of methyl petroselinate standard

(6c-18:1 FAME) was passed through the Teflon tubing with a variable length exposed to the ozone. In all cases, the bottle was filled with ozone from an ozone generator at a measured concentration of 35.6 g/m^3 and used immediately (the half life of ozone at 20 °C is 3 days [74]). Without in-line ozonolysis (L= 0cm), 6c-18:1 FAME appears in the APPI (+) mass spectrum as the protonated molecular ion $[M+H]^+$ at *m/z* 297 along with fragment ions at *m/z* 265 and 247 that correspond to the neutral loss of CH_3OH and the further loss of H_2O (**Figure 3-1(a)**). As L increases from 0cm to 40cm, the intensity of the $[M+H]^+$ ion at *m/z* 297 decreases whilst the intensity of ions at *m/z* 145 and 113, which are not present in the L=0cm case, increase (**Figure 3-1**). This is clear evidence that the ozonolysis reaction occurs inside of the Teflon tubing. Furthermore, increasing L can be seen to promote the reaction since the lipid has a longer contact time with ozone in the in-line reaction apparatus. The ions at *m/z* 145 and 113 are actually the ozonolysis product ions and indicate the double bond position at *n*-12, as explained in detail in Section 3.3.2. A similar series of experiments were also performed at constant L but using ozone concentrations of 35.6, 40.1, 46.5 and 52.1 g/m^3. As expected, a higher ozone concentration is found to promote the ozonolysis reaction inside of the semi-permeable tubing under the same L.

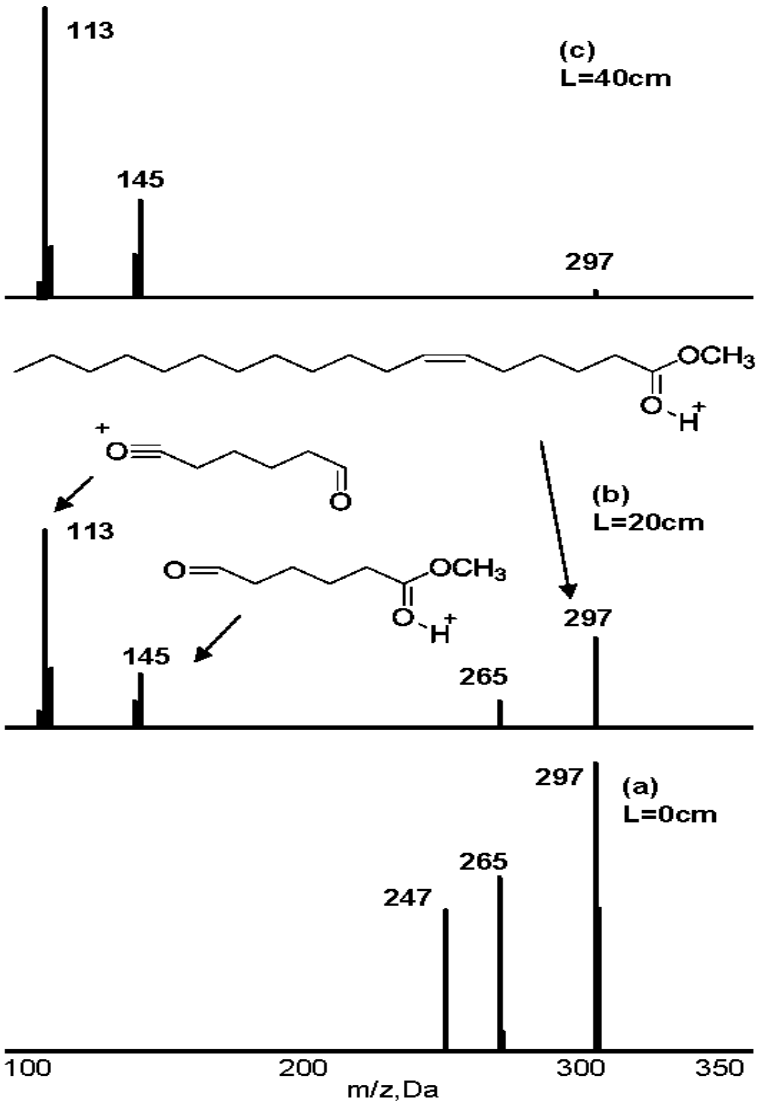

Figure 3-1. In-line O_3-APPI(+)/MS spectrum of 6c-18:1 FAME using tubing length L of (a)0cm, (b)20cm and (c)40cm.

It should be noted that the tubing length L within the glass bottle containing ozone vapor can be easily adjusted. Hence, the in-line ozonolysis reaction apparatus is readily adaptable for lipids at different concentrations even using the same ozone concentration. In general, it is more convenient to alter the tubing length than the ozone concentration. For FAME analysis, it is desirable

that both the intact FAME molecular ion and the ozonolysis product ions can be observed in the same mass spectrum, so that both the number and position of double bonds could be obtained in one flow injection analysis (FIA). From **Figure 3-1** it can be seen that that at the ozone concentration used (35.6 g/m^3 on loading), the ions at *m/z* 297, 145 and 113 can all be observed with good abundance when L is 20cm (tubing internal volume of $1.0x10^{-8}$ m^3). Thus, this reaction condition was selected as the optimum for use in this work.

3.3.2. In-line O_3-MS analysis of monounsaturated FAME

In this experiment, unsaturated FAME react with ozone that penetrates through the Teflon AF-2400 tubing giving rise to products that are analyzed in real time by APPI/MS. **Scheme 3-2** shows the ozonolysis reaction pathway in the case of methyl petroselinate (6c-18:1 FAME). First, ozone specifically reacts with the carbon-carbon double bond forming 1,2,3-trioxolane as the primary ozonide. This primary ozonide readily decomposes into aldehydes and the corresponding Criegee intermediates shown in Pathway 1 and 2. These aldehydes and Criegee intermediates can further react with each other to form secondary ozonides, which can also decompose back to aldehydes and the corresponding Criegee intermediates [37].

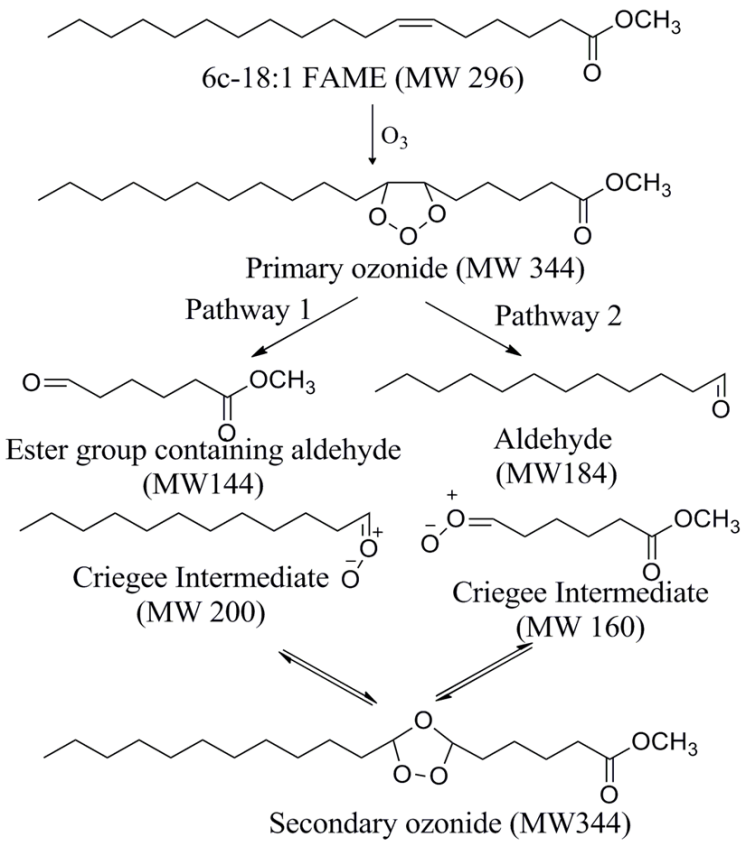

Scheme 3-2. Ozonolysis pathway of methyl petroselinate (6c-18:1). Each compound is labeled with its molecular weight.

The APPI mass spectrum of methyl petroselinate is shown in **Figure 3-1**. Following ozonolysis, reaction products at *m/z* 145 and 113 appear along with a large decrease in the intensity of the $[M+H]^+$ ion at *m/z* 297. The elemental composition of the ion measured at *m/z* 145.0857 is $C_7H_{13}O_3$ (Δ=-1.4 ppm) which is consistent with the protonated ion of an aldehyde that retains the methyl ester group (see inset in **Figure 3-1(b)**). This ion is consistent with analogous ions seen by Zhang *et al.* following oxidative cleavage of the unsaturated FAME under positive LTP ionization [58]. Since the ion at *m/z* 145 contains the ester group and the fatty acid chain up to the point of carbon-carbon double bond cleavage

(which becomes an aldehyde), it is the unique marker of a double bond at *n*-12. The ion at *m/z* 113 results from the neutral loss of CH_3OH from the ion at *m/z* 145. However, we did not observe the ion formation of Criegee intermediates (MW160 and 200) and the aldehyde without ester group (MW184 in **Scheme 3-2**). This may be due to the low stability of the ions of these compounds, or be because Pathway 1 is the major decomposition route of the primary ozonide.

There are no ions present at higher *m/z* value than *m/z* 297, either. This is in contrast to other work that has observed ozonides of phospholipids and triacylglycerols as sodium adduct ions under DESI(+) [68] and ESI(+) [40]. We have shown in a previous report that secondary ozonides of FAME can also be observed as sodium and ammonium ion adducts but only under ESI (+); these undergo in-source fragmentation under APPI (+) and APCI (+). FAME molecular species are not observed, or are extremely weak, using ESI(+) [75]. In contrast, both the intact FAME and the ozonolysis aldehyde products can be observed using either APCI(+) or APPI(+). Thus, in the present study, APPI(+) was chosen for in-line O_3-MS analysis. Not only did this result in significantly better sensitivity and signal stability compared to APCI(+) but additionally both FAME $[M+H]^+$ ions and the diagnostic aldehyde ions are present in the mass spectra.

In order to further prove that the aldehyde ions seen in the APPI mass spectra of the ozonolysis products can be used for double bond localization, the positional isomers methyl oleate (9c-18:1 FAME) and methyl *cis*-vaccenate (11c-18:1 FAME) have also been analyzed by in-line O_3-MS (**Figure 3-2**). In each

case the common molecular ion $[M+H]^+$ at *m/z* 297 is seen in the mass spectrum whereas the ozonolysis product ions in the lower *m/z* range are very different from each other. Using in-line ozonolysis with methyl oleate (**Figure 3-2(a)**), ions at *m/z* 187 and 155 (methanol loss from *m/z* 187) are the main ozonolysis cleavage products observed. These ions are characteristic of a double bond located at *n*-9. For methyl *cis*-vaccenate (**Figure 3-2(b)**), ions at *m/z* 215 and 183 indicate a double bond at the *n*-7 position. It is clear that the mass differences (Δm) between intact unsaturated FAME molecular ions and the corresponding aldehyde ions resulting from in-line O_3-MS are different for each isomer and can be used to unambiguously identify double bond positions. If "*n*"is the position of the double bond in the FAME counting from the methyl terminus and the nominal masses of an oxygen atom and methylene group are 16 and 14 respectively, the following equation can be used to determine n and hence the double bond location in the FAME:

$$n = (\Delta m+16)/14$$

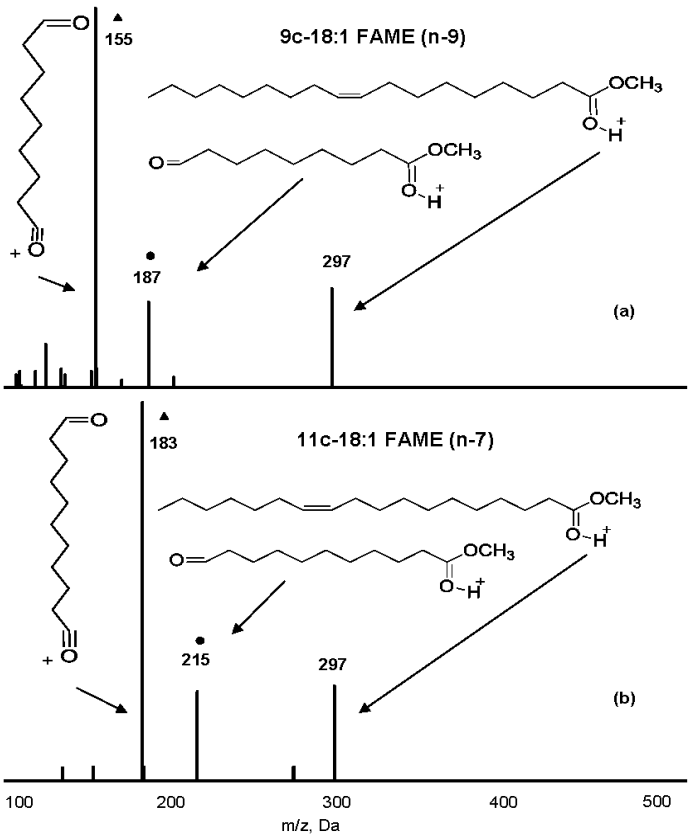

Figure 3-2. In-line O_3-APPI(+)/MS spectrum of 9c-18:1(a) and 11c-18:1(b) FAME. Ozonolysis cleavage aldehyde ions are labeled with ●, and methanol loss ions are labeled with ▲.

3.3.3. Application of the in-line O_3 -MS method for the analysis of polyunsaturated FAME

Since in-line O_3-MS proved effective in the case of monounsaturated FAME, we expanded the use of this method to polyunsaturated FAME. **Figure 3-3** is the in-line ozonolysis mass spectra of methyl linolenate (6c,12c,15c-18:3 FAME) and eicosapentaenoic acid (EPA) methyl ester (5c,8c,11c,14c,17c-20:5 FAME). Compared to **Figure 3-2**, more ions appear in the lower *m/z* range as a result of the oxidative cleavage of each double bond by ozone. In **Figure 3-3(a)**,

the ions at *m/z* 267, 227 and 187 are aldehydes containing the methyl ester group formed due to ozonolysis cleavage of double bonds at *n*-3, -6 and -9. As seen for monounsaturates, these aldehyde ions also lose methanol, giving rise to fragment ions at *m/z* 235, 195, 155. For EPA methyl ester, a highly unsaturated FAME, we still observe the aldehyde ions at *m/z* 291, 251, 211, 171 and 131, resulting from oxidative cleavage of each double bond (**Figure 3-3(b)**). This allows assignment of the 5 double bond positions at *n*-3, -6, -9, -12 and -15, respectively. However, the mass spectrum becomes a little more complicated due to losses of H_2O and CH_3OH from these aldehyde ions. For example, ion at *m/z* 273 comes from the dehydration of ion at *m/z* 291, and ion at *m/z* 241 is from further loss of CH_3OH (291-18-32). The same pattern of fragmentation is also seen for the aldehyde ions at *m/z* 251 and 211. Note that the equation $n = (\Delta m+16)/14$ only applies to the determination of the double bond closest to the methyl group terminus, because of the complication of having both methylene and methane groups along the chain. For both methyl linolenate and EPA methyl ester, the mass difference between the intact molecular ions and ester group containing aldehyde ions from oxidative cleavage at *n*-3 double bond is 26 Da. This specific mass loss after ozonolysis can only occur to *n*-3 FAME. Hence, the in-line O_3-MS method can be used for the identification of *n*-3 PUFA that have been shown to have benefit for heart health and are critical for brain function [76].

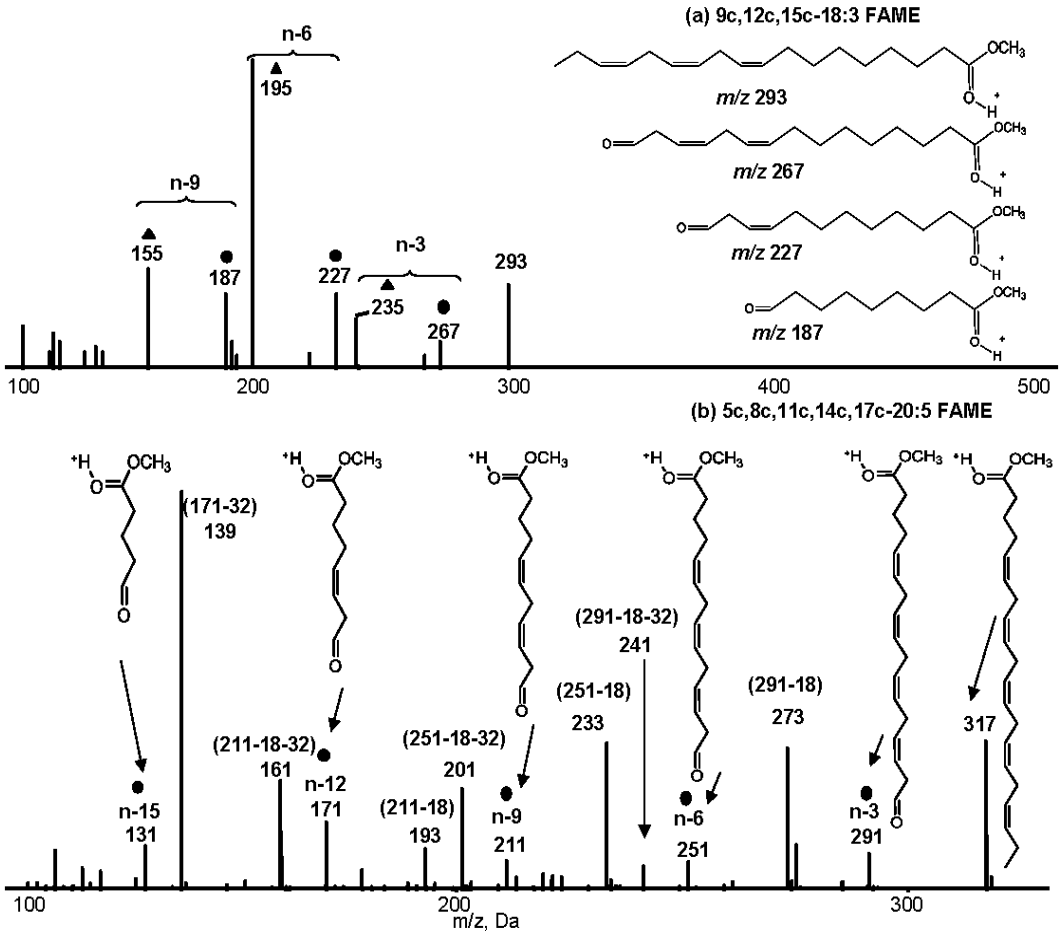

Figure 3-3. In-line O_3-APPI(+)/MS spectrum of 9c,12c,15c-18:3(a) and 5c,8c,11c,14c,17c-20:4 (b) FAME. Ozonolysis cleavage aldehyde ions are labeled with ●, the ions from the loss of methanol are labeled with ▲.

Thus, using the in-line O_3-MS method, in a single FIA the number of double bonds can be determined from the exact mass measurement of FAME molecular ions and the positions of double bonds can be identified from the measured *m/z* values of the aldehyde products arising from ozonolysis at each double bond.

3.3.4 Application of the LC/O_3-MS method for the analysis of a bovine fat sample

The above discussion has demonstrated how in-line O_3-MS analysis of FAME can readily be used to identify double bond positions, when individual FAME is analyzed. Here, as an example of the potential use of LC/O_3-MS for direct double bond determination in lipid mixtures, we have investigated the use of Ag^+-LC for the analysis of a bovine fat sample. Currently, most complex FAME mixtures are analyzed by high resolution GC methods, although an important advantage of Ag^+-LC over GC methods is that *cis/trans* unsaturated FAME as well FAME with different number of double bonds can be easily separated [77]. However, a drawback is that most FAME positional isomers can only be partially separated [78]. As described below, this limitation can be overcome by the use of the extra dimension of information available by coupling LC to the O_3-MS method.

The retention in Ag^+-LC is affected by the interaction strength between the Ag^+ ions and double bonds. The general pattern seen in the Ag^+-LC separation of FAME is that saturated FAME elute first followed by groups of FAME of increasing degree of unsaturation with increasing retention times (t_R). Within each group, *trans* isomers elute ahead of *cis* isomers due to the weaker interaction with Ag^+ ions [77]. **Figure 3-4(a)** shows the total ion current (TIC) trace for an Ag^+-LC/O_3-MS analysis of a bovine fat sample. There are five major peaks at t_R of 3.78, 3.99, 4.50, 6.26 and 12.66 min. The O_3-MS spectrum of peak at 3.78 min (**Figure 3-4(b)**) shows no ions in the lower *m/z* range, indicating the lack of double bonds. The ions at *m/z* 271 and 299 are identified as methyl

palmitate (16:0 FAME) and methyl sterate (18:0 FAME), which are consistent with the exact mass measurements (**Table 3-1**). In **Figure 3-4(c)**, the O_3-MS spectrum of peak at 3.99 min, ions at *m/z* 169 and 201, 183 and 215, 211 and 243 appear along with the ion at *m/z* 297 which is the $[M+H]^+$ ion of 18:1 FAME. Using the equation $n = (\Delta m + 16)/14$ for double bond location in monounsaturated FAME, ions at *m/z* 201, 215 and 243 are the characteristic aldehyde ions formed by ozonolysis cleavage of double bonds at *n*-8, *n*-7 and *n*-5; ions at *m/z* 169, 183 and 211 result from the loss of CH_3OH from each aldehyde species. It can be seen in **Figure 3-4(a)** that the small 18:1 FAME peak at 3.99 min elutes ahead of the major peak centered at 4.50 min, which is also identified (**Figure 3-4(d)** and **Table 3-1**) as 18:1 FAME. Since *trans* isomers elute ahead of *cis* isomers in Ag^+-LC, the three positional isomers of 18:1 FAME (*n*-8, *n*-7 and *n*-5) eluting at 3.99 min must have the *trans* configuration. The mass spectra of the peak at 4.50 min assigned to *cis* monounsaturated FAME have been averaged over two t_R windows. **Figure 3-4(d)** is the mass spectrum averaged between 4.20 and 4.40 min, where ions m/z at 187 and 155 indicate a double bond at the *n*-9 position. In addition, the *n*-7 (*m/z* 215 and 183) and *n*-5 (*m/z* 243 and 211) isomers of 18:1 FAME are present. The mass spectrum averaged between 4.40 and 4.70 min (**Figure 3-4(e)**) is different, showing an additional 16:1 FAME molecular ion at *m/z* 269 and the ozonolysis product ions at *m/z* 187 and 155 indicating a double bond at *n*-7. All of these positional isomers of 18:1 FAME (*n*-9, *n*-7 and *n*-5) and 16:1(*n*-7) FAME seen in the peak centered at 4.50 min are in the *cis* form. **Figure 3-4(f)** shows the O_3-MS spectrum of peak at 6.26 min which contains the ion at *m/z* 295 that is the

protonated molecular ion of 18:2 FAME (**Table 3-1**). The ozonolysis product ions at *m/z* 227(195) and 187(155) can be used to assign the double bonds at *n*-6 and *n*-9. Finally, the mass spectrum of the peak at 12.66 min (**Figure 3-4(g)**) is the same as that shown in **Figure 3-3(a)**, which identifies the ion at *m/z* 293 as the $[M+H]^+$ ion of 18:3 FAME with double bonds at *n*-3, -6 and -9. In addition, it has been found that 9,12-18:2 and 9,12,15-18:3 FAME in the sample have the same retention times as 9c,12c-18:2 FAME and 9c,12c,15c-18:3 FAME standards under the same chromatographic conditions, which supports the identification that these are both in the all *cis* configuration.

Table 3-1. Identification of FAME in bovine fat sample by using Ag^+-LC/O_3-(APPI+)MS analysis.

Experimental *m/z*	Thoretical *m/z*	Error (ppm)	Elemental Composition	Fragment Ions[a]	t_R (min)	FAME Identification
271.2627	271.2637	-3.7	$[C_{17}H_{34}O_2]^+$	N/A	3.78	16:0
299.2943	299.2945	-2.4	$[C_{19}H_{39}O_2]^+$	N/A	3.78	18:0
297.2796	297.2788	2.7	$[C_{19}H_{37}O_2]^+$	243(211)	3.83	13t-18:1(*n*-5)
				215(183)	3.98	11t-18:1(*n*-7)
				201(169)	3.98	10t-18:1(*n*-8)
				243(211)	4.28	13c-18:1(*n*-5)
				215(183)	4.33	11c-18:1(*n*-7)
				187(155)	4.37	9c-18:1(*n*-9)
269.2484	269.2475	3.3	$[C_{17}H_{33}O_2]^+$	187(155)	4.58	9c-16:1(*n*-7)
295.2639	295.2632	2.4	$[C_{19}H_{35}O_2]^+$	187(155),227(195)	6.26	9c,12c-18:2(*n*-9,*n*-6)
293.2479	293.2475	1.4	$[C_{19}H_{33}O_2]^+$	187(155), 227(195),267(235)	12.66	9c,12c,15c-18:3(*n*-9,*n*-6,*n*-3)

[a] *m/z* of protonated aldehyde ions $[M+H]^+$ from oznolysis oxidative cleavage of double bond, with *m/z* of $[M+H-32]^+$ ions in parentheses.

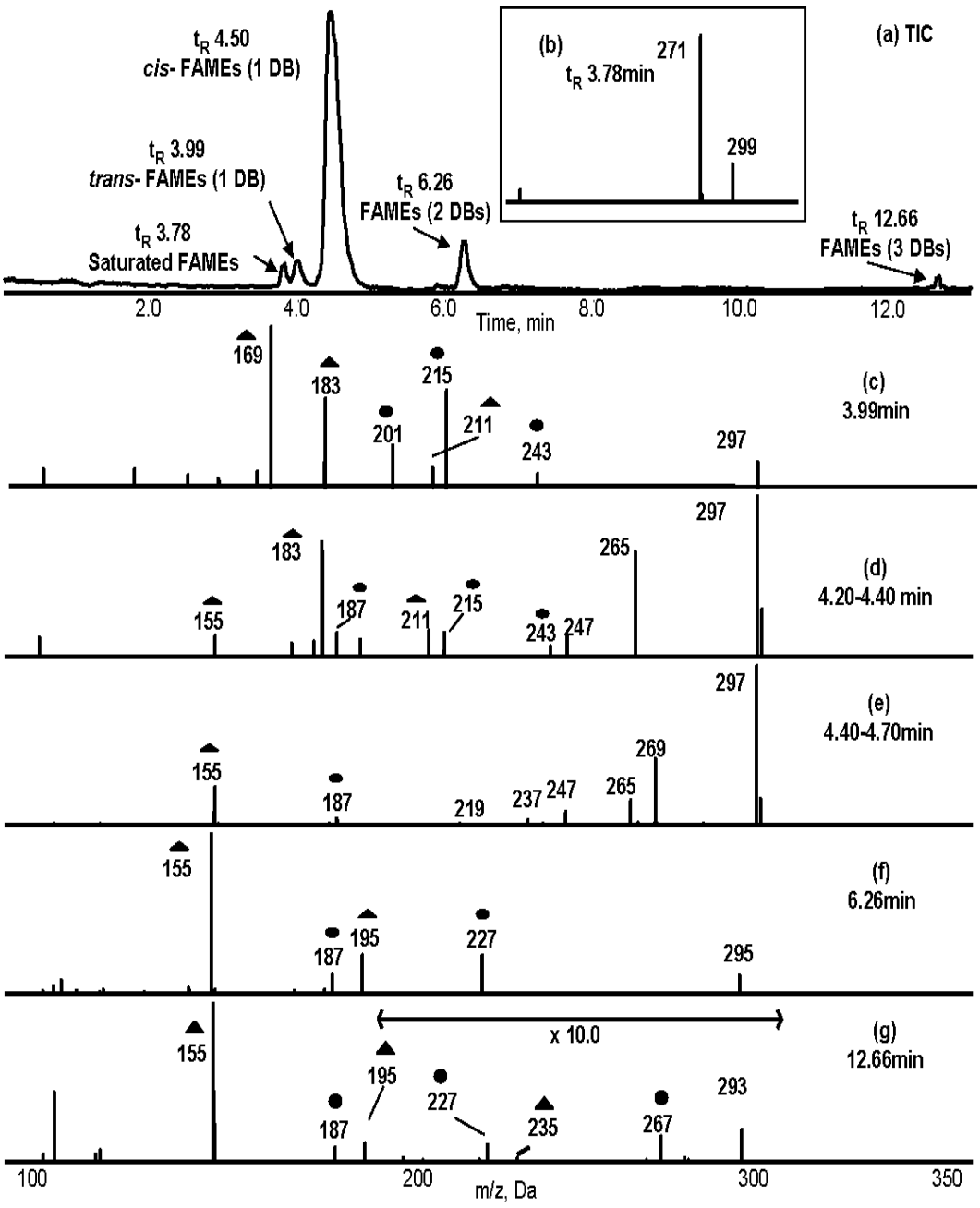

Figure 3-4. (a) Ag^+ -LC/O_3-(APPI+)MS TIC chromatogram of bovine fat sample; (b) mass spectrum averaged at t_R of 3.78min; (c) mass spectrum averaged at t_R of 3.99min;(d) mass spectrum averaged between 4.20 and 4.40min; (e) mass spectrum averaged between 4.40 and 4.70min;(f) mass spectrum averaged at t_R of 6.26min; (g) mass spectrum averaged at t_R of 12.66 min. Ozonolysis cleavage aldehyde ions are labeled with ●, the ions from the loss of methanol are labeled with ▲. DB means double bond.

The assignment of *cis*/*trans* geometry and double bond position can also be clearly illustrated by the extracted ion chromatograms (XIC) of ozonolysis product aldehyde ions seen in the O_3-MS spectra (**Figure 3-5**). As an example, the ion at *m/z* 243 (**Figure 3-5(b)**) is a characteristic ozonolysis product of a FAME with a double bond at *n*-5 and has the same retention time as ion at *m/z* 297, the $[M+H]^+$ ion of 18:1 FAME (**Figure 3-4(a)**). The two peaks seen in the XIC *m/z* of 243 (**Figure 3-5(b)**) indicate that 18:1(*n*-5) FAME exists in both *trans* and *cis* configurations. A peak at 12.66 min appears in the XIC of ozonolysis product aldehyde ions at *m/z* 187, 227 and 267(**Figure 3-5(d) (e) and (f)**). This peak is identified as 18:3 FAME in **Figure 3-4(a)** and **(g).** Hence, the data reveals that the peak at 12.66 min is due to an 18:3 FAME with double bonds at position *n*-9, -6 and -3.

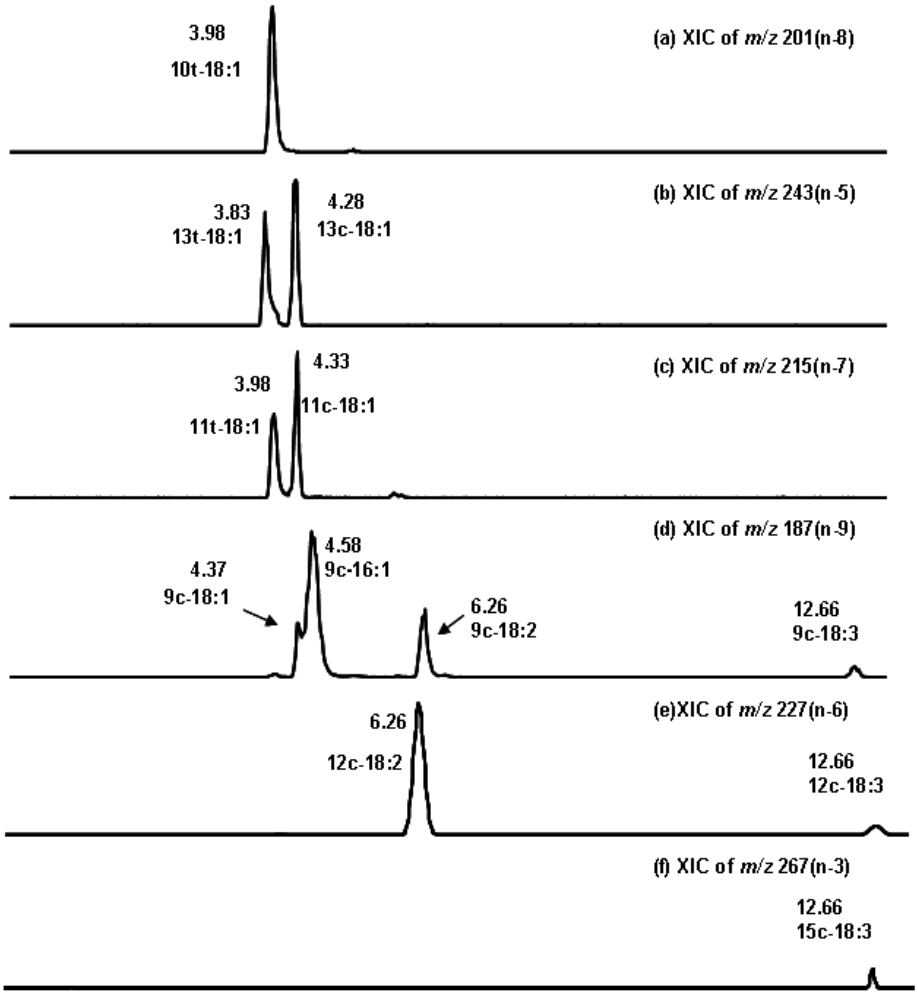

Figure 3-5. XIC of ion at *m/z* 201(a),243(b),215 (c), 187 (d), 227 (e) and 267 (f) from Ag^+ -LC/O_3-(APPI+)MS TIC of bovine fat sample.

The ions at *m/z* 243 (**Figure 3-5(b)**, t_R 4.28 min), *m/z* 215 (**Figure 3-5(c)**, t_R 4.33 min) and *m/z* 187 (**Figure 3-5(d)**, t_R 4.37 min) are from the *cis* isomers of 18:1 FAME with double bond at *n*-5, *n*-7 and *n*-9. This elution order is consistent with earlier reports that FAME positional isomers with double bonds closer to the methyl terminus elute earlier in Ag^+-LC [78]. The 18:1(*n*-5), 18:1(*n*-7) and 18:1(*n*-9) FAME isomers are not well resolved under current chromatographic

conditions in which they all elute under the peak centered at 4.50 min in **Figure 3-4(a)**. Nonetheless, using the unique *m/z* values of their corresponding ozonolysis product aldehyde ions, a partial separation of these positional isomers is revealed by their differing t_R. Hence, even though the current Ag^+-LC method has little chromatographic resolution between FAME positional isomers, the additional dimensions of information available from O_3-MS (molecular weight, characteristic ozonlysis product from cleavage of each double bond) still allow the identification of positional isomers in the lipid mixture.

In the bovine fat sample a total of 2 saturated FAME and 9 unsaturated FAME were identified (**Table 3-1**) including both double bond location and geometric configuration. Among the 18:1 FAME isomers, vaccenic acid (11t-18:1 FA) was shown to be present; this is believed to be a precursor in the formation of conjugated linoleic acid (CLA), a group of isomeric fatty acids some of which may have anti-cancer potential [79,80]. Finally, it should be noted that we have found that the use of Teflon AF-2400 tubing in-line with conventional LC columns have little effect on chromatographic resolution due to the small inner diameter of the tubing (0.01" ID). Hence, LC/O_3-MS using other higher resolution LC columns and methods are now being investigated.

3.4. Conclusions

The in-line O_3 -MS method presented here can be used to unambiguously assign double bond positions in mono- and poly-unsaturated FAME. The assignment is based on the observation by APPI(+)/MS of aldehydes arising from

the cleavage of each double bond by ozonolysis. The Ag^+-LC/O_3-MS analysis of a bovine fat sample has also demonstrated the capability of the method to determine double bond positions in complex lipid extracts. Even though the Teflon AF-2400 tubing is used as an in-line ozonolysis reaction apparatus, this method does not have any requirement for a specific type of mass spectrometer and no instrumental modification is needed. We have found that the in-line ozonolysis apparatus is easy to use and the O_3-MS mass spectra of FAME are simple to interpret. All of these advantages make it straightforward for the LC/O_3-MS method to be adopted by LC/MS laboratories and used for double bond determination in a range of applications, such as the identification of *n*-3 PUFA and specific *trans* FAs. Further work is underway to couple O_3-MS with other LC separations and ionization sources for the analysis of a wider range of lipids, including triacylglycerides and phospholipids.

CHAPTER 4

The Identification of Conjugated Linoleic Acid Isomers by Silver Ion- Liquid Chromatography/ In-line Ozonolysis-Mass Spectrometry [4]

4.1. Introduction

Conjugated linoleic acid (CLA) is the group of octadecadienoic acid isomers (18:2) with conjugated double bonds, as distinct from the more abundant non-conjugated $\Delta^{9,12}$ linoleic acid. Each CLA positional isomer may also exist in *cis,cis*-, *cis,trans*-, *trans,cis*- and *trans,trans*- configurations. In the fat of ruminants, such as in milk or beef, rumenic acid (*cis*9, *trans*11-18:2) is the most abundant CLA, formed by bacterial biohydrogenation of linoleic and linolenic acid [81,82]. It has been reported that some of CLA isomers may result in anti-carcinogenic and anti-atherogenic effects, and may bring about changes in body composition [83-85]. Although the exact biological mechanisms for CLA activity are still under investigation, current research has shown that individual CLA isomers may have different impacts on lipid metabolism, cancer and diabetes [11,12,80,86,87].

Due to the diversity of individual CLA positional and geometric isomers and their isomer-specific biological effects, an analytical method is required that

[4] A version of this chapter has been published. Sun, C., Black, B.A., Zhao, Y., Gänzle, M.G. and Curtis, J.M. *Anal. Chem.* 2013, *85*, 7345−7352
Reprinted with permission.

readily allows for accurate identification of CLA isomers. Gas chromatography coupled with flame ionization detection (GC-FID) is widely used for analysis of fatty acid methyl esters (FAME) including CLA methyl esters [88,89]. However, even with the best separation achieved using long (100m) polar columns with cyanopropyl type stationary phases CLA isomers, especially the *trans,trans*-positional isomers, are still not well resolved from each other. Furthermore, interferences, such as the coelution of 20:1 FAME with CLA methyl esters, may occur [90]. In addition, GC-FID requires a standard mixture of CLA for identification of isomers in food and biological samples, but only a limited number of CLA isomers are available as pure standards.

For the unambiguous identification of each CLA positional isomer, GC combined with electron ionization mass spectrometry (GC/EI-MS) has been used following the specific derivatization that is necessary for double bond localization. The latter is required since the EI mass spectra of positional isomers of CLA methyl ester are indistinguishable. Commonly employed derivatives for CLA analyses include picolinyl esters, Diels-Alder adducts [16] and especially dimethyloxazolines (DMOX) [17], which are easily formed and can be well separated by GC. The fragment ions in the EI mass spectra of DMOX derivatives of unsaturated fatty acids directly indicate the location of the double bonds and the diagnostic fragment ions from the DMOX derivative of CLA positional isomers from $\Delta^{6,8}$ to $\Delta^{13,15}$ have all been reported [91]. Reconstructed ion chromatograms of these diagnostic ions have been used for CLA isomer

identification [92]. However, the abundance of these ions may be too low for their use in the identification of minor CLA isomers.

Separation by silver ion liquid chromatography (Ag^+- LC) has been used as a complementary tool along with GC for better separation of CLA isomers, especially the *trans,trans*- positional isomers [91]. Since conjugated dienes show characteristic absorptions at 233 nm, a UV detector is normally coupled with the Ag^+- LC [93]. The reported Ag^+- LC separation of CLA isomers has often used an isocratic separation with 0.1- 1.0 % acetonitrile in hexane on a ChromSpher 5 Lipids column [91,94,95]. In this way, CLA isomers can be separated into *trans,trans*-, *cis/trans*- (*cis,trans*- or *trans,cis*-) and *cis,cis*- geometric groups in this order of increasing retention time. Furthermore, studies have shown that CLA positional isomers with conjugated double bonds located closer to carboxyl group elute later within each geometric group [91,94,95]. Multiple Ag^+- LC columns, even up to six, have also been connected in series in order to improve peak resolution [95]. Recently, the relative retention order of all *cis,trans*- and *trans,cis*- CLA isomers from $\Delta^{6,8}$ to $\Delta^{13,15}$ were established using three Ag^+- LC columns in series [96]. Although it may be possible to resolve *trans,trans*-, *cis,cis*- and most of *cis/trans*- positional isomers using multiple Ag^+- LC columns under optimal conditions, there is still a significant challenge to identify each peak, especially closely eluting peaks. This is made worse by the instability of retention times on Ag^+- LC columns and the very different concentrations of CLA isomers in natural samples [97]. Since *cis*9, *trans*11-CLA is the most abundant CLA isomer existing in nature, the peak of highest intensity in the Ag^+-LC

chromatogram is normally assumed to be *cis*9, *trans*11-CLA, and from this the identification of the other CLA isomers can be made by their relative retention times. Furthermore, in research on the biological function of specific CLA isomers, CLA isomers other than *cis*9, *trans*11-CLA have been used. This gives rise to the situation where *cis*9, *trans*11-CLA is no longer the most abundant CLA isomer in these sample [98].

The ambiguity in CLA positional isomer identification is also present when mass spectrometry and tandem mass spectrometry (MS/MS) is used. For example, when three Ag^+- LC columns in series were coupled to atmospheric pressure photo ionization mass spectrometry (APPI-MS), the ion $M^{+\cdot}$ at *m/z* 294 was used to identify CLA methyl esters, but the assignment of each specific CLA positional isomer could only be made based on the elution order in Ag^+- LC [99]. To date, there is no single definitive method for the identification of CLA positional isomers.

Ozone can specifically react with carbon-carbon double bonds producing cleavage products of predictable mass and hence the ozonolysis of unsaturated lipids has been used to determine double bond locations [30,38]. Blanksby et al. have developed ozone induced dissociation (OzID-MS) in which gas phase ozonolysis takes place within a mass spectrometer to allow for the elucidation of double bond locations [39,40]. In recent OzID research on the identification of CLA positional isomers, sodium adducts of aldehydes from ozonolysis at each double bond were observed under ESI (+), and used for the assignment of double bond positions [100]. However, this technique requires the specialized

introduction of ozone into a mass spectrometer; furthermore it may not be suitable for the identification of low abundance CLA isomers in complex samples.

It is highly desirable to have a single technique that could determine double bond positions, and also achieve *de novo* identification of CLA positional isomers even in complex lipid mixtures. Recently, we reported a simple approach for the direct determination of double bond positions in FAME by coupling ozonolysis in-line with mass spectrometry (in-line O_3-MS) (Chapter 3) [101]. In that method, the unsaturated FAME within the LC mobile phase passed through gas permeable, liquid impermeable tubing housed within a vessel containing ozone. With this arrangement, ozone passed through the tubing wall resulting in the ozonolysis of unsaturated FAME directly within the mobile phase. The aldehydes, that were the products of ozonolysis and were characteristic of FAME double bond positions, were then analyzed in real-time by APPI-MS. A great advantage of this technique is that it readily allows the coupling of liquid chromatography with O_3-MS (LC/O_3-MS). Hence, the complete identification of each FAME in the chromatogram of complex lipid mixtures can be achieved.

In this study, we explore the feasibility of using in-line O_3-MS for the *de novo* identification of CLA positional isomers. Then, we describe the development of the LC/O_3-MS method for the identification of CLA isomers in complex lipid samples. Using this approach, we demonstrate the identification of CLA isomers in natural matrices through the examples of a commercial CLA supplement, bovine milk fat and a lipid extract from a bacterial culture.

4.2. Experimental

4.2.1. Material

HPLC grade hexanes (HEX), acetonitrile (ACN), isopropanol (IPA) were purchased from Fisher Scientific Company (Ottawa, ON, Canada). All the CLA methyl ester standards (*cis*9, *trans*11-, *cis*9, *cis*11-, *trans*9, *trans*11- and *trans*10, *cis*12-18:2) were purchased from Matreya Inc. (Pleasant Gap, PA, USA). FAME standards (*cis*9-18:1 and *trans*11-18:1) were purchased from Nu-Chek Prep Inc. (Elysian, MN, USA). Each standard solution was prepared in HEX at a concentration of 200 μg/mL. A solution of porcine renin substrate tetetradecapeptide at 10 pmol/μL in acetonitrile/water (1:1, v/v) from a chemical standards kit (Applied Biosystems, Foster City, CA, USA) was used for the tuning and calibration of mass spectrometer. The Teflon AF-2400 tubing (0.020" OD, 0.010" ID) was purchased from Biogeneral Inc. (San Diego, CA, USA).

4.2.2. Lipid extraction and methylation

The commercial CLA supplement was obtained from a local supermarket. It was manufactured from safflower oil and sold in capsule form for weight control purposes. Approximately 0.05 g of CLA supplement was dissolved in toluene and methylated using 1% sulfuric acid in methanol at 50 ºC overnight [102]. The methylated lipid was dissolved in hexane to a concentration of approximately 50 μg/mL for analysis.

Bovine milk with 3.25 % fat content was purchased from local market. Lipid extraction was performed on 1 g of milk using the Bligh and Dyer method

[103]. The chloroform layer that contained lipid was dried under a flow of nitrogen, and the residual lipid was dissolved in toluene for methylation as above. The entire methylated lipid extract was dissolved in 10 mL hexane and diluted a further 20 times in hexane before analysis.

Lactobacillus plantarum TMW1460 was incubated in modified DeMan-Rogosa-Sharpe broth, supplemented with 4 g/L linoleic acid, at 30 °C for 48 h and extracted according to Black et al. [104]. After extraction, the fatty acids were methylated as above. The resulting FAME was resuspended in a total volume of 2 mL hexane. Each of two 1 mL FAME aliquots was loaded onto a separate conditioned silver ion- solid phase extraction (Ag^+ - SPE) cartridge (750 mg/6 mL, Supelco Inc., Bellefonte, PA) and 6 mL hexane/acetone (99:1, v/v) was used to elute the unretained FAME. Following this, fractions were eluted using 6 mL hexane/acetone (96:4, v/v) and 6 mL hexane/acetone (90:10, v/v) [105]. The fractions collected from each of the two 1mL FAME aliquots were combined, dried under nitrogen and dissolved into 1 mL of hexane.

4.2.3. In-line O_3-MS analysis of CLA methyl ester standard

The in-line O_3-MS method was described in detail in Chapter 3 [101]. In this study, a 10 cm length of gas permeable tubing passed through a chamber filled with oxygen and ozone gas (ozone concentration 35.6 g/m^3) at room temperature. A 3 µL volume of the 200 µg/mL CLA standard solution was delivered through the gas permeable tubing by an Agilent 1200 series HPLC system (Agilent Technologies Inc, Palo Alto, CA, USA) with hexane as the

mobile phase and at the flow rate of 0.2 mL/min. The ozonolysis products were analyzed using an APPI ion source in the positive ion mode attached to a hybrid quadrupole time - of - flight mass spectrometer (QSTAR Elite, Applied Biosystems/MDS Sciex, Concord, ON, Canada). The APPI ion source temperature was held at 375 °C while the source region gas flows in arbitrary units assigned by the data system were as follows: curtain gas 25; auxiliary gas 10; nebulizing gas 50. In all cases, high purity nitrogen was the gas used. The ionspray voltage, declustering potential (DP), focus potential (FP), and DP2 were 1300 V, 35 V, 130 V and 10 V, respectively. The mass spectrometer was tuned using the ion at *m/z* 879.9723 and fragment ion at *m/z* 110.0713 obtained by infusing porcine renin substrate tetetradecapeptide into the ESI ion source in the positive ion mode and at a resolution of above 10,000 (full width at half maximum). This solution was also used for calibration of the mass range *m/z* 100-1,300.

4.2.4. Ag^+-LC/O_3-MS analysis of FAME mixtures from lipid extracts

Isocratic separation on a ChromSpher 5 Lipids column (2 mm i.d.×250 mm, 5 μm particles) (Agilent Technologies Inc, Lake Forest, CA, USA) was used with all of the samples. The mobile phase consisted of 20% HEX: IPA: ACN (100:1:0.1, v/v/v) and 80% of HEX. The sample injection amount was 2 μL and the flow rate was 0.2 mL/min. The in-line O_3-MS conditions were the same as above except that only 5 cm tubing was used for sample analysis.

4.3. Results and Discussion

4.3.1. In-line O_3-MS analysis of CLA standard

In Chapter 3, we showed that the ozonolysis product aldehydes resulting from the oxidative cleavage at each double bond can be used as indicators of double bond positions for monounsaturated and non-conjugated polyunsaturated FAME [101]. Here, in-line O_3-MS analysis is performed on a *cis*9, *trans*11- and *trans*10, *cis*12- CLA methyl ester standard, in order to see whether conjugation will have any affect on double bond assignment by ozonolysis. For both CLA positional isomers, protonated molecular ions $[M+H]^+$ at *m/z* 295 are observed in the O_3-MS mass spectra under positive ion APPI (**Figure 4-1**). From the in-line O_3-MS analysis of *cis*9, *trans*11- CLA methyl ester, we observe product ions at *m/z* 213, 181, 187 and 155 (**Figure 4-1(a)**). The ions at *m/z* 213 and 187 correspond to the protonated aldehyde ions from the ozonolysis cleavage at Δ^{11} and Δ^{9} position, and the ions at *m/z* 181 and 155 are due to methanol loss from *m/z* 213 and 187. In contrast, for the *trans*10, *cis*12- CLA methyl ester the ions at *m/z* 227, 195, 201 and 169 are observed by in-line O_3-MS (**Figure 4-1(b)**). The ions at *m/z* 227 and 201 are indicative of double bonds located at Δ^{12} and Δ^{10} positions and the ions at *m/z* 195 and 169 are due to the methanol loss from these ions.

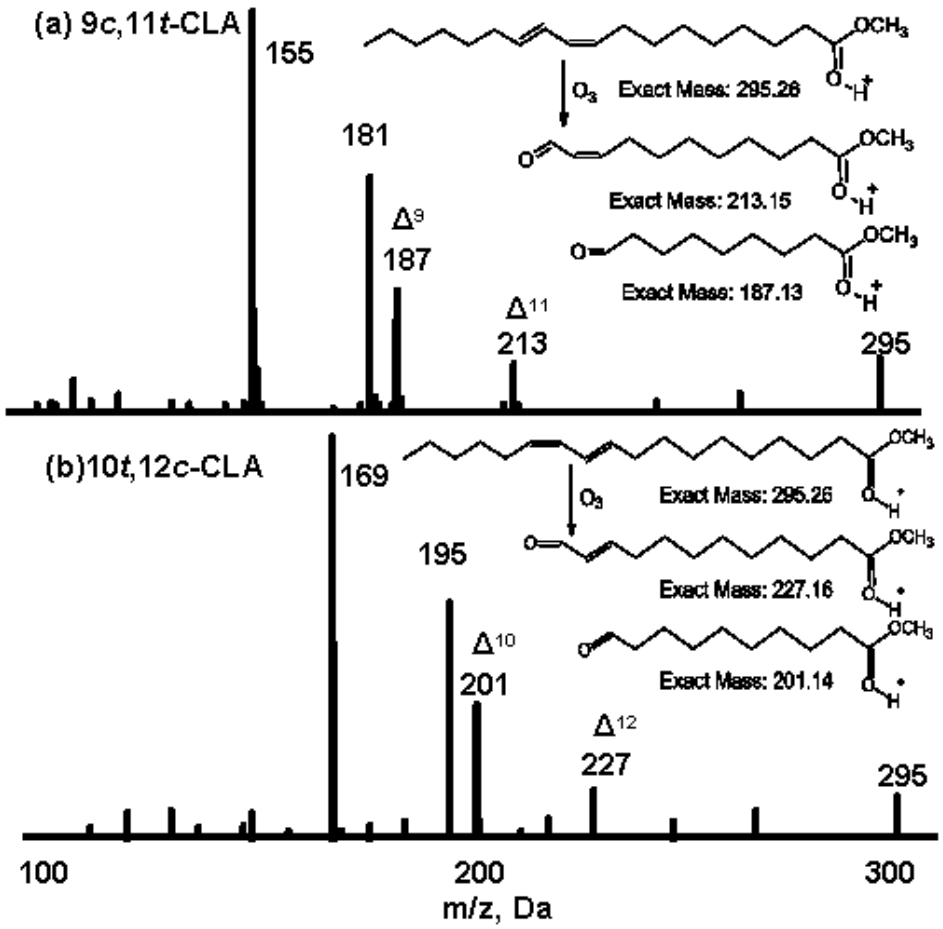

Figure 4-1. In-line O_3-APPI(+)-MS spectrum of (a) 9*c*,11*t*-CLA methyl ester and (b) 10*t*,12*c*-CLA methyl ester.

In-line O_3-MS analysis of *cis*9, *cis*11- and *trans*9, *trans*11- CLA methyl ester (**Figure 4-2**) gives the same ozonolysis product ions as those seen for *cis*9, *trans*11- CLA methyl ester. This result demonstrates that double bond geometry does not affect the ozonolysis product ions observed. However, ozonolysis of CLA isomers is generally seen to proceed at an accelerated rate compared to the non-conjugated *cis*9, *cis*12-18:2 methyl ester. Thus, under the same reaction condition (tubing length of 20 cm, ozone concentration 35.6 g/m^3, 3 µL of 200 µg/mL standard solution), only ozonolysis product ions of CLA methyl esters can

be observed, whereas the $[M+H]^+$ ion at *m/z* 295 of intact non-conjugated *cis*9, *cis*12-18:2 methyl ester still exists. For this reason, only a 10 cm length of the semi-permeable tubing is used here for the in-line O_3-MS analysis of CLA methyl esters so that some CLA molecular ions can still be seen in the mass spectrum. An enhanced reaction rate for gas phase ozonolysis of CLA was also observed in the OzID/MS experiment [100].

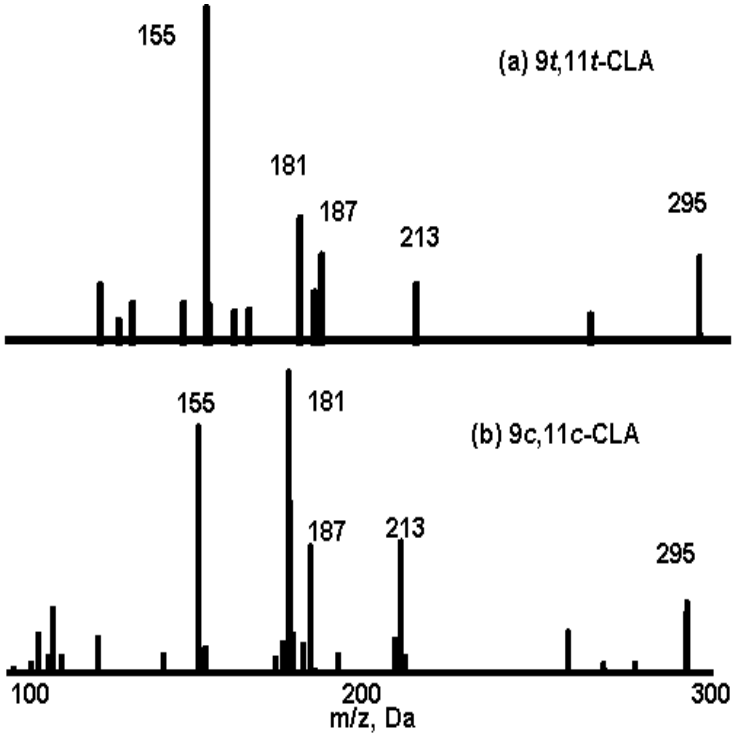

Figure 4-2. In-line O_3-APPI(+)-MS spectrum of (a) 9*t*,11*t*-CLA methyl ester and (b) 9*c*,11*c*-CLA methyl ester.

In summary, the in-line O_3-MS spectra of two CLA positional isomers indicate that the observed ozonolysis product aldehydes are indicative of double bond locations even when the double bonds are conjugated. Even though pure standards of every CLA positional isomer are not available, the pair of diagnostic

aldehyde ions arising from ozonolysis cleavage at each double bond can still be used to reliably differentiate CLA positional isomers. All of the predicted diagnostic aldehyde ions and their corresponding methanol loss fragment ions for CLA positional isomers from $\Delta^{6,8}$ to $\Delta^{13,15}$ are listed in **Table 4-1**.

Table 4-1. In-line O_3/APPI(+)-MS diagnostic ions for CLA positional isomer identification.

CLA Isomer	A. *m/z* of aldehyde ions from O_3 cleavage at Δ^a position	*m/z* of ions due to methanol loss from A	B. *m/z* of aldehyde ions from O_3 cleavage at Δ+2 position	*m/z* of ions due to methanol loss from B
6, 8	145	113	171	139
7, 9	159	127	185	153
8, 10	173	141	199	167
9, 11	187	155	213	181
10, 12	201	169	227	195
11, 13	215	183	241	209
12, 14	229	197	255	223
13, 15	243	211	269	237

[a] Position of double bond counted form the carboxyl group end.

4.3.2. Ag^+-LC/O_3-MS analysis of FAME mixtures from lipid extracts

In order to demonstrate the relative retention order of *cis,cis-, cis/trans- and trans,trans-* CLA isomers in silver ion chromatography, Ag^+-LC/APPI(+)-MS analysis was performed on a standard mixture of CLA isomers (*cis*9, *trans*11-; *cis*9, *cis*11-; *trans*9, *trans*11- and *trans*10, *cis*12- CLA methyl esters), methyl oleate (*cis*9-18:1) and methyl vaccenate (*trans* 11-18:1) (**Figure 4-3**). In the extracted ion chromatogram (XIC) of *m/z* 297, the peaks at 6.4 and 12.9 min represent *trans*11-18:1 and *cis*9-18:1. In the XIC of *m/z* 295, the first eluting peak is *trans*9, *trans*11- CLA, the last eluting peak is *cis*9, *cis*11-CLA, and the two

peaks in the middle are *trans*10, *cis*12- and *cis*9, *trans*11- CLA, respectively. Within the 30 min isocratic separation, CLA geometric isomers (with the same double bond positions) are well separated from each other and also separated from *cis*- and *trans*- 18:1 methyl esters. Hence, coupling Ag^+-LC to in-line O_3-MS provides the extra dimension of information needed to determine the double bond geometries in addition to identifying the double bond positions from the mass spectra.

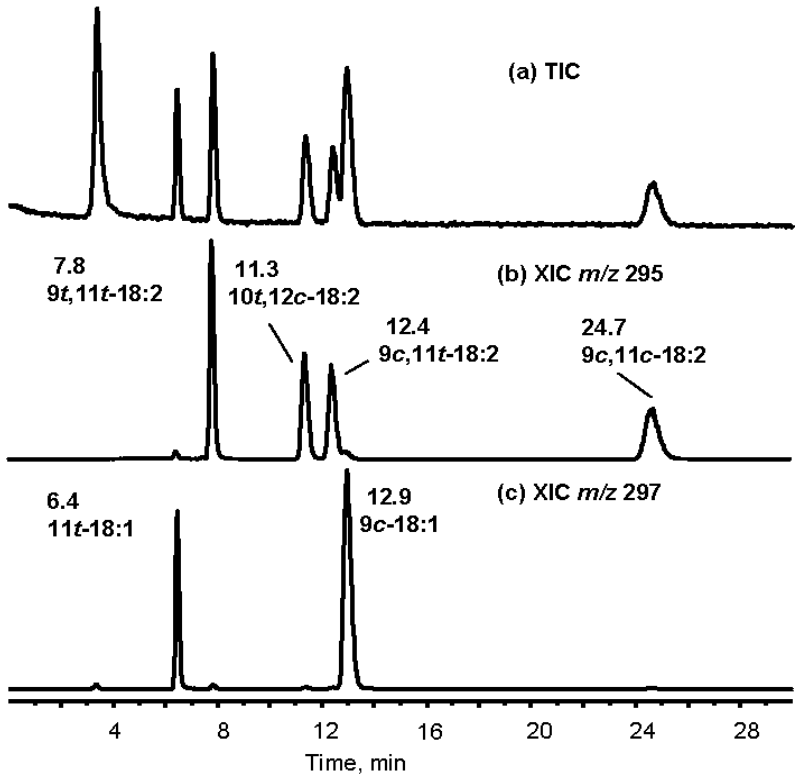

Figure 4-3. (a) Ag^+-LC/APPI(+)-MS TIC trace of a mixture of FAME standards including 11*t*-18:1, 9*c*-18:1, 9*t*,11*t*-18:2, 9*c*,11*t*-18:2, 9*c*,11*c*-18:2 and 10*t*,12*c*-18:2 methyl esters; (b) Extracted ion chromatogram (XIC) of *m/z* 295; (c) XIC of *m/z* 297.

In the following sections, we demonstrate the application of the Ag^+-LC/O_3-MS method for the identification of CLA isomers in a commercial CLA supplement, bovine milk fat and the lipid extract of *L. plantarum* culture. These

examples include distinctly different CLA sources having different levels and distributions of CLA isomers and possible matrix interferences. In order to observe both of the diagnostic aldehyde ions from the ozonolysis of CLA that is present in low amounts in these samples, a shorter length of semi-permeable tubing (5 cm) was used, reducing the extent of ozonolysis.

4.3.2.1. Commercial CLA supplement

Because of the proven and potential health benefits of CLA consumption, foods enriched in CLA and CLA supplements have become available to consumers. CLA supplements can be manufactured from soybean and safflower oil that are rich in linoleic acid through either photo- or alkali-induced isomerization [106,107]. Since these isomerization processes are not isomer specific, multiple CLA isomers are believed to exist in these synthetic CLA mixtures.

The FAME mixture from the CLA supplement was first analyzed by Ag^+-LC/APPI(+)-MS without ozonolysis (**Figure 4-4**). In the XIC for $[M+H]^+$ ions at *m/z* 295 of linoleic acid isomers, there are two major peaks at 10.8 and 11.8 min with four other minor peaks at 6.4, 6.7, 23.1 and 24.9 min. The mass spectra of these peaks are identical and thus the double bond positions in these isomers cannot be distinguished directly. **Figure 4-5(a)** is the total ion current chromatogram (TIC) of the same sample after in-line O_3-MS; the mass spectra of each visible peak at 6.8, 7.2, 11.2 and 12.3 min are also shown. The mass spectra of the peaks at 6.8 (**Figure 4-5(b)**) and 11.2 min (**Figure 4-5(d)**) are almost the

same; the pair of diagnostic ions at *m/z* 227 (methanol loss ion at *m/z* 195) and 201(methanol loss ion at *m/z* 169) can be used to unambiguously assign the double bond position at Δ^{12} and Δ^{10}. Similarly, in **Figure 4-5(c)** and **(e)** the same pair of diagnostic ions at m/z 213 (methanol loss ion at *m/z* 181) and 187 (methanol loss ion at *m/z* 155) can be seen, which identify these peaks as $\Delta^{9,11}$ CLA isomers. In all of these mass spectra, the $[M+H]^+$ ion at *m/z* 295 is not seen, partly because of the accelerated ozonolysis reaction rate of CLA compared to non-conjugated isomers, as described above. In addition, the CLA content of a natural sample such as milk, cheese and butter is only up to 2% of the total fatty acids [108,109]. This much lower abundance also contributes to the failure to observe CLA molecular ions in the mass spectra after ozonolysis.

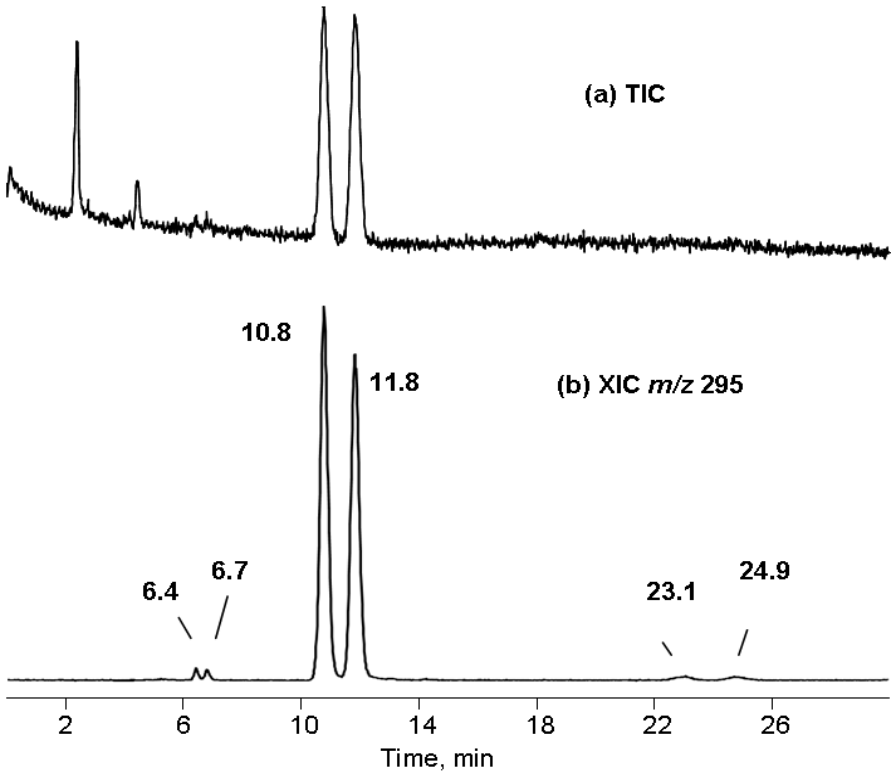

Figure 4-4. The Ag^+-LC/APPI(+)-MS analysis of a CLA supplement (a) TIC; (b) XIC *m/z* 295.

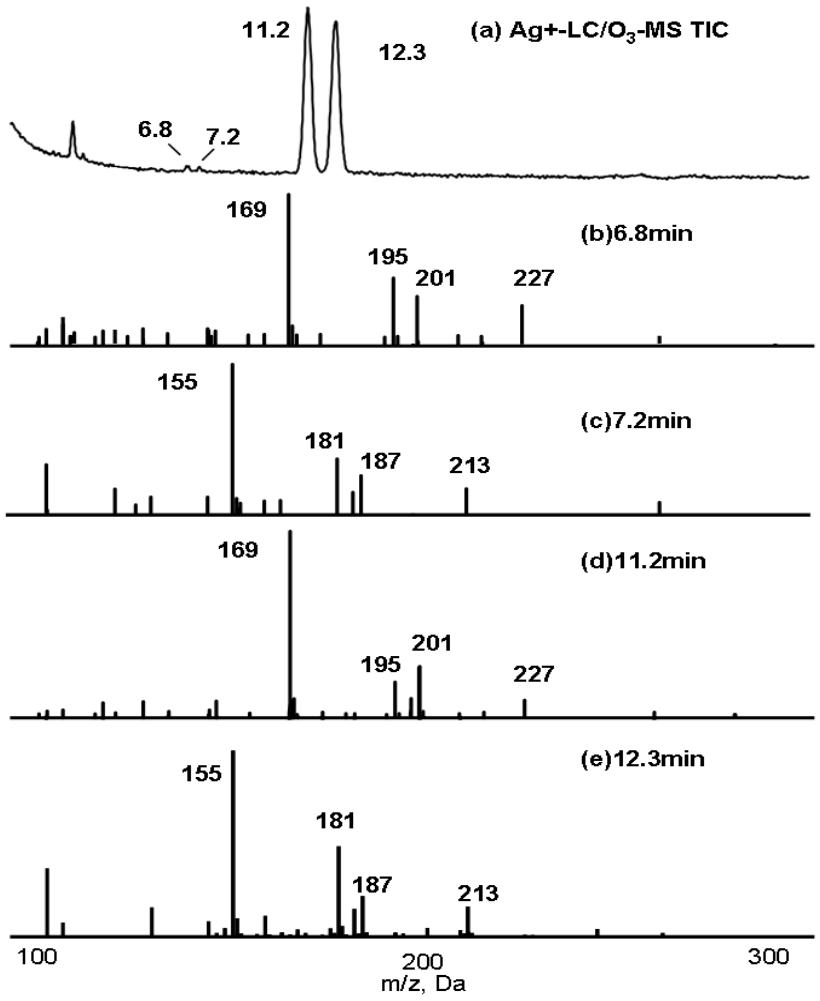

Figure 4-5. The Ag^+-LC/O_3-APPI(+)-MS analysis of a CLA supplement (a) TIC; (b) mass spectrum averaged at 6.8min; (c) mass spectrum averaged at 7.2min; (d) mass spectrum averaged at 11.2min; (e) mass spectrum averaged at 12.3min.

Even though there are two small peaks at 23.1 and 24.9 min in the XIC of *m/z* 295 (**Figure 4-4(b)**), these peaks are difficult to see in Ag^+-LC/O_3-MS TIC trace in **Figure 4-5(a)** and hence some CLA isomers might be overlooked. However, a simple screening for all possible CLA positional isomers can be performed by generating XICs for each pair of diagnostic ions listed in **Table 4-1**. Peaks appearing at the same retention time (t_R) in these XICs correspond to the

specific CLA positional isomer. For example, in **Figure 4-6(a)**, the three peaks at 7.2, 12.3 and 25.1 min in the XIC of *m/z* 213 are also present in the XIC of *m/z* 187 meaning that these peaks are all due to CLA isomers with double bonds located at Δ^{11} and Δ^{9}. From the known elution order of CLA geometric isomers in Ag^{+}-LC, the peaks at 7.2 min and 25.1 min must be *trans*9, *trans*11- and *cis*9, *cis*11- CLA. The peak at 12.33 min could be either *cis*9, *trans*11- or *tran*9, *cis*11- CLA which are not readily distinguished by their retention time. However, in this particular case, the peak at 12.3 min is identified as *cis*9, *trans*11-CLA which is confirmed by addition of *cis*9, *trans*11- CLA standard to the sample (**Figure 4-7**). Similarly, the XICs of another pair of diagnostic aldehyde ions at *m/z* 227 and 201 reveals three geometric isomers of $\Delta^{10,12}$ CLA at 6.8, 23.9 and 11.2 min (**Figure 4-6(b)**), which are identified as *trans*10, *trans*12-, *cis*10, *cis*12- and *trans*10, *cis*12- CLA (the latter confirmed by addition of *trans*10, *cis*12- CLA standard to the sample). In summary, the results show that the commercial CLA supplement sample contains primarily *cis*9, *trans*11- and *trans*10, *cis*12-CLA, along with minor amounts of their geometric isomers *trans*9, *trans*11-, *cis*9, *cis*11-, *trans*10, *trans*12- and *cis*10, *cis*12-CLA. This finding is consistent with a previous publication that used Ag^{+}-LC and GC- (EI) MS to analyze a commercial CLA mixture [110].

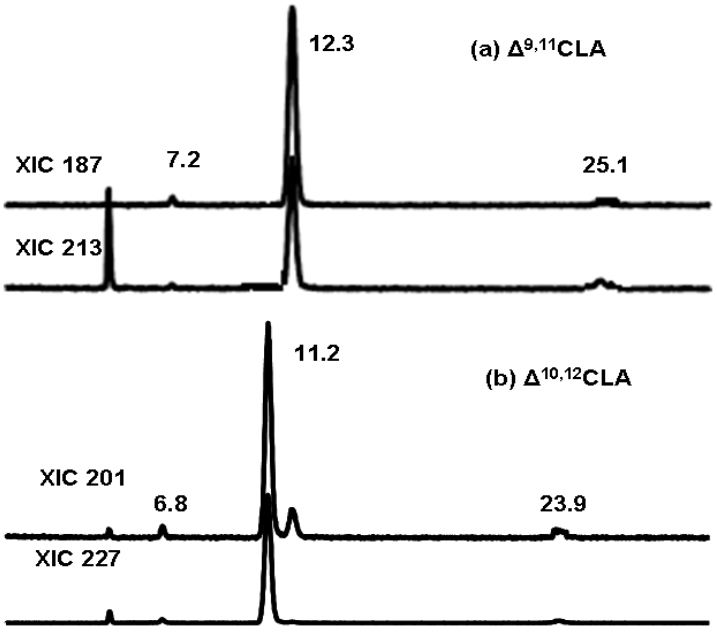

Figure 4-6. The Ag^+-LC/O_3-APPI(+)-MS analysis of a CLA supplement (a) XIC of *m/z* 187 and 213; (b) XIC of *m/z* 201 and 227; (*c.f.* TIC trace in **Figure 4-5(a)**).

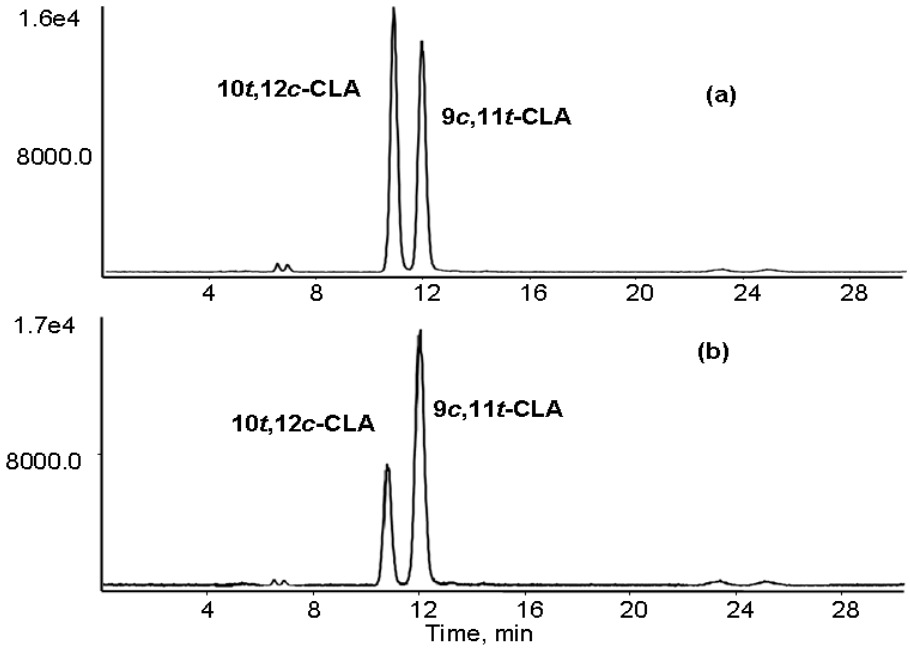

Figure 4-7. XIC of *m/z* 295 from Ag^+-LC/APPI(+)-MS analysis of (a) CLA supplement ; (b) CLA supplement sample with addition of *cis*9, *trans*11- CLA standard 1:1 (v/ v) mixed.

It is important to clarify that as in this example, in-line O_3-MS can directly identify CLA positional isomers without requiring standards, but it is not able to differentiate the geometric isomers. On the other hand, the elution order in Ag^+-LC provides complementary information on double bond geometry, especially when both double bonds are in the same configuration (*trans,trans*- and *cis,cis*-). However, the elution order of a positional isomer having double bonds in *cis,trans*- and *trans*,*cis*- configurations is less definite, and may depend upon column conditions, temperature and mobile phase composition [96,97]. The addition of a CLA standard can help the identification of *cis/trans*- geometric isomer as shown above, but only if the CLA isomer is available as a pure standard. Overall, this example demonstrates that the Ag^+-LC/O_3-MS method is capable of *de novo* identification of CLA positional isomers in lipid mixtures, despite the fact that it is not in itself able to differentiate *cis,trans*- and *trans,cis*-CLA geometric isomers.

4.3.2.2. Bovine milk fat

Milk fat is complicated mixture that contains up to 20 CLA isomers, among them rumenic acid (*cis*9, *trans*11-18:2) is normally the most abundant CLA isomer [111]. CLA content and isomer distribution in cow milk is greatly influenced by the season, feeding practice and by the diet of the cow. Identification of CLA isomers in milk is important for the dairy industry and also for nutritional research [112,113].

The XICs of $[M+H]^+$ ions at *m/z* 295 and 297 for 18:2 and 18:1 FAME from Ag^+-LC/APPI(+)-MS analysis of a milk fat FAME mixture is shown in **Figure 4-8**. The peak at 12.2 min in the XIC trace of *m/z* 297 that is present at high intensity is due to methyl oleate (*cis*9-18:1), the most abundant 18:1 fatty acid in milk. Due to this high abundance of methyl oleate, the peak at 12.2 min in the TIC appears to be a single component. However, the separation of all minor CLA species can still be observed in the XIC of *m/z* 295 because of the high selectivity achieved in this trace.

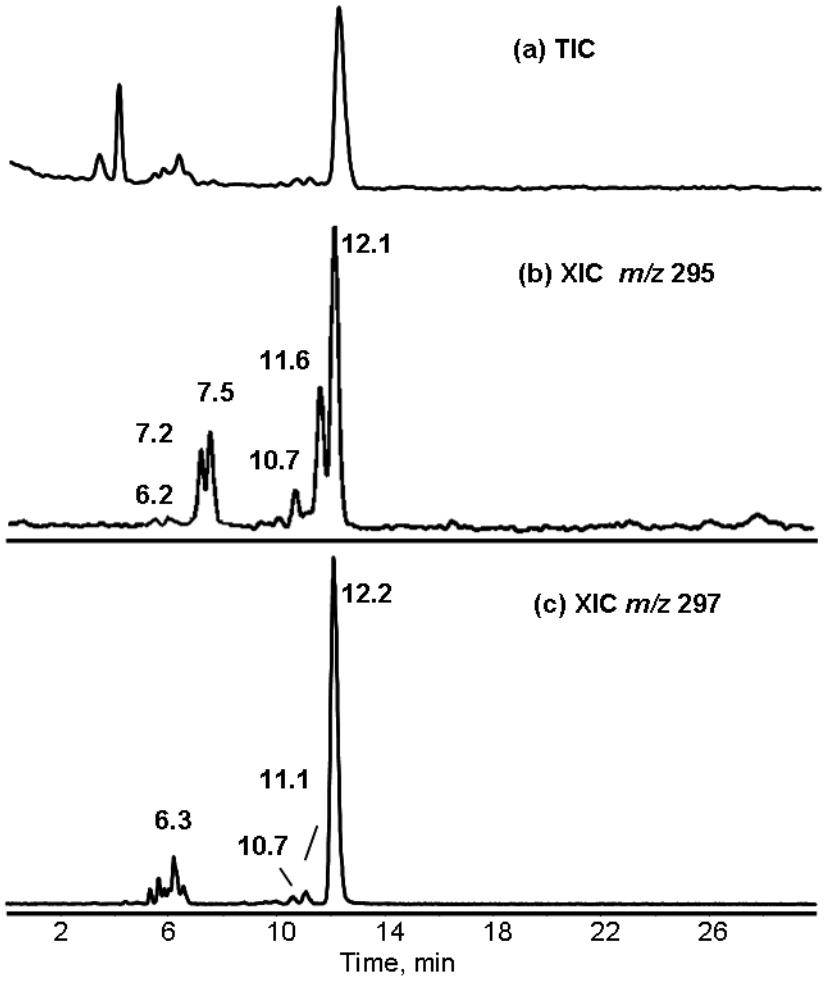

Figure 4-8. The Ag^+-LC/APPI(+)-MS analysis of milk fat (a) TIC; (b) XIC of *m/z* 295; (c) XIC of *m/z* 297.

It is apparent from **Figure 4-8(b)** that more than one CLA isomer must exist in the sample, so Ag^+-LC/O_3-MS analysis was performed for the elucidation of the double bond positions in the CLA positional isomers. In **Figure 4-9**, both the traces showing the characteristic aldehyde ions (in dark blue) and methanol loss fragment ions (in light red) are overlaid in order to avoid false positives - especially important for complex samples like the milk fat. For example, in **Figure 4-9(a)** there is a peak at around 3.0 min in the XIC of *m/z* 215 (diagnostic aldehyde ions of Δ^{11} double bond), 241 (diagnostic aldehyde ions of Δ^{13} double bond) and 209 (methanol loss from ion at *m/z* 241), but this peak is totally missing from the XIC of *m/z* 183 (methanol loss from ion at *m/z* 215). As seen in the O_3-MS of two CLA standards (**Figure 4-1**) and also the CLA supplement sample (**Figure 4-5**), methanol loss from the ozonolysis product aldyhyde ions occurs during APPI ionization and the fragment ions have even higher intensity than their aldehyde ion precursors. Therefore, the peak at 3.0 min in XIC of *m/z* 215 is not due to cleavage of double bond at Δ^{11} by ozonolysis. The peaks in the XIC of ions at *m/z* 241, 209, 215 and 183 overlay each other at 10.5 min (**Figure 4-9(a)**), which is thus identified as $\Delta^{11,13}$ CLA in *cis,trans*- or *trans,cis*- configuration. The peaks that superimpose at 6.9, 11.2 and 11.6 min in the XICs of ions at *m/z* 227, 195, 201 and 169 (**Figure 4-9(b)**) are identified as *trans*10, *trans*12-, *trans*(or *cis*)10, *cis*(or *trans*)12-, *cis*(or *trans*)10, *trans*(or *cis*)12- CLA.

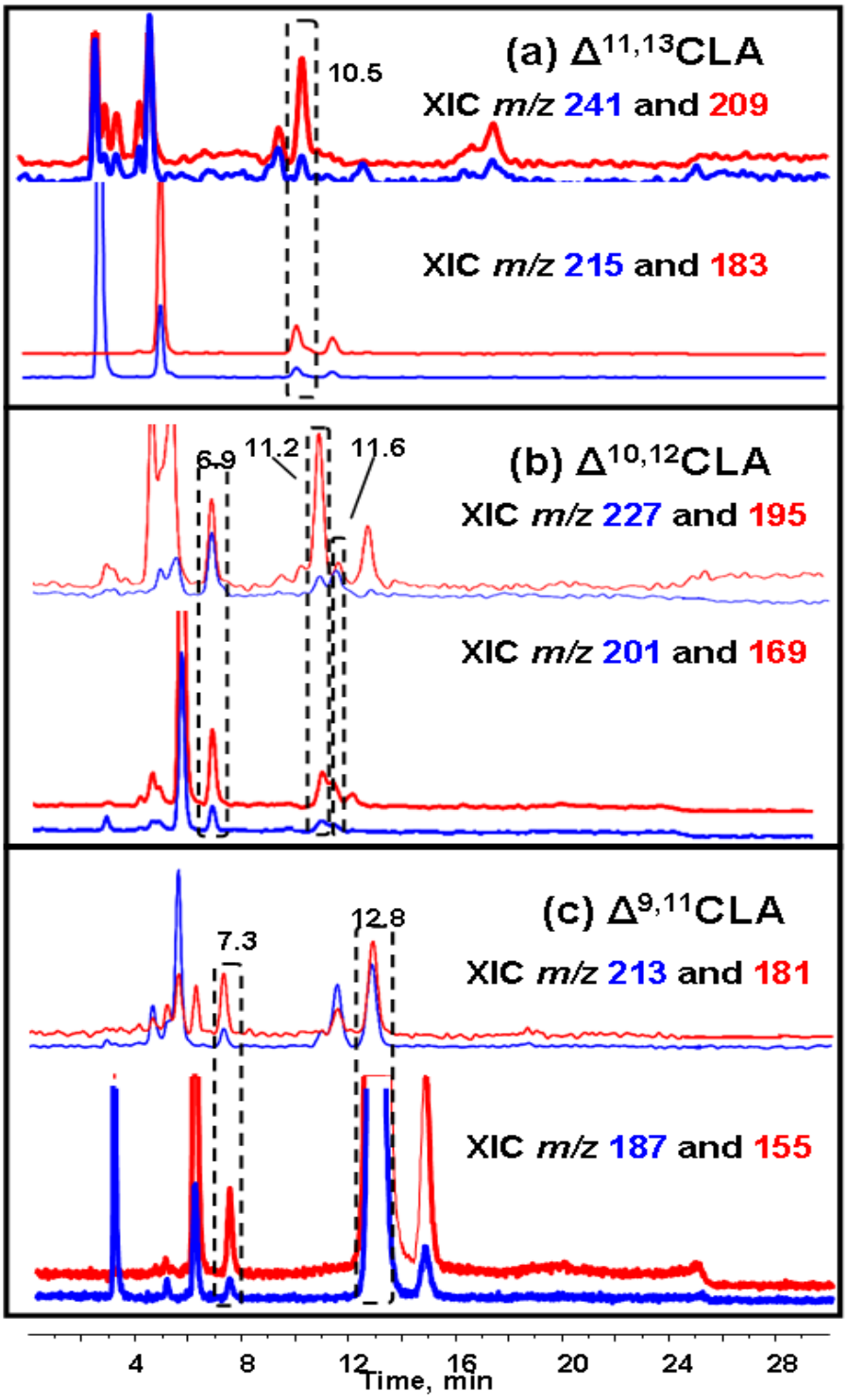

Figure 4-9. The Ag^+-LC/O_3-APPI(+)-MS analysis milk fat (a) XIC of *m/z* 183 and 209 (in red), *m/z* 215 and 241(in blue); (b) XIC of *m/z* 169 and 195 (in red), *m/z* 201 and 227 (in blue); (c) XIC of *m/z* 155 and 181(in red), *m/z* 187 and 213 (in blue).

We can also confirm the existence of $\Delta^{9,11}$ CLA positional isomers at 7.3 min as *trans*9, *trans*11- CLA and at 12.8 min as *cis*9, *trans*11- CLA (proved by the addition of a standard of *cis*9, *trans*11- CLA in the sample). We notice that the peak at 10.8 min in XIC of *m/z* 187 and 155 are much wider and of much higher intensity than the corresponding peak in XIC of *m/z* 213 and 181 (**Figure 4-9(c)**). This is because the abundant methyl oleate (*cis*9-18:1) elutes just behind *cis*9, *trans*11- CLA and the characteristic ions indicating Δ^9 double bond are also *m/z* 187 and 155. Despite this coelution, extracting the two pairs of characteristic ions still allows for the correct identification of *cis*9, *trans*11- CLA.

Thus, by using Ag^+-LC/O_3-MS we are able to positively identify six CLA isomers including *trans*(or *cis*)11, *cis*(or *trans*)13- CLA at 10.5 min, *trans*10, *trans*12- CLA at 6.9 min, *trans*(or *cis*)10, *cis*(or *trans*)12- CLA at 11.2 min, *cis*(or *trans*)10, *trans*(or *cis*)12- CLA at 11.6 min, *trans*9, *trans*11- CLA at 7.3 min and *cis*9, *trans*11- CLA at 12.8 min (**Figure 4-9**) in the milk fat sample.

Unlike other reports that used multiple Ag^+-LC columns in series, resulting in long separations for CLA isomers [91], only a 30 min isocratic separation on a single column is needed in this study to provide adequate separation of the CLA isomers. Then, the in-line O_3-MS results can be used for the *de novo* identification of CLA positional isomers irrespective of any coelution or interference. In addition, the poor retention time stability often seen with Ag^+-LC and also observed in our study, has no impact on CLA positional isomer identification since the *de novo* assignment only depends on the extraction of the two pair of characteristic ions listed in **Table 4-1** instead of a comparison against

the retention times of CLA standards. This is especially an advantage for complex lipid samples containing a low abundance of CLA isomers.

4.3.2.3. Lipid extract from L. plantarum culture

Although animal studies testing the activity of CLA show promise, conflicting results have arisen in studies attempting to show human health benefit when natural sources of CLA were used, for example CLA from food grade bacteria [114]. This inconsistency could relate to the fact that different CLA isomers may elicit a different biological response, and at the same time suitable methods for identification of CLA isomers at low concentration are still lacking. *Lactobacillus* species have a safe history of use in food production and can be utilized to transform linoleic acid to CLA for human consumption [114,115]. However, a majority of studies do not report on the geometric isomers produced by *Lactobacillus* species and other food-grade bacteria [114,115]. Here, we have employed *L. plantarum* for bioconversion of linoleic acid as it is known to produce *trans*9, *trans*11-, *cis*9, *trans*11-, and *trans*10, *cis*12-CLA [116,117].

A lipid extraction from *L. plantarum* culture was purified and converted to FAME for analysis by the Ag^+-LC/O_3-MS method. The XICs of the two pairs of characteristic ions clearly show the presence of $\Delta^{8,10}$, $\Delta^{9,11}$, $\Delta^{10,12}$ and $\Delta^{12,14}$ CLA positional isomers (**Figure 4-10**), and the retention times allow for the partial assignment of CLA geometric isomers. Finally, it can be concluded that *trans*9, *trans*11- (8.2 min), *cis*9, *trans*11- (12.9 min), *trans*10, *trans*12- (7.8min), *trans*10, *cis*12- (11.8min), *trans*12, *trans*14- (6.1min) and *trans*8, *trans*10- CLA (9.5min)

are found in *L. plantarum* culture sample. Hence, in addition to CLA isomers previously elucidated from the conversion of linoleic acid by *L. plantarum*, the use of the Ag^+-LC/O_3-MS method in this study has revealed that three additional CLA isomers are also produced. These additional, previously unidentified isomers may partially be responsible for the lack of definitive and reproducible results in human studies involving CLA from lactobacilli cultures.

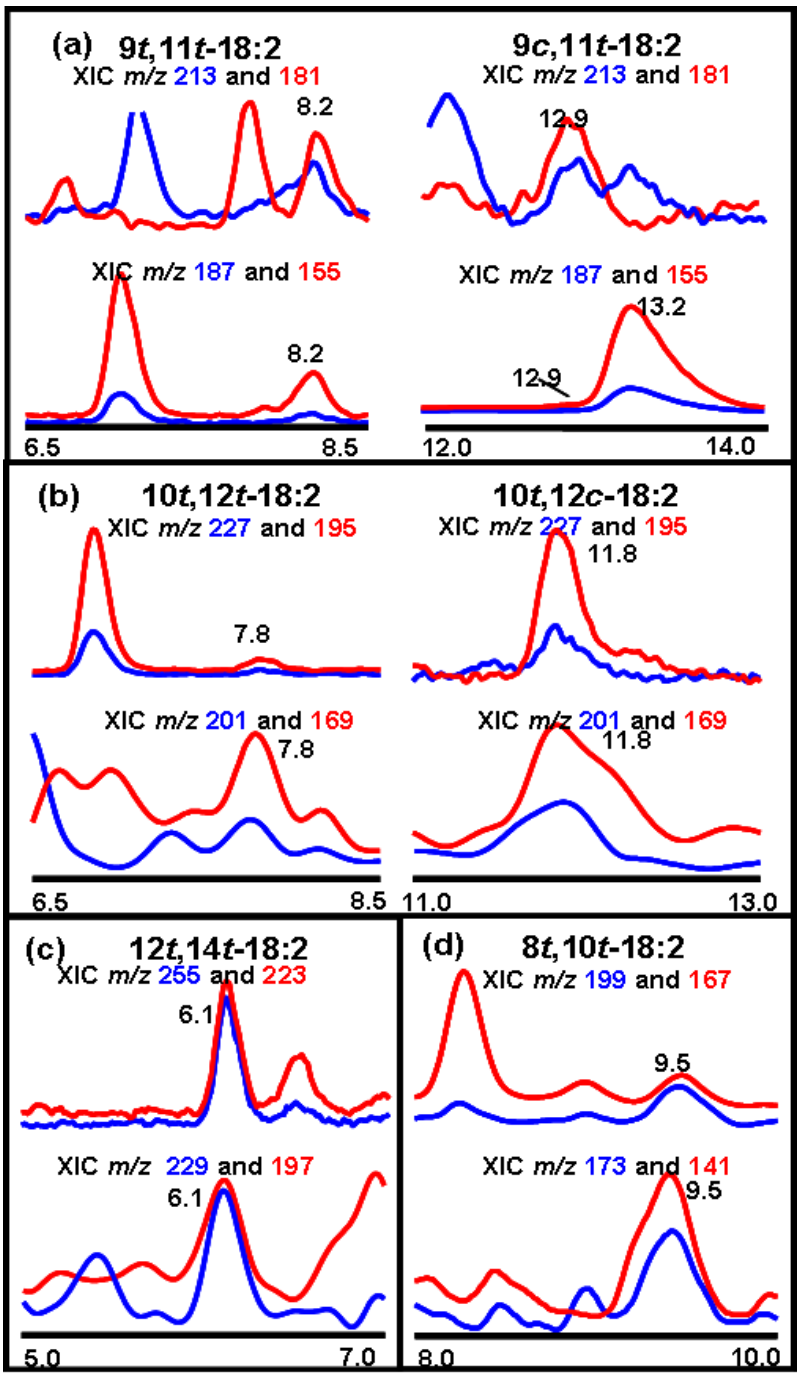

Figure 4-10. The Ag^+-LC/O_3-APPI(+)-MS analysis of a lipid extract from *L. plantarum* culture. Each identified CLA isomer is indicated by its retention time. (a) XIC of *m/z* 155 and 181(in red), *m/z* 187 and 213 (in blue); (b) XIC of *m/z* 169 and 195 (in red), *m/z* 201 and 227 (in blue); (c) XIC of *m/z* 197 and 223 (in red), *m/z* 229 and 255 (in blue); (d) XIC of *m/z* 141 and 167 (in red), *m/z* 173 and 199 (in blue).

4.4. Conclusions

In this study, we have demonstrated that ozonolysis product aldehyde ions from in-line O_3-MS can be used for the identification of CLA positional isomers. Coupling Ag^+-LC to in-line O_3-MS successfully identifies CLA positional isomers and most of geometric isomers in complex samples, which has been shown in the analysis of CLA isomers in a CLA supplement and even complex lipid mixture such as milk fat and lipid extract of *L. plantarum* culture. Since the diagnostic ozonolysis aldehyde ions and methanol loss fragment ions are predictable, it is easy to extract these target ions (**Table 4-1**) for the *de novo* identification of CLA positional isomers. Furthermore, the Ag^+-LC/ O_3-MS method is unaffected by the retention time instability of Ag^+-LC columns because the identification solely relies on extracting the diagnostic ions without reference to the retention times of CLA standards. Future work will apply Ag^+-LC/ O_3-MS for quantitation of CLA, dependent on the availability of suitable isotopically labeled internal standards. In summary, the Ag^+-LC/ O_3-MS method described here could be expected to facilitate the fast and direct identification of the CLA isomers present in lipid extracts from any source.

CHAPTER 5

Elucidation of Phosphatidylcholine Isomers using Two Dimensional Liquid Chromatography coupled in-line with Ozonolysis- Mass Spectrometry [5]

5.1. Introduction

Phospholipids (PL) are important structural and functional components of cell membranes [1]. Phosphatidylcholine (PC), which is comprised of the characteristic choline head group and fatty acyl chains at *sn*-1 and *sn*-2 position of the glycerol backbone, is the most abundant PL class in eukaryotic cell membranes. The chain length, number and position of double bonds along the fatty acyl chains of PC can greatly influence the structural and dynamic properties of membranes. For example, membrane fluidity is at a maximum when the double bond is located in the middle of the fatty acyl chain [118]. Despite the importance of double bond locations to the function of phospholipids, it remains a challenge in lipidomic studies to differentiate all of the isobaric species that may exist. Strategies to differentiate between phospholipid isomers with different head groups have been described [119] but assumptions are often made in order to assign substituent fatty acid isomers.

[5] A version of this chapter has been published. Sun, C., Zhao, Y. and Curtis, J.M. *J. Chromatogr. A* 2014, *1351*, 37-45.
Reprinted with permission.

The use of electrospray ionization- mass spectrometry (ESI-MS) not only achieves sensitive detection of PL [120], but also can achieve the identification of PL classes and even PL molecular species when combined with the high separating power of liquid chromatography (LC) [14,121,122]. Normal phase LC (NPLC) retains analytes based on their polar interaction with a silica stationary phase. Thus, PL are separated into classes, depending on the nature of their head group, such that the more polar PL class has a longer retention time (t_R) in NPLC. Chloroform, methanol, hexane and 2-propanol are typical mobile phases used for NPLC separations of PL classes but in addition, electrospray compatible aqueous buffers such as ammonium hydroxide and ammonium formate are also added in the mobile phase to improve peak shape and response [122-124]. Reverse phase LC (RPLC) has been mainly used for the separation of molecular species within a single PL class, since the hydrophobicity of acyl chains depends on the chain length and the number of double bonds. Both isocratic [125-127] and gradient elutions [128] on C18 columns have been used for the separation of PC molecular species in food and biological samples. When the retention orders of PC molecular species were established under different separation conditions, most species retained the same relative elution order, which could be helpful for the identification of unknown PC isomers. However, differences in PC elution orders were found between literature reports, probably due to differences in mobile phase composition [125-127]. Furthermore, despite achieving good separations between PC species, many PC assignments remain ambiguous especially for those identified by LC methods not compatible with MS.

Due to the natural diversity present within PL classes and molecular species, no single technique can provide adequate separation for all PL molecules. Hence, the idea of combing the NPLC separation of PL classes and the RPLC separation of molecular species was proposed in order to achieve a nearly complete separation of all PL molecules in complex biological samples [129]. Houjou et al used NPLC to separate PL extracts into classes that were separately collected then analyzed by C30 RPLC/ESI-MS for molecular species identification [130]. This off-line two dimensional (2D) LC/MS experiment did reveal the diversity of PL species present in rat liver, but had some disadvantages due to the need for fraction collection, potentially leading to sample loss and oxidation. The first application of on-line NPLC×RPLC/MS analysis for PL profiling was realized by a solvent-evaporating interface [131]. In this system, the mobile phase from the NPLC first dimension was evaporated by a vacuum pump at the interface; then the mobile phase from RPLC passed through the interface and transferred the fraction into the second dimension C18 column for further molecular species separation. In this way, the problem of immiscibility between the mobile phases from NPLC and RPLC was solved, and the components of interest were also enriched at the interface. Another solution to the problem of solvent incompatibility between NPLC and RPLC is the use of hydrophilic interaction chromatography (HILIC), a version of NPLC. However, unlike other NPLC that uses high proportions of organic solvents, a partially aqueous mobile phase with a polar organic solvent such as acetonitrile can be used on a HILIC column. A stop-flow 2D-LC/MS method for PL analysis was

recently developed in which 23 fractions separated by HILIC were collected and injected onto a C18 column for species separation via a 100 μL sample loop [132].

Even though MS and tandem MS (MS/MS) have emerged as powerful tools for the structural elucidation of PL, they still fail to provide some key aspects of PL structure information such as the position of double bonds in the fatty acyl chains that are critical to certain biological function. The assignment of the specific fatty acyl chains still relies heavily on the natural abundance of the fatty acids that are present in the PC fraction, as determined by gas chromatography coupled to flame ionization detector (GC-FID) following PC hydrolysis and methylation [133-135]. However, this is not a definite identification of the fatty acyl substituents of a particular PC molecular species. In order to confirm the identification of unsaturated fatty acids where many positional isomers are possible, GC coupled to electron ionization mass spectrometry (GC/EI-MS) analysis was performed on dimethyloxazolines (DMOX) derivatives of fatty acids from PC [17,123]. In another approach, multiple-stage MS (MS^n) analysis of lithiated adducts of PL was performed on a linear ion-trap mass spectrometer. The product ions arising from MS^n scans of $[M+Li]^+$ and $[M-H+2Li]^+$ ions were used for assignment of the polar head group and fatty acyl substituents, as well as for the localization of double bonds along the chains [136]. However, not all mass spectrometers have the capacity of performing MS^n analysis and this method is likely only suitable for major PL species.

Ozone-induced dissociation (OzID-MS) is another approach for the determination of double bond locations that has been shown to be applicable to PL [39]. During OzID-MS analysis, ozone vapor was introduced into an ion trap MS for *in-situ* ozonolysis, and the ozonolysis products with characteristic *m/z* were used for localization of double bonds in PL. However, this may not be directly compatible with LC and introduction of ozone into the mass spectrometer is needed. In order to have an ozonolysis method compatible with LC separations of complex lipid extracts, we have developed a method utilizing a type of gas-permeable, liquid-impermeable Teflon tubing as an in-line ozonolysis device (O_3-MS) (Chapter 3) [101]. In the O_3-MS experiment, a length of the semi-permeable tube passes through a glass chamber filled with ozone. The ozone penetrates the tubing walls and reacts with unsaturated lipids in the sample within the mobile phase flowing along the tube. The characteristic ozonolysis products that result from the oxidative cleavage of double bonds are then detected in real- time by MS. With an LC column placed prior to the in-line ozonolysis device, each eluting compound can undergo ozonolysis at the site of any unsaturations. Hence, double bond positions from complex lipid mixtures can be determined, as we have demonstrated for fatty acid methyl ester mixtures (Chapter 3 and 4) [101,137]. Potentially, this approach could also be applied to lipid extracts for the identification of PL molecular species.

In this study, we further develop in-line O_3-MS method for the unambiguous assignment of double bond positions in both fatty acyl chains of PC molecules. On-line 2D-LC is developed for the separation of PC molecular

species, and the 2D-LC is also coupled to in-line O_3-MS for the detailed structural determination of PC molecules in the mixture. In addition, 2D-LC/O_3-MS approach is applied to the rat liver PL extract for the identification of PC molecular species.

5.2. Experimental

5.2.1. Nomenclature

We adopted as much as possible the nomenclature and abbreviation conventions from Fahy et al [8]. Diacyl-phosphatidylcholine is described by the PC (n:j/s:t) nomenclature, where n is the number of carbon atoms and j is the number of double bonds in one substituent; s is the number of carbons, and t is the number of double bonds in the other substituent. They only indicate the composition of these two chains; the order does not necessary represent their *sn*-1 or *sn*-2 position, except for the PC standards. In this study, it is advantageous to locate the double bond by counting from the terminal methyl group, thus the "*n*-" terminology is used. For example, 1-octadecanoyl-2-(9Z,12Z-octadecadienoyl)-*sn*-glycero-3-phosphocholine is expressed as PC(18:0/18:2 (*n*-6,9)).

5.2.2. Materials

HPLC grade water, tetrahydrofuran (THF), chloroform, methanol, acetonitrile (ACN), isopropanol (IPA) were purchased from Fisher Scientific Company (Ottawa, ON, Canada). HPLC grade ammonium formate and formic acid were obtained from Sigma (St. Louis, MO, USA). All the standards PC(18:0/22:6(*n*-3,6,9,12,15,18)), PC(18:0/20:4(*n*-6,9,12,15)), PC(18:1(*n*-

9)/18:1(*n*-9)), PC(18:0/18:2(*n*-6,9)), PC(18:1(*n*-12)/18:1(*n*-12)) and PC(18:0/18:1(*n*-9)) were purchased from Avanti polar lipids, Inc. (Alabaster, AL, USA). Each standard solution was prepared in methanol at a concentration of 200 μg/mL. The Teflon AF-2400 tubing (0.020" OD, 0.010" ID) was purchased from Biogeneral Inc. (San Diego, CA, USA).

5.2.3. Extraction of PL from rat liver

Rat livers from suckled rats were collected and ground in liquid nitrogen. The ground rat liver was used as the sample for PL extraction according to a modified Bligh and Dyer method developed by Xiong et al [138]. In brief, 100 mg of samples were mixed with 2 mL of extraction solvent (chloroform/methanol/water, 1:2:0.8) and homogenized at 10,000 rpm for 5 min with a Polytron PT1300 D homogenizer (Kinematica AG, Switzerland) and then centrifuged at 3000 rpm for 5 min. The extraction procedure was repeated three times and all of the supernatants were combined in a 10 mL volumetric flask and made up to volume with methanol. The extract solution was diluted a further 10-fold with methanol prior to analysis.

5.2.4. LC and MS instrument

An Agilent 1200 series HPLC system (Agilent Technologies Inc, Palo Alto, CA, USA) coupled to a hybrid quadrupole time - of - flight mass spectrometer (QSTAR Elite, Applied Biosystems/MDS Sciex, Concord, ON, Canada) with ESI source was used for all the LC-MS analysis. The mass spectrometer was tuned using the ion at *m/z* 879.9723 and fragment ion at *m/z*

110.0713 obtained by infusing porcine renin substrate tetetradecapeptide into the ESI ion source in the positive ion mode and at a resolution of above 10,000 (full width at half maximum). This solution was also used for calibration of the mass range *m/z* 100-1,300 under ESI (+). Taurocholic acid (*m/z* 514.2844 and the fragment ion at *m/z* 79.9568) was used for calibration of the mass range *m/z* 70-1500 under ESI (-). The ion source temperature was kept at 375 ºC and the ionspray voltage was at 5500V for positive (ESI (+)) and -4500V for negative ionization mode (ESI (-)). Source region nitrogen gas flows assigned by the data system in arbitrary units were as follows: curtain gas 25; auxiliary gas 10, nebulizing gas 50. The declustering potential (DP), focus potential (FP), and DP2 were 40 V, 150 V, 10 V and -40 V, -150 V, -10 V for ESI (+) and ESI (-), respectively. MS/MS analysis was performed using collision induced dissociation (CID) with collision gas at 8, and collision energy of 35 eV under ESI (+) and -38 eV under ESI (-). Analyst QS 2.0 software was used for data acquisition and analysis.

5.2.5. On-line 2D-LC

A 10-port 2-position switching valve (Rheodyne, Rohnert Park, CA) was used to interface between the HILIC column as the first dimension of LC and the C18 column as the second LC dimension (**Scheme 5-1**). The conditions of gradient separation used for the HILIC column and isocratic separation used for the C18 column were shown below.

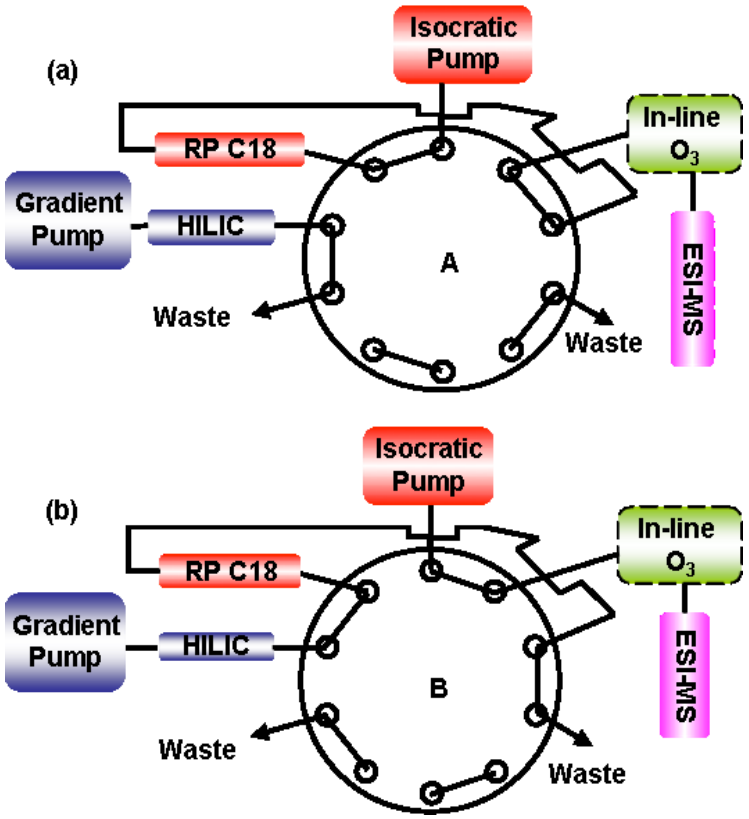

Scheme5-1. The 2D-LC/MS configuration: (a) valve position A (b) valve position B.

5.2.5.1. First dimension- HILIC

Gradient elution on an Ascentis Express HILIC column (2.1 mm i.d.×150 mm, 2.7 µm particles) (Sigma, St. Louis, MO) was used for PL class separation. The mobile phase A was ACN and B was 10 mM ammonium formate in water at pH 3.0, adjusted using formic acid. The gradient was as follows: 0–0.1 min, 8% B; 0.1–10 min, from 8% to 30% B; 10.0-10.1 min, from 30% to 95% B, and hold at 95% B until 17 min; then back to 8% B at 17.1 min until the end of run at 30 min. The flow rate was at 0.2 mL/min except the period between 23.0 and 29.0 min which was at 0.4 mL/min for quicker equilibrium of the column.

5.2.5.2. Second dimension- C18 RPLC

An Ascentis Express C18 column (2.1 mm i.d. ×150 mm, 2.7 μm particles) (Supelco, Bellefonte, PA USA) was used for RPLC separation of PC molecular species. The isocratic mobile phase at 0.475 mL/min (selected to maximize flow rate at acceptable back-pressure) was composed of THF: ACN: IPA: 10 mM ammonium formate in water at pH 3.0 (5:20:16:9, v/v/v) at 60 ºC, modified from the method used by Dugo et al [132]. Both dimensions of LC and the switching valve were controlled by Analyst software. The valve switching program was: 0-8.2 min, valve at position A; 8.2-9.0 min, valve at position B; 9.0-30 min, valve at position A (see **Scheme 5-1**).

5.2.6. In-line O_3-MS analysis of PC molecular species

The development and setup of the in-line ozonolysis device was described in detail in Chapter 3 [101]. Briefly, a 20 cm length of gas permeable and liquid impermeable Teflon tube passed through a chamber filled with oxygen and ozone gas (ozone concentration 56.2 g/m^3) at room temperature. One end of the tube was connected to the 10-port 2-position switching valve; the other end was directly connected to the ESI source, as seen in **Scheme 5-1**. All the PC species eluting from the C18 column passed through the semi-permeable tube where ozone vapor immediately reacted with the carbon-carbon double bonds in the PC molecules. The ozonolysis products were then carried directly towards the ESI source by mobile phase for ESI-MS analysis.

5.3. Results and Discussion

5.3.1. MS and in-line O_3-MS analysis of PC standards

The following experiments were performed in order to illustrate how detailed PC structural information can be obtained, including fatty acyl chain composition and double bond locations. Firstly, flow injection ESI-MS and ESI–MS/MS was performed to identify molecular formulae and fatty acid compositions. This was followed by in-line O_3-MS analyses to locate double bond positions.

5.3.1.1. MS analysis of PC

ESI (+)-MS analysis was performed on PC(18:1(*n*-9)/18:1(*n*-9)) and PC(18:0/20:4(*n*-6,9,12,15)) using ACN/ water with 10 mM ammonium formate (85:15, v/v) as the mobile phase at 0.2 mL/min. Since the phosphate anion in PC can be easily protonated, PC(18:1(*n*-9)/18:1(*n*-9)) and PC(18:0/20:4(*n*-6,9,12,15)) readily form $[M+H]^+$ ions at *m/z* 786 and 810. The following MS/MS analysis of these two $[M+H]^+$ ions reveals fragments that are phosphocholine ions at *m/z* 184 as the dominant products, as expected for all choline containing PL. Due to the high intensity of *m/z* 184 fragment ions, other fragment ions that might be used for the determination of fatty acyl chain composition, are barely observed under ESI(+)-MS/MS. As a result, it is necessary to perform ESI(-)-MS and MS/MS analysis to identify the fatty acyl composition. Under the conditions used, formate adduct $[M+ HCOO]^-$ at *m/z* 830 and 854 for PC(18:1(*n*-9)/18:1(*n*-9)) and PC(18:0/20:4(*n*-6,9,12,15)) are formed under ESI(-). Although CID of $[M+ HCOO]^-$ at *m/z* 830 and 854 yields the demethylated ions $[M-CH_3]^-$ at *m/z* 770 and

794 as the main product ions, likely due to loss of a choline methyl group, fatty acid carboxylate anions are also generated with high intensity which can be used to assign PC fatty acyl chain composition (**Figure 5-1**). In **Figure 5-1a**, the product ion at *m/z* 281 corresponds to 18:1 fatty acid chains in PC(18:1(*n*-9)/18:1(*n*-9)), and the very low intensity product ions at *m/z* 488 and 506 are due the loss of a methyl group plus the 18:1 fatty acid chain or the 18:1 ketene, respectively. Similarly in the MS/MS spectrum of the ion at *m/z* 854, the product ions at *m/z* 283 and 303 correspond to the 18:0 and 20:4 fatty acid chains while the product ions at *m/z* 508 and 528 arise from the loss of a methyl group plus 18:0 and 20:4 ketene (**Figure 5-1b**). We also notice another fragment ion with much lower intensity at *m/z* 259, which is 44 Da lower than the 20:4 product ion at *m/z* 303. This fragment ion is probably formed by the loss of CO_2 from *m/z* 303, consistent with that observed in other research [123].

Overall, it was found that for unknown sample analyses, even though the intensities of PC molecular ions are generally lower in negative ionization mode than in positive mode, the PC species still need to be analyzed under ESI(-) for the determination of the fatty acid compositions.

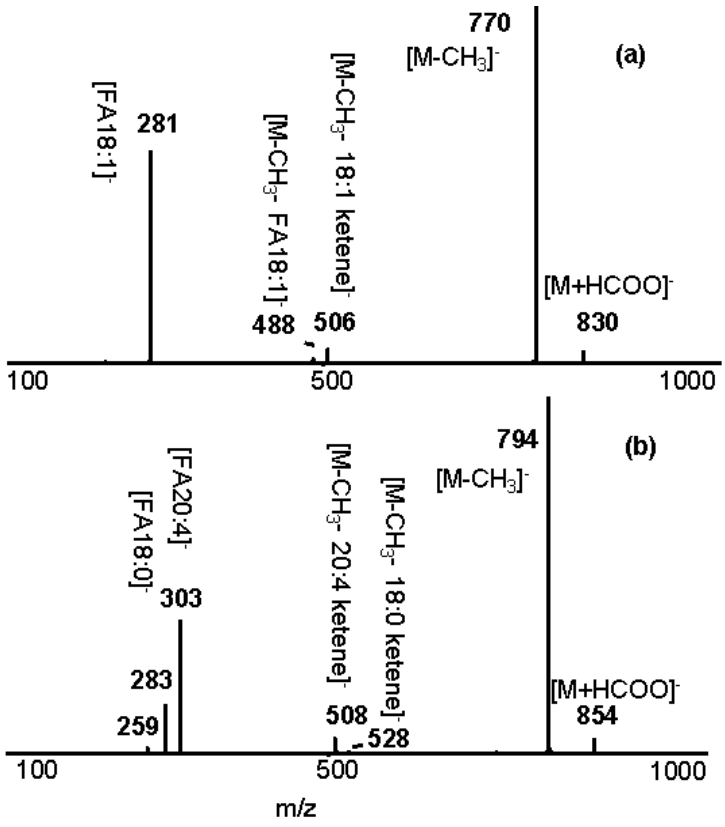

Figure 5-1. ESI(-)-MS/MS analysis of (a) PC(18:1(*n*-9)/18:1(*n*-9)) and (b) PC(18:0/20:4(*n*-6,9,12,15)).

5.3.1.2. In-line O_3-MS analysis

The ESI-MS and -MS/MS analyses of PC reveal the fatty acid composition but no insight into the positions of double bonds can be derived since no product ions characteristic of fragmentation at double bonds are generated. In other work, the in line O_3-MS method has been successfully applied to the determination of double bond positions in fatty acid methyl esters [101]. Here, we expand on this approach for the assignment of double bond positions in the fatty acyl chains of PC.

First, a flow injection of PC(18:1(*n*-9)/18:1(*n*-9)) (400ng) was delivered in the mobile phase (0.4 mL/min) through gas-permeable tubing surrounded by ozone. The resulting ozonolysis products were directly detected under ESI(+)/MS. As seen in **Figure 5-2a**, the ozonolysis product ions at *m/z* 676 and 566 appear in the O_3-MS spectrum along with the intact $[M+H]^+$ ions of PC(18:1(*n*-9)/18:1(*n*-9)) at *m/z* 786. The neutral loss of 110 Da giving the ion at *m/z* 676, is the same neutral loss as that observed previously in the in-line ozonozlysis of 18:1(*n*-9) fatty acid methyl ester [101]. This ion arises from the oxidative cleavage of the *n*-9 double bond located in one of the 18:1 fatty acyl chains. The accurate mass measurement of this ozonolysis product at *m/z* 676.4539 (Δ=1.3 ppm) is consistent with the proposed aldehyde product (see **Figure 5-2a**). The ion at *m/z* 566 corresponds to the other ozonolysis product aldehyde resulting from oxidative cleavage of both *n*-9 double bonds in PC. In-line O_3-MS analysis was also performed on PC(18:0/20:4(*n*-6,9,12,15)), which has a long chain poly unsaturated fatty acid (PUFA) as one of the acyl chains. In addition to the intact $[M+H]^+$ ions at *m/z* 810, ions at *m/z* 742, 702, 662, 622 are present in the O_3-MS spectrum (**Figure 5-2b**). The ozonolysis product ions at *m/z* 742 are due to the neutral loss of 68 Da as expected from ozonolysis of an *n*-6 double bond, as explained in Chapter 3 [101]. The observed mass difference of 40 Da (C_3H_4) between the four ozonolysis product ions is due to the presence of methylene interrupted double bonds. These ozonolysis product aldehydes formed in solution reflect the exact location of double bonds along the 20:4 fatty acyl chain of this PC species, which are at *n*-6, *n*-9, *n*-12 and *n*-15 positions. This is

consistent with the earlier reports of the products from gas phase ozonolysis of PC ions by OzID which were used for the assignment of double bond positions [39].

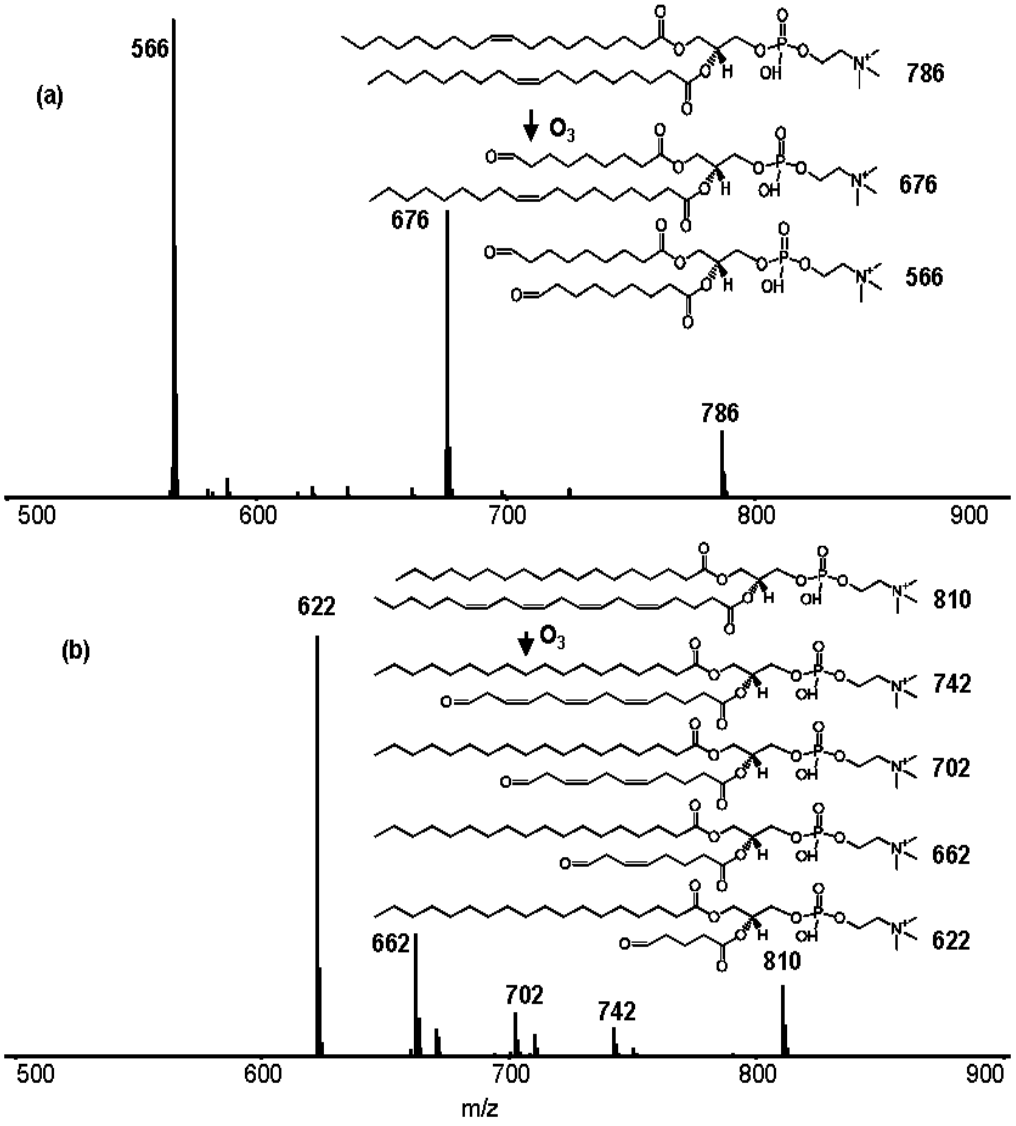

Figure 5-2. In-line O_3-MS spectrum of (a) PC(18:1(*n*-9)/18:1(*n*-9)) and (b) PC(18:0/20:4(*n*-6,9,12,15)) in positive ion mode.

In-line ozonolysis products of PC(18:1(*n*-9)/18:1(*n*-9)) and PC(18:0/20:4(*n*-6,9,12,15)) were also analyzed by ESI(-)-MS and characteristic ozonolysis product aldehydes were observed as formate adducts ions, although at

much lower intensity than the corresponding ions under ESI (+). For this reason, the in-line ozonolysis products of PC are observed under ESI (+) for all the later sample analyses.

In summary, ozonolysis product aldehyde ions that are characteristic of the double bond locations along the fatty acyl chains of PC are observed due to the specific oxidative cleavage of each double bond by ozone vapor. This allows the unambiguous localization of double bonds in the fatty acyl chains of PC.

5.3.2. Development of HILIC×C18 LC

2D-LC using NPLC for PL class separation and RPLC for molecular species separation has shown great promise of comprehensive analysis of PL [122,130,132]. For a natural complex PL sample, such chromatographic separation will not only be necessary for the confident identification of minor species, but also allows for the unambiguous assignment of double bond locations in each PC species by combining with in-line ozonolysis. Here, on-line 2D LC is achieved by using a HILIC column in the first dimension and a C18 column in the second dimension, and is directly coupled to O_3-MS.

5.3.2.1. Optimization of HILIC and C18 LC separation

Recently, we have successfully used gradient elution on a HILIC column for PL class separation in both food and biological samples [138,139]. Using this approach, a PL standard mixture composed of phosphatidylinositol (PI), phosphatidylethanolamine(PE), lysophosphatidylethanolamine(LPE), PC, lysophosphatidylcholine (LPC) and sphingomyelin (SM) was analyzed by

HILIC/ESI (+)-MS under full scan mode. As seen in the total ion current (TIC) chromatogram (**Figure 5-3a**), the PL standard mixture is successfully separated into PI, PE, LPE, PC, SM and LPC with increasing t_R. The PC class elutes between 8.2 and 9.0 min and is well separated from other PL classes. This makes the separation suitable to perform a heart-cut of the PC fraction for the second dimension RPLC separation of molecular species. In general, C18 column separates the PC species by their hydrophobicity due to constituent fatty acyl chains. Equivalent carbon number (ECN) is defined as the number of carbon atom minus two times the number of double bonds in the acyl chains and is used to describe the retention of lipid species on the RPLC column. The PC standard mixture containing six PC molecular species with ECN between 28 and 34 was used to test separation efficiency of the C18 column used here. As seen in **Figure 5-3b**, good separation between PC species with different ECN is realized and the species with higher ECN are retained longer. In addition, isomeric PC species with the same ECN such as PC(18:1(*n*-9)/18:1(*n*-9)), PC(18:0/18:2(*n*-6,9)), PC(18:1(*n*-12)/18:1(*n*-12)) (3,4 and 5 in **Figure 5-3b**) are also almost baseline separated from each other.

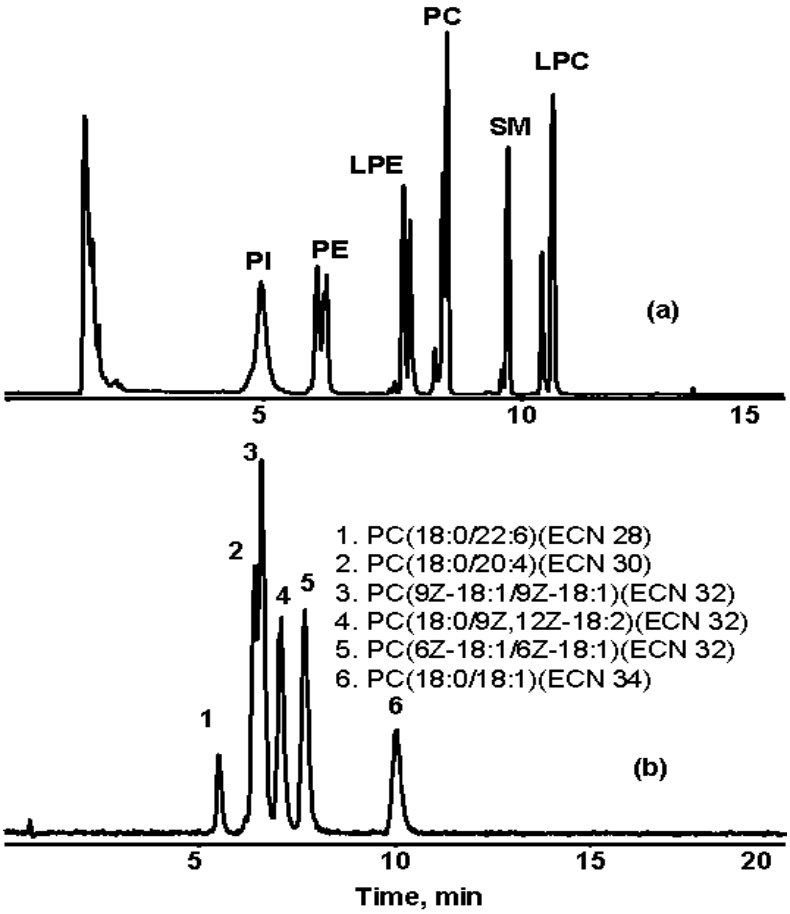

Figure 5-3. (a) HILIC/ESI(+)-MS analysis of a PL standard mixture TIC trace; (b) C18 LC/ESI(+)-MS analysis of a PC standard mixture TIC trace.

5.3.2.2. Configuration of heart-cut HILIC×C18 LC

A 10-port 2-position switching valve is used to divert all of the PC species eluting in the first dimension of LC onto the second dimension of LC, as shown in **Scheme 5-1**. Before 8.2 min, the valve position is at A and all of the eluting PL compounds from HILIC column are discarded. Between 8.2 and 9.0 min, the valve is switched to position B so that the HILIC mobile phase containing the PC fraction is directed onto the C18 column. Then, since the mobile phase from the HILIC column is too weak to elute the PC fraction from C18 column, the PC

fraction is retained at the head of C18 column. After 9.0 min, the valve switches back to position A and a mobile phase with much higher strength in RPLC passes through the C18 column allowing the PC molecular species to elute according to their hydrophobicity. During this period the HILIC eluent goes to waste.

In on-line 2D-LC separations, peak distortion and band broadening in the second dimension of LC can be encountered due to immiscibility of the mobile phases [140]. In this study, HILIC was used as the first LC dimension since the mobile phase used in HILIC column is completely miscible with that used in C18 column. Furthermore, band focusing onto the head of the second dimension C18 column is achieved between 8.2- 9.0 min (valve position B) due to the relative strength of the HILIC mobile phase on the C18 column. The C18 column used in this work is composed of particles having a solid core and a porous shell [141]. These fused-core columns allow fast separations without high back pressure and at flow rates that are still compatible with ESI (0.475 mL/min was used in this work). The relatively high flow rate into the 2.1 mm ID second dimension C18 column also allows for fast equilibrium of this column after valve switching. In addition, the column used is composed of 2.7 μm fused-core particles that provide high peak resolution and separation efficiency comparable to ultra performance LC [141]. Hence, the second dimension column is effective for the separation of many PC molecular species that are present in the sample.

5.3.3. Structural determination of PC molecules in rat liver PL extract

The above results demonstrate that detailed structural identification of a PC in a complex mixture can be achieved. The PL extract is first analyzed by HILIC/MS in positive ion mode in order to obtain the elemental composition of PC and also the retention time of the PC class on the HILIC column. HILIC/MS/MS analysis is then performed in negative ion mode for the determination of fatty acyl chain composition. HILIC×C18 LC/MS analysis is performed for the separation of molecular species in the PC class selected in the first dimension. The second dimension of separation also allows for confirmation of the presence of minor PC species. Finally, 2D-LC is coupled to in-line O_3-MS so that the double bond positions within each molecular species can be assigned unambiguously.

This approach was applied to a PL extract from rat liver for the identification of PC molecular species. This is of interest since it has been shown that hepatic PC biosynthesis can regulate the metabolism of plasma lipoprotein, and it is also related to liver and heart diseases [142].

5.3.3.1. HILIC/MS analysis for the determination of PC composition

2 μL of rat liver PL extract was first analyzed by HILIC/ESI (+)-MS. As expected, the PC class is well separated from other PL classes (**Figure 5-4a**). The mass spectrum averaged across the PC peak at between 8.2 and 9.0 min (**Figure 5-4b**) indicates the presence of many individual PC species. The accurate masses of $[M+H]^+$ ions of these PC species allow determination of their elemental

formulae which are listed in **Table 5-1**. When HILIC analysis was coupled with ESI (-)/MS, PC is present as $[M+ HCOO]^-$ ions that are 44 Da higher in mass than the corresponding $[M+H]^+$ ions formed under ESI(+). This helps to confirm the identification of these PC molecular species (compare **Figure 5-5a** and **Figure 5-4b**).

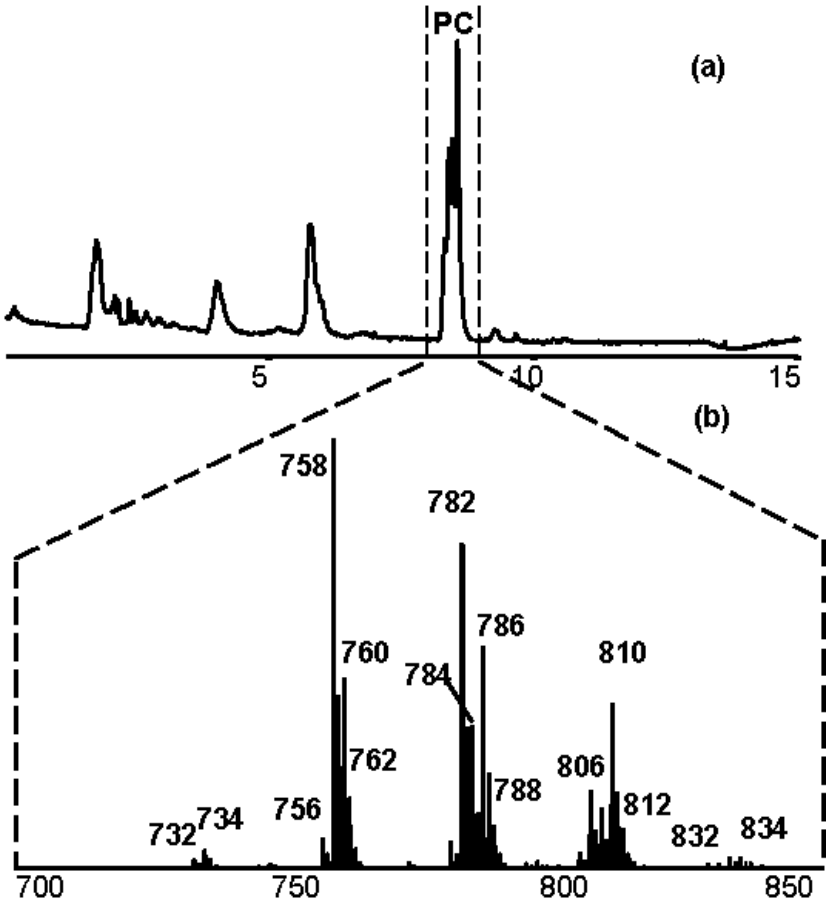

Figure 5-4. (a) HILIC/ESI(+)-MS analysis of rat liver PL extract TIC trace; (b) Mass spectrum of the PC class averaged between 8.2 and 9.0 min.

Table 5-1. PC species identified in rat liver PL extract.

Ion (*m/z*)	Formula	Mass Accuracy (ppm)	Molecular species		t_R (min)	Double Bond Position *n*-	Ozonolysis Product Aldehyde Ions (*m/z*)
732.5534	$C_{40}H_{79}NO_8P^+$	-0.5	PC 32:1 (ECN=30)	16:0/16:1	14.74	*n*-7	650
				14:0/18:1	14.74	*n*-17	510
734.5696	$C_{40}H_{81}NO_8P^+$	-0.5	PC 32:0 (ECN=32)	16:0/16:0	17.01	Saturated	Saturated
756.5535	$C_{42}H_{79}NO_8P^+$	-0.4	PC 34:3 (ECN=28)	16:0/18:3	14.11	*n*-6,9,12	688, 648, 608
				16:1/18:2	13.49	*n*-4/ *n*-9,12	716/ 606,566
758.5712	$C_{42}H_{81}NO_8P^+$	2.3	PC 34:2 (ECN=30)	16:0/18:2	15.15	*n*-6,9	690, 650
760.5814	$C_{42}H_{83}NO_8P^+$	-4.8	PC 34:1 (ECN=32)	16:0/18:1	16.98	*n*-9	650
762.5993	$C_{42}H_{85}NO_8P^+$	-1.8	PC 34:0 (ECN=34)	16:0/18:0	20.14	Saturated	Saturated
782.5706	$C_{44}H_{81}NO_8P^+$	1.5	PC 36:4 (ECN=28)	16:0/20:4	14.76	*n*-6,9,12,15	714, 674, 634, 594
				18:2/18:2	13.77	*n*-6,9/n-6,9	714, 674/ 606,566
784.5823	$C_{44}H_{83}NO_8P^+$	-3.5	PC 36:3 (ECN=30)	16:0/20:3	15.71	*n*-6,9,12	636, 676, 716
				18:1/18:2	15.29	*n*-9/*n*-6,9	674/ 606, 566
786.5995	$C_{44}H_{85}NO_8P^+$	-1.5	PC 36:2 (ECN=32)	18:1/18:1	17.43	*n*-9/*n*-9	676/ 566
				18:0/18:2	17.94	*n*-6,9	718,678
788.6166	$C_{44}H_{87}NO_8P^+$	0.3	PC 36:1 (ECN=34)	18:0/18:1	21.27	*n*-9	678
806.5696	$C_{46}H_{81}NO_8P^+$	0.2	PC 38:6 (ECN=26)	16:0/22:6	14.19	*n*-3,6,9,12,15,18	780, 740, 700, 660, 620, 580
				18:2/20:4	13.50	N/A	N/A[a]
810.5998	$C_{46}H_{85}NO_8P^+$	-1.1	PC 38:4 (ECN=30)	18:0/20:4	17.36	*n*-6,9,12,15	742, 702, 662, 622
812.6159	$C_{46}H_{87}NO_8P^+$	-0.6	PC 38:3 (ECN=32)	18:0/20:3	18.82	*n*-6,9,12	744, 704, 664
832.5821	$C_{48}H_{83}NO_8P^+$	-3.6	PC 40:7 (ECN=26)	18:1/22:6	14.29	N/A	N/A[a]
834.5990	$C_{48}H_{85}NO_8P^+$	-2.0	PC 40:6 (ECN=28)	18:0/22:6	16.49	*n*-3,6,9,12,15,18	808, 768, 728, 688, 648, 608

[a] The ozonolysis product aldehyde ions are too weak to observe.

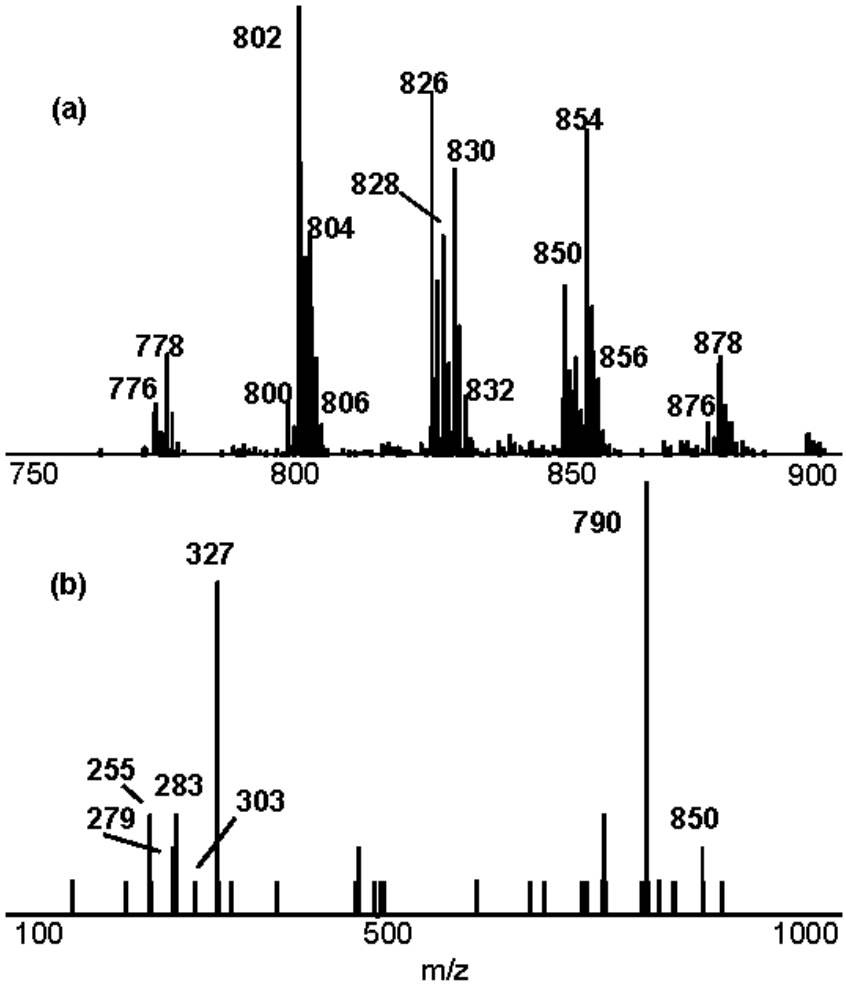

Figure 5-5. (a) Mass spectrum across the PC class from the HILIC/ESI(-)-MS analysis of rat liver PL extract; (b) ESI(-)-MS/MS spectrum of the ion at *m/z* 850 in the rat liver PL extract.

As seen in the MS/MS analysis of PC standards (**Figure 5-1a and b**), CID of $[M+ HCOO]^-$ ions generates carboxylate anions that can be used for the assignment of fatty acyl chains. Hence, ESI (-)-MS/MS analysis of rat liver PL extract was performed under information dependent acquisition (IDA) mode, selecting precursor ions between *m/z* 700 and 1000 of intensity higher than 10 cps. As an example, **Figure 5-5b** is the MS/MS spectrum of the ion at *m/z* 850

from the rat liver sample. The elemental composition of this ion is $[C_{46}H_{80}NO_8P+HCOO]^-$, corresponding to PC 38:6. The product ion at *m/z* 327 is identified as 22:6 fatty acid which indicates that the other fatty acid should be 16:0 according to the elemental composition. This would give rise to a deprotonated ion at *m/z* 255, which is indeed observed in the MS/MS spectrum (**Figure 5-5b**). However, other product ions are also observed, indicating that the PC species at *m/z* 850 is actually a mixture of isomers with different fatty acyl chain combinations. The product ions at *m/z* 303 and 279 correspond to 20:4 and 18:2 fatty acids generated from CID of the isomeric PC(18:2/20:4). We observe the neutral loss of CO_2 from *m/z* 327 (22:6 fatty acid) resulting in the formation of fragment ion at *m/z* 283, similar to the CO_2 loss from *m/z* 303 in the MS/MS spectrum of PC(18:0/20:4) in **Figure 5-1b**, and as described elsewhere [123]. The loss of CO_2 from caboxylate anions of PUFA was also observed for other PC species such as PC(16:0/20:4), PC(18:0/20:4), PC(18:0/22:6) that are present in the sample. Several studies have showed that the *sn*-2 carboxylate anion had higher intensity than *sn*-1 carboxylate anion, which could be useful for the assignment of *sn*-1/*sn*-2 position [120,143]. However, it has been proved that this ion ratio is greatly affected by chain length, degree of unsaturation and the collision energy used during CID [144,145]. For example, the neutral loss of CO_2 from carboxylate anions of PUFA can result in changes in the intensity ratio between *sn*-1 and *sn*-2 fragment ions and so complicate the region-isomer assignment. When it comes to complex natural PL samples, the relative abundances of the carboxylate anion fragments are also affected by the mixture of regio-isomers that co-elute. Hence,

there is considerable uncertainty in assigning the *sn*-1/*sn*-2 positions of fatty acyl chains from relative intensities [146]. Therefore, in this study regio-specific *sn*-1/*sn*-2 position of the fatty acyl chains in PC are not assigned.

5.3.3.2. 2D-LC/MS analysis for molecular species separation

HILIC×C18 LC/MS analysis was first performed on the rat liver PL extract in positive ion mode. There is no peak in the first 8 min of the 2D-LC/MS TIC trace (**Figure 5-6**), since all of the PL fractions eluting before PC class on the HILIC column is discarded. Between 8 and 10 min, there is a fluctuation of the baseline due to the valve switching from A to B and back to the A position while transferring and loading the PC class onto C18 column. The least retaining PC species elutes at around 13.5 min, about 3 min past the baseline fluctuation. Hence, the PC fraction is sufficiently retained by the C18 column to allow the desired further species separation. Other PC molecular species are much better separated from each other on the second dimension C18 column than on the first dimension HILIC column on which they are barely resolved. At least 10 peaks are clearly visible in **Figure 5-6**, indicating the diversity of PC molecular species present in the sample. The extracted ion chromatograms (XIC) also reveal the existence of many other minor PC species, as listed in **Table 5-1**. The retention of most PC species on C18 column increases proportionally with their ECN, which ranged from 26 to 34. However, the PC species containing PUFA as one of the fatty acyl chains retain more strongly than the PC species with even higher ECN. For example, 16:0/18:3 PC (t_R 14.11 min) and 16:1/18:2 PC (t_R 13.49 min) with the same ECN of 28 elute earlier than 16:0/22:6 PC (t_R 14.19 min) with ECN

of 26. This kind of elution exception has also been observed in other studies [126,132] and demonstrates that the use of relative retention times alone for the assignment of specific PC species is insufficient.

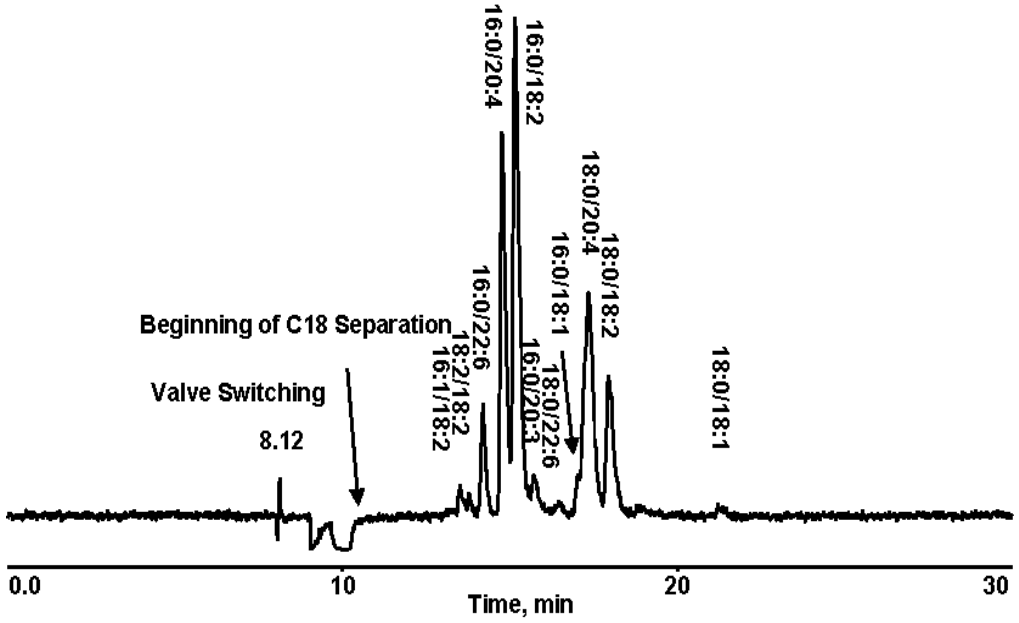

Figure 5-6. The 2D-LC/ESI(+)-MS analysis of rat liver PL extract TIC trace.

In the current second dimensional C18 separation most of the major PC isomeric species are well resolved. For example, in the XIC of the PC 36:4 at *m/z* 782, PC(18:2/18:2) at 13.77 min is well separated from PC(16:0/20:4) at 14.76 min (**Figure 5-7c**). The resolution between other isomeric PC species is also observed in the XIC of PC 38:6 at *m/z* 806 (**Figure 5-7b**), PC 36:3 at *m/z* 784 (**Figure 5-7d**), PC 36:2 at *m/z* 786 (not shown) and PC 34:2 at *m/z* 756 (not shown). A further comparison of t_R within each group of PC isomers also indicates that the isomer with PUFA as one of the fatty acyl chains is normally retained longer than the other PC isomer. For example, PC(16:0/20:4) has a longer retention time than PC(18:2/18:2) (**Figure 5-7c**).

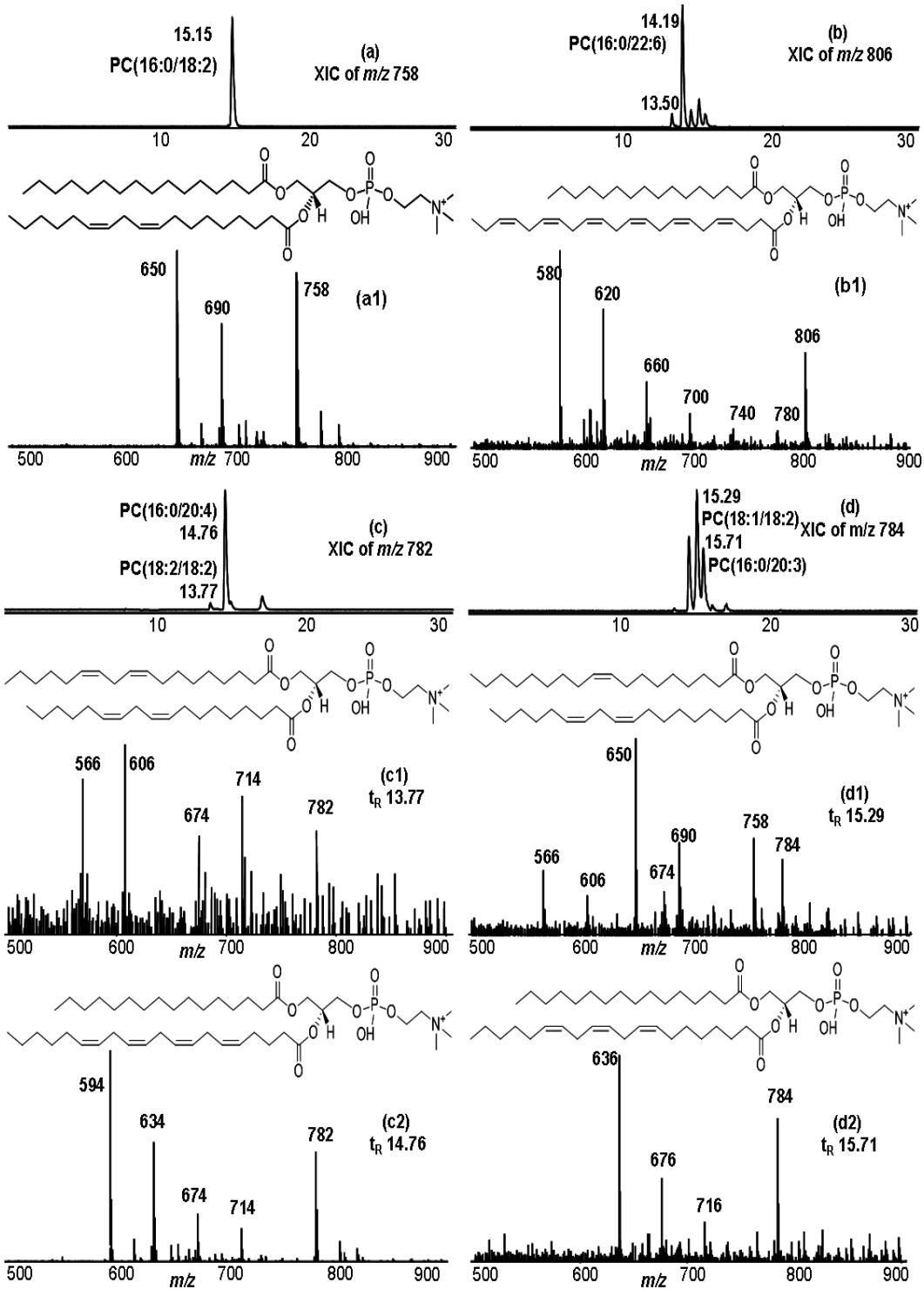

Figure 5-7. XIC of the PC $[M+H]^+$ ion at *m/z* (a)758, (b)806, (c)782 and (d) 784; The O_3-MS spectra of the labeled peak at (a1)15.15 min, (b1)14.19 min, (c1)13.77 min, (c2)14.76 min, (d1)15.29 min and (d2)15.71 min.

5.3.3.3. 2D-LC/O_3-MS analysis for detailed structural elucidation of PC

Although HILIC×C18 LC/MS analysis is successfully used to isolate the PC class and separate PC molecular species, unambiguous identification of each PC species is not possible without the assignment of double bond positions. This may be especially important for PC with PUFA chains with distinctively different biological functions for *n*-3 and *n*-6 PUFA isomers [76]. Hence, the in-line ozonolysis device was placed between the second dimension C18 column and the ionization source of mass spectrometer while keeping other experimental settings the same. Each PC species eluting from the 2D-LC separation passes through the gas-permeable tube surrounded by ozone vapor and the ozonolysis products that are characteristic of double bond positions are detected in real-time by ESI (+)-MS.

Here, the 2D-LC/O_3-MS spectra of the ions at *m/z* 758, 806, 782 and 784 arising from PC species in the rat liver extract are shown in **Figure 5-7**. In **Figure 5-7a1**, the intact PC(16:0/18:2) molecular ion at *m/z* 758 is present along with the ozonolysis product aldehyde ions at *m/z* 690 and 650 indicating that the two double bonds in the 18:2 chain are located at the *n*-6 and 9 positions. This method is also applicable for PC containing PUFA. For example, in **Figure 5-7b1** the ozonolysis product ion at *m/z* 780, 26 Da lower than the $[M+H]^+$ ion of PC(16:0/22:6) at *m/z* 806, is used to assign one of the double bonds at *n*-3 position. Other ions at *m/z* 740, 700, 660, 620 and 580 indicate the locations of the other double bonds to be *n*-6, -9, -12, -15 and -18. Thus, PC(16:0/22:6) must contain docosahexaenoic acid. In **Figure 5-7c**, the PC isomer at 14.76 min is

identified as PC(16:0/20:4) containing arachidonic acid, based on the observation of ozonolysis product aldehyde ions at *m/z* 714, 674, 634 and 594 that are used to locate double bonds at *n*-6,-9,-12,-15 position (**Figure 5-7c2**). The other peak at 13.77 min in the XIC of *m/z* 782 is identified as PC(18:2(*n*-6,9)/18:2(*n*-6,9)) by the O_3-MS spectrum shown in **Figure 5-7c1**. The ozonolysis product ions at *m/z* 714 and 674 with a 40 Da mass difference between them, indicates that they are located at *n*-6 and *n*-9 in one 18:2 chain; the other ozonolysis product ions at *m/z* 606 and 566 are due to oxidative cleavage of the two double bonds located at *n*-6 and *n*-9 in the other 18:2 chain.

A more complicated example of PC containing two unsaturated fatty acyl chains is the PC(18:1/18:2) eluting at 15.29 min (**Figure 5-7d**). In the O_3-MS spectrum of PC(18:1/18:2) (**Figure 5-7d1**), an ion at *m/z* 758 arising from PC(16:0/18:2(*n*-6,9)) (t_R 15.15 min) appears due to a partial co-elution, and the ions at *m/z* 690 ad 650 are its ozonolysis product ions that were described above (**Figure 5-7a1**). Despite this interference, the ozonolysis product ion at *m/z* 674 is used to assign the double bond at *n*-9 in an 18:1 chain; the ions at *m/z* 606 and 566 are due to the ozonolysis of double bonds at *n*-6 and -9 in an 18:2 chain. The isomeric PC at 15.71 min (**Figure 5-7d**) is identified as PC(16:0/20:3(*n*-6,9,12)) due to the presence of ozonolysis product ions at *m/z* 716, 676 and 636 (**Figure 5-7d2**). Using a similar approach, the double bond positions could be determined for virtually all of the PC molecular species that are present in the extract and are listed in **Table 5-1** along with the diagnostic ozonolysis product aldehyde ions. There are only two PC species, PC(18:2/20:4) and PC(18:1/22:6), for which the

double bond positions could not be assigned since both these PC are present in very low abundances and consequently the ozonolysis product ions are too weak to observe.

Overall, 21 PC molecular species were positively identified and the specific fatty acyl chains, including the double bond positions, were assigned for 19 of these PC species. It can be seen that in-line ozonolysis is not only suitable for the determination of double bond positions in PC species that contain only one unsaturated fatty acyl chain such as PC(16:0/22:6), but is also applicable where both PC fatty acyl chains are unsaturated, as shown in **Figure 5-7c1** and **5-7d1**. Isocratic elution on the second dimension C18 column provides adequate separation between PC molecular species in many cases, but co-elutions do still occur and are especially evident where one of the PC species is present in high abundance. However, even in these cases, in-line ozonolysis product aldehydes can still be used for the assignment of double bond positions, as seen for the example shown in **Figure 5-7d1**.

5.4. Conclusions

This study demonstrates that double bond locations within the fatty acid chains of PC molecules can be directly assigned from the ozonolysis product aldehyde ions observed by in-line O_3-MS analysis. The 2D-LC method can achieve both on-line PL class and species separation, in addition to being compatible with in-line ozonolysis. Hence, 2D-LC/O_3-MS allows the unambiguous identification of PC species in complex mixtures. This approach

was successfully applied to a rat liver PL extract for the detailed structural elucidation of PC molecules. Although lipidomic analyses using various LC/MS and MS/MS methods can reveal abundant structural information about lipids in complex mixtures, many isomeric species remain unidentified. The in-line O_3-MS experiment can provide complementary insight into the specific structure of PL molecules and can be easily incorporated into the LC/MS analyses. In addition, the potential exists to develop algorithms that automatically identify the ozonolysis diagnostic product ions, which have predictable *m/z* values, and hence identify specific PC isomers.

CHAPTER 6

Profiling of Phospholipids by Two Dimensional Liquid Chromatography coupled in-line with Ozonolysis- Mass Spectrometry [6]

6.1. Introduction

Glycerophospholipids (GPL) and sphingomyelins (SM), the two main classes of phospholipids (PL), are important structural and functional components of eukaryotic cell membranes [1]. Dietary PL from animal and plant sources often with unsaturated fatty acids (FA) located at the *sn*-2 position, can be delivered and incorporated directly into the cell membranes [147]. Thus, the fatty acid composition of dietary PL can potentially change membrane components of certain cells and so ultimately influence cellular function and have implications in the treatment of diseases. For example, in a mouse model dietary intake of SM has shown a preventive effect on the formation of colon cancer [148]. Also, an *n*-3 polyunsaturated fatty acid (PUFA) rich GPL extract from a marine source has shown a blood cholesterol lowering effect in patients suffering from hyperlipidaemia [149]. Since PL are known to be safe and ubiquitous components in food, a recommendation to increase dietary intake of specific PL for the prevention of disease does not carry the risks associated with an increased consumption of other non-food compounds. Therefore, a systematic study of the

[6] A version of this chapter has been submitted for publication.

PL profile of foods may increase understanding of how PL interacts with other metabolites after digestion and absorbance, which may lead to results that could be beneficial in studies of nutrition and health.

GPL can be divided into different "classes" depending on the polar head group at the *sn*-3 position of the glycerol backbone, such as phosphatidylethanolamine (PE), phosphatidylinositol (PI), phosphatidylcholine (PC) and phosphatidylserine (PS). Within each class, a range of molecular species exists due to different fatty acid substituents at *sn*-1 and 2 positions. In lipidomics, electrospray ionization mass spectrometry (ESI-MS) and tandem MS (ESI-MS/MS) have become powerful tools for analysis of PL species [120,125,129]. Since most PL molecules have a characteristic head group, lipidomic studies can target these characteristic features by using specific scanning modes, such as a precursor ion scan of *m/z* 184 for choline-containing PL, and a neutral loss scan of 260 Da for PI. Such experiments can be used for both identification and quantification of these PL classes [150,151]. Since ion suppression can occur in ESI when multiple species co-elute and thus compete in the ESI process, an attempt must be made to optimize chromatographic separations of complex lipids mixtures. A long established strategy in PL separation is the use of normal phase liquid chromatography (NPLC), which can be used for class separation of PL prior to MS analysis [122]. Even though the number of PL species that can be identified increases greatly after NPLC class separation, the lack of separation between species within each PL class means that only the major molecular species can be positively identified by NPLC-MS

methods. Thus, two dimensional LC (2D-LC) using NPLC for PL class separation combined with reverse phase LC (RPLC) for molecular species separation is highly desirable for the detailed analysis of a complex PL mixture. This approach has been described in a few recent studies. In a PL profiling study of rat liver, the PL extract was first separated by NPLC, then the PE and PC fractions were collected off-line and injected onto a C30 column for further molecular species separation. Identification of the individual molecular species containing targeted fatty acyl chains was achieved by a precursor ion scan of targeted carboxylate anions $[RCOO]^-$ under ESI (-) [130]. Later, PL profiling in biological and food samples was achieved by on-line 2D-LC/MS, employing a multiple-port, 2-position switching valve and a sample loop as the interface [131,132,140]. For the analysis of a milk PL extract, 23 fractions of PI, PE, PS, PC, SM and lysophosphatidylcholine (LPC) from the first dimensional hydrophilic interaction liquid chromatography (HILIC) column, were injected one at a time onto the second dimensional C18 column under the stop-flow mode during one analysis. In this work, the mass measurements of PI $[M-H]^-$ ions and of the $[M+H]^+$ ions of other PL classes, were used for the identification of molecular species. These were also confirmed using PL standards and by comparison with literature results [132].

In general, 2D-LC/MS and -MS/MS analyses have revealed a large diversity in both PL classes and in PL molecular species within each class. However, the identification of a specific molecular species may rely on a combination of LC/MS analysis with the separate identification of the overall

fatty acid profile, as determined by gas chromatography coupled to flame ionization detector (GC-FID) [133,134] or from the literature [132,139,152]. A necessary part of the full identification of fatty acids is the specific assignment of double bond positions. In GC-FID, this can often be achieved via the retention times of fatty acid methyl ester (FAME) derivatives. In other cases, the fatty acids from hydrolysis of PL have been converted into dimethyloxazolines (DMOX) derivatives. Under conditions of electron ionization mass spectrometry, DMOX derivatives of fatty acids undergo charge remote fragmentations and these fragmentation patterns can reveal double bond locations [17,123]. However, in these GC/MS analyses of DMOX or FAME derivatives, the precise PL molecular structure is lost and the derivitization procedures add additional complexity to the analysis.

Recently, we have successfully coupled on-line 2D-LC with in-line ozonolysis-MS (O_3-MS) to allow the detailed structure determination of PC molecular species, as demonstrated for a PL extract from rat liver (Chapter 5). In that study, HILIC/MS analysis was first performed on the PL extract under ESI (+) for the separation PL classes. From these data, the elemental compositions of all PC species were determined. HILIC/MS analysis was also performed under ESI (-), during which the collision induced dissociation (CID) of PC formate adducts generated carboxylate anions $[RCOO]^-$ that were used for the determination of the molecular formulae for the fatty acyl chains present in PC. Then, 2D-LC was developed for the on-line separation of PC molecular species. The fraction containing PC species eluted from the first dimension HILIC column

at between 8.2 and 9.0 min were directly injected onto the second dimension C18 column through a 10-port 2-position switching valve. The PC molecular species, eluting from the HILIC × C18 LC separation, then passed through the ozonolysis device that was connected between the C18 column and the ESI source. The ozonolysis device is a length of gas-permeable Teflon tube that passes through a chamber filled with ozone vapor, as described in Chapter 3 [101]. The ozonolysis reaction occurred for all double bonds in the PC molecules eluting from C18 column and passing through the device. This resulted in the formation of characteristic ozonolysis product aldehydes that were detected as protonated molecular ions under ESI (+), and used for the direct assignment of double bond positions in unsaturated PC species. Therefore, by performing HILIC/MS, HILIC/MS/MS and 2D-LC/O_3-MS analysis the PC molecular species in a complex PL mixture can be unambiguously identified without any off-line derivatization or comparison with standards.

In this study, the in-line O_3-MS method will be applied to PL classes such as PI, PE, SM, lysophosphatidylethanolamine (LPE) and LPC for the direct assignment of double bond positions. The on-line 2D-LC method will also be extended to allow the molecular species separation of other PL classes such as PI and PE. Overall, we show for the first time this strategy can allow for the complete profiling of PL mixtures, including the assignment of each significant molecular species, as demonstrated here for egg yolk PL extract.

6.2. Experimental

6.2.1. Material

HPLC grade water, tetrahydrofuran (THF), chloroform, methanol, acetonitrile (ACN), isopropanol (IPA) were purchased from Fisher Scientific Company (Ottawa, ON, Canada). HPLC grade ammonium formate and formic acid were obtained from Sigma (St. Louis, MO, USA). All the standards PI(18:0/20:4 (*n*-6,9,12,15)), PE(18:0/20:4 (*n*-6,9,12,15)), SM(d18:1/18:1(*n*-9)), LPE(18:1(*n*-9)) and LPC(18:1(*n*-9)) were purchased from Avanti polar lipids, Inc. (Alabaster, AL, USA). Each standard solution was prepared in methanol at a concentration of 200 μg/mL. The Teflon AF-2400 tubing (0.020" OD, 0.010" ID) was purchased from Biogeneral Inc. (San Diego, CA, USA).

6.2.2. Extraction of PL from egg yolk

Fresh eggs were purchased from local markets, and the egg yolks from six eggs were separated from the whites and mixed together. The fresh egg yolks were used for PL extraction according to a modified Bligh and Dyer method [139]. In brief, 100 mg of samples were mixed with 2 mL of extraction solvent (chloroform/methanol/water, 1:2:0.8) and homogenized at 10,000 rpm for 5 min on a Polytron PT1300 D homogenizer (Kinematica AG, Switzerland) and then centrifuged at 3000 rpm for 5 min. The extraction procedure was repeated three times, and all supernatants were combined and made up to 10 mL using methanol. The extract was further diluted 10-fold with methanol prior to analysis.

6.2.3. LC and MS instrument

An Agilent 1200 series HPLC system (Agilent Technologies Inc, Palo Alto, CA, USA) coupled to a hybrid quadrupole time - of - flight mass spectrometer (QSTAR Elite, Applied Biosystems/MDS Sciex, Concord, ON, Canada) with ESI source was used for all the LC-MS analysis. The ion source temperature was kept at 375 ºC and the ionspray voltage was at 5500V for ESI (+) and -4500V for ESI (-). Source region nitrogen gas flows in arbitrary units assigned by the data system were as follows: curtain gas 25; auxiliary gas 10, nebulizing gas 50. The declustering potential (DP), focus potential (FP), and DP2 were 40 V, 150 V, 10 V and -40 V, -150 V, -10 V for ESI (+) and ESI (-), respectively. Analyst QS 2.0 software was used for data acquisition and analysis.

6.2.4. HILIC×C18 LC/MS analysis

The 2D-LC configuration was the same as described in Chapter 5 (**Scheme 5-1**) using a 10-port 2-position switching valve (Rheodyne, Rohnert Park, CA) as the interface between the HILIC column and the C18 column. Separation conditions were modified for the shorter analysis time. The Ascentis Express HILIC column (2.1 mm i.d.×150 mm, 2.7 μm particles) (Sigma, St. Louis, MO) was used as first dimension LC for PL class separation. The mobile phase A was ACN and B was 10 mM ammonium formate in water at pH 3.0, and the flow rate was at 0.2 mL/min. The gradient was as follows: 0–10 min, from 8% to 30% B; 10.0–10.1 min, from 30% to 95% B; 10.1-15.0 min, held at 95% B; 15.0-15.1 min, from 95% to 8% B; 15.1-20.0 min, held at 8% B. In order to

achieve molecular species separation of PI, PE and PC class within 20 min, the Ascentic Express C18 column with half-length of that was used in the study described in Chapter 5 (2.1 mm i.d. × 75 mm, 2.7 μm particles, Supelco, Bellefonte, PA USA) was used as the second dimension LC. The mobile phase at 0.475 mL/min was composed of THF: ACN: IPA: water with 10 mM ammonium formate at pH 3.0 (5:20:16:9, v/v/v) at 45 ºC.

The injection of the fraction from the HILIC column to the C18 column was done by switching the valve from A to B position and back to A position. For PI class, the fraction between 4.0-4.8 min from the first dimension HILIC column was transferred to the second dimension C18 column and detected under ESI (-); For PE and PC, the fractions between 5.6-6.4 min and 8.2-9.0 min were transferred onto C18 column and analyzed under ESI (+), respectively. In this study, LPE, LPC and SM were analyzed by one dimension HILIC/MS instead of 2D-LC/MS, which would be discussed later.

6.2.5. In-line O_3-MS analysis

The method development of in-line O_3-MS approach for double bond position determination has been described in details in Chapter 3 [101]. In this study, a 20 cm length of gas permeable and liquid impermeable Teflon tube passed through a chamber filled with oxygen and ozone gas (ozone concentration 56.2 g/m^3) at room temperature. This ozonolysis device was placed in-line between 2D-LC and ESI source of the mass spectrometer for the analysis of PI, PE can PC molecular species. For the analysis of LPE, LPC and SM species,

ozonolysis device was coupled in-line with HILIC column. In this way, each PL species eluting from either the second dimension C18 column or the HILIC column passed through the semi-permeable tube, ozone vapor immediately reacted with carbon-carbon double bonds existing in the molecules, and the ozonolysis products of which would be directly detected by ESI-MS.

6.3. Results and Discussion

In Chapter 5, the mass measurements of PC $[M+H]^+$ ions were used for the determination of elemental compositions. Carboxylate anions $[R_1COO]^-$ and $[R_2COO]^-$ generated from CID of PC $[M+HCOO]^-$ ions were used for the determination of fatty acyl chains compositions. Then, double bond positions in these fatty acyl chains were unambiguously assigned by in-line O_3-MS analysis using the diagnostic ozonolysis product aldehyde ions. In this study, PE, LPE, SM, LPC and PI standards were first used for ESI-MS, MS/MS and in-line O_3-MS analysis to see whether we can get similar structure information as from PC that was achieved by our previous study.

6.3.1. ESI-MS and MS/MS analysis of PE, LPE, SM, LPC and PI standards

Flow injection analysis (FIA) was performed on PI(18:0/20:4 (*n*-6,9,12,15)), PE(18:0/20:4 (*n*-6,9,12,15)), SM(d18:1/18:1(*n*-9)), LPE(18:1(*n*-9)) and LPC(18:1(*n*-9)) standard in positive ion mode using a mobile phase of ACN/ water with 10mM ammonium formate (85/15, v/v). PE, SM, LPE and LPC $[M+H]^+$ ions were observed with high abundance. In contrast, in the ESI (+)-MS spectrum of PI(18:0/20:4 (*n*-6,9,12,15)), the $[M+H]^+$ ion at *m/z* 887 appeared at

very low intensity, and the spectrum was dominated by the ion at *m/z* 627 that arise from the neutral loss of 260 Da. The mass measurement of $[M+H]^+$ ions of LPE and LPC were directly used for the determination of fatty acyl chain composition, since there is only one fatty acyl chain in these molecules. For PE and SM, the mass measurement of $[M+H]^+$ ions were used to deduce the elemental composition. However, the ESI (+)-MS/MS analyses of PE and SM $[M+H]^+$ ions failed to provide fragment ions that could be used for the determination of fatty acyl chain composition. The dominant product ions in these MS/MS spectra arose from the fragmentation of the head group, such as phosphocholine ions at *m/z* 184 for SM, and the product ions from neutral loss of phosphoethanolamine (141 Da) from $[M+H]^+$ ions of PE, which has also been observed in other studies [139,150,153].

FIA of PE(18:0/20:4 (*n*-6,9,12,15)) in negative ion mode resulted in $[M-H]^-$ ions at *m/z* 766. MS/MS analysis using collision energy (CE) at -35 eV of the ion at *m/z* 766 generated carboxylate anions at *m/z* 283 and 303 that are characteristic of 18:0 and 20:4 fatty acyl chains (**Figure 6-1a**). For SM(d18:1/18:1(*n*-9)), $[M+HCOO]^-$ ions at *m/z* 773 were observed by FIA. The MS/MS analysis of these ions using CE of -42 eV (**Figure 6-1b**) resulted in the demethylated ions $[M-CH_3]^-$ at *m/z* 713 as the dominant product ions. A similar ionization and fragmentation pattern was previously observed for MS/MS analysis of PC under ESI (-), since both PC and SM have a phosphocholine head group. However, unlike the MS/MS spectrum of PC, fragment ions directly corresponding to the N-acyl chain or long-chain base (LCB) were not observed

for SM. Instead the ion at *m/z* 449 was observed, which was formed by the neutral loss of N-acyl chain (18:1 ketene) from the demethylated ion at *m/z* 713. Thus, the mass difference between the ion $[M\text{-}CH_3\text{-}\ R_1CO]^-$ (*m/z* 449 in this case) and the demethylated ion $[M\text{-}CH_3]^-$ (*m/z* 713 in this case) can be used to assign the N-acyl chain. Then the composition of LCB can be deduced. The same fragmentation pattern of SM $[M+HCOO]^-$ ion was also observed in another study and used for molecular species assignment of SM [151].

In contrast to the weak $[M+H]^+$ ions seen under positive ion mode, PI(18:0/20:4 (*n*-6,9,12,15)) molecular ions $[M\text{-}H]^-$ at *m/z* 885 were seen with high intensity under ESI (-). Thus, the mass measurements of $[M\text{-}H]^-$ ions can be used for the determination of elemental composition of PI class. The MS/MS spectrum (CE= -42 eV) of the ions at *m/z* 885 is presented in **Figure 6-1c**. The $[RCOO]^-$ ions at *m/z* 283 and 303 corresponded to the 18:0 and 20:4 fatty acyl chain, and the inositol phosphate ion at *m/z* 241 were present with high intensity. Other product ions at *m/z* 599 ($[\text{lysostearoyl PI-H}]^-$) and 581 ($[\text{lysostearoyl PI-H-}\ H_2O]^-$) were also observed, probably formed by the loss of 20:4 acyl chain and the further loss of H_2O. The product ion at *m/z* 419 was due to the further loss of inositol from the $[\text{lysostearoyl PI-H}]^-$ ion at *m/z* 599. The similar fragmentation pattern of PI under ESI(-)-MS/MS were also observed by other studies [124,154].

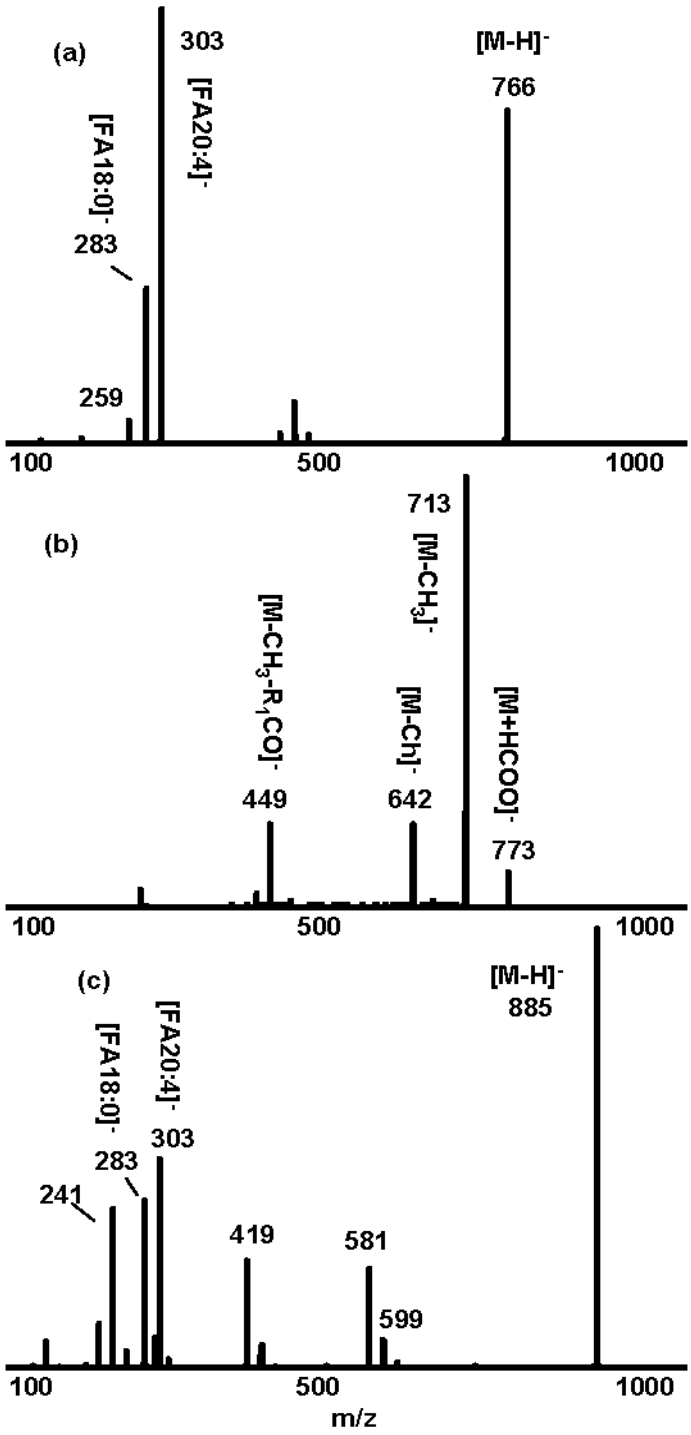

Figure 6-1. ESI (-)-MS/MS analysis of (a) PE(18:0/20:4 (*n*-6,9,12,15)); (b) SM(d18:1/18:1(*n*-9)); (c) PI(18:0/20:4 (*n*-6,9,12,15)).

6.3.2. In-line O_3-MS analysis of PE, LPE, SM, LPC and PI standards

For LPE and LPC, even though the chain length and number of double bonds can already be determined by the mass measurement of $[M+H]^+$ ions, the position of double bonds along the chain can not be assigned. Hence, in-line O_3-MS analysis of LPE(18:1(*n*-9)) and LPC(18:1(*n*-9)) were performed under ESI (+) (**Figure 6-2a** and **b**). The ozonolysis product of LPE(18:1(*n*-9)) was observed at *m/z* 370 as well as the intact $[M+H]^+$ ion at *m/z* 480 (**Figure 6-2a**). The ion at *m/z* 370 corresponded to the characteristic ozonolysis product aldehyde that was formed by oxidative cleavage of the *n*-9 double bond in LPE. The mass loss of 110 Da after ozonolysis has also been observed in other lipids with double bonds located at *n*-9 position such as methyl oleate [101] and PC(16:0/18:1(*n*-9)). The ion at *m/z* 352 was probably due to the neutral loss of one H_2O molecule from the ion at *m/z* 370. For LPC(18:1(*n*-9)), a similar mass loss of 110 Da from the intact molecular ion at *m/z* 522 was observed resulting in the ion at *m/z* 412 after in-line ozonolysis (**Figure 6-2b**).

In the O_3-MS spectrum of PE(18:0/20:4 (*n*-6,9,12,15)) (**Figure 6-2c**), the ozonolysis product aldehyde ions at *m/z* 700, 68 Da mass lower than intact $[M+H]^+$ ion at *m/z* 768, were generated by the ozonolysis of the double bond at *n*-6 position. The product ions at *m/z* 660, 620 and 580 corresponded to the further oxidative cleavage of successive methyle interrupted double bonds. In addition, the neutral loss of one H_2O molecule from the aldehyde ion at *m/z* 580 was observed at *m/z* 562. This kind of neutral loss of H_2O molecule from the

ozonolysis product aldehyde ions apparently involves the ethanolamine head group, since it is only observed in the O_3-MS spectra of LPE and PE.

The O_3-MS spectrum of SM(d18:1/18:1(*n*-9)) (**Figure 6-2d**) contained the intact $[M+H]^+$ ion at *m/z* 729 and the high intensity ozonolysis product at *m/z* 619, which resulted from ozonolysis of the double bond at *n*-9 position in the N-18:1 chain. The low intensity ions at *m/z* 549, 180 Da lower mass than $[M+H]^+$ ions at *m/z* 729, were formed by ozonolysis of the double bond located in the d18:1 chain. The ozonolysis of both double bonds in SM(d18:1/18:1(*n*-9)) resulted in the ion at *m/z* 439. The ozonolysis product aldehydes formed by oxidative cleavage of double bonds located along N-acyl chain (*m/z* 619 in this case) can be used for the direct assignment of double bond positions in N-acyl chain.

The in-line ozonolysis products of PI(18:0/20:4 (*n*-6,9,12,15)) were detected in negative ion mode, since the molecular ions of PI can only be observed as $[M-H]^-$ ions. In the resulting O_3-MS spectrum (**Figure 6-2e**), intact $[M-H]^-$ ions at *m/z* 885 were still observed along with the deprotonated ozonolysis product aldehydes ions at *m/z* 817, 777, 737 and 697, due to the oxidative cleavage of double bonds at *n*-6,-9,-12,-15 positions. The same group of ozonolysis product aldehyde ions were also observed during OzID-MS analysis of PI(18:0/20:4 (*n*-6,9,12,15)) under ESI (-) [39]. Along with these characteristic ozonolysis aldehyde ions, another set of ions at *m/z* 851, 811, 771 and 731 were also observed. These ions with mass difference of 40 Da between each other have 34 Da higher masses than the corresponding deprotonated aldehydes ions at *m/z* 817, 777, 737 and 697. We suspect that these ions are generated from the further

reaction of "Criegee intermediate" that are carbonyl oxides formed by ozonolysis of each double bond. The possible structure of the product ion at *m/z* 731 has been shown in the inset of **Figure 6-2e**, and these products are probably due to the adduction of H_2O molecule in the mobile phase to the Criegee intermediates. The Criegee intermediates were observed as the carbonyl oxide ions with 16 Da higher mass than their corresponding aldehyde ions during the OzID-MS analysis of PI under ESI (-) [39]. Whether these Criegee intermediate adducts form during in-line ozonolysis reaction or during the negative electrospray ionization is not clear, but it does not diminish the use of the ozonolysis product aldehydes for the direct assignment of double bond positions as shown in **Figure 6-2e**.

In summary, for in-line ozonolysis of LPE, LPC, PE and SM, both the intact molecules and ozonolysis product aldehydes that are characteristics of double bond positions were detected as $[M+H]^+$ ions. For PI, the molecular ions could only be observed as $[M-H]^-$ ions under negative ion mode; and the in-line ozonolysis products were also detected under ESI (-) among which the aldehyes could still be used for the unambiguous assignment of double bond locations.

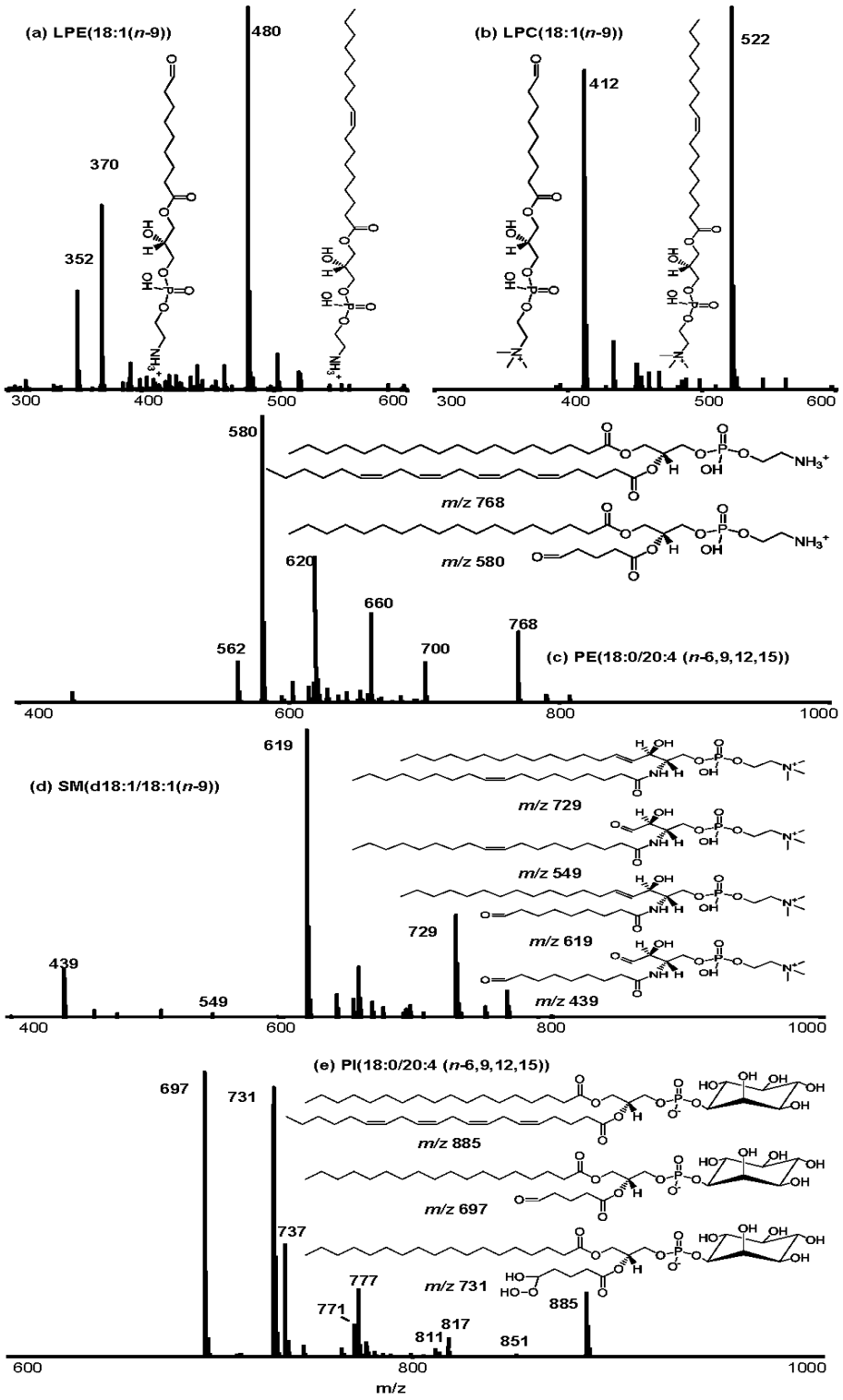

Figure 6-2. In-line O_3-MS spectrum of (a) LPE(18:1(*n*-9)) (+ve); (b) LPC(18:1(*n*-9)) (+ve); (c) PE(18:0/20:4 (*n*-6,9,12,15)) (+ve); (d) SM(d18:1/18:1(*n*-9)) (+ve); (e) PI(18:0/20:4 (*n*-6,9,12,15)) (-ve).

6.3.3. PL profiling of egg yolk PL extract

Egg yolk is a good source of dietary PL, and PL from egg yolk has been introduced as a novel food in EU recently [148]. In addition, the egg yolk fatty acid profile can be possibly changed through the hen's diet. For example, the abundance of *n*-3 PUFA in egg yolk can be increased by enriching seal blubber oil in hen's diet [124]. The main class of PL in egg yolk includes PI, PE, LPE, PC, SM and LPC [124,138,139]. In the following sections, we demonstrate the use of HILIC/MS and HILIC/MS/MS analyses for PL class separation and for the determination of elemental and fatty acyl chain composition. Additionally, on-line 2D-LC/MS analysis is carried out for the separation of molecular species within each PI, PE and PC class, and 2D-LC/O_3-MS analysis is also performed to assign the double bond positions directly. Finally, HILIC is coupled to O_3-MS (HILIC/O_3-MS) in order to determine the double bond positions in LPE, LPC and SM class, since the molecular species within these three classes are relatively simple and can be already separated on HILIC column.

6.3.3.1. HILIC/MS and HILIC/MS/MS analysis

We have previously demonstrated the separation of PL classes using HILIC column with gradient elution (Chapter 5). The egg yolk PL extract was analyzed by HILIC/ESI-MS under both positive and negative ion mode in order to observe molecular ions from each PL class (**Figure 6-3**). In HILIC/ESI(+)-MS spectrum (**Figure 6-3a**), the PL from egg yolk were separated into PE, LPE, PC, SM and LPC classes within 20 min, these classes formed abundant positive ions

especially for PC which had the highest intensity. Under ESI (-) (**Figure 6-3b**), the PI class, which did not form abundant positive ions, appeared between 4.0 and 5.0 min. PE, LPE, PC, SM and LPC classes could still be observed under negative mode, but with about half of the intensity of that seen under ESI (+). Thus, the mass measurements of PE, PC and SM $[M+H]^+$ ions and PI $[M-H]^-$ ions were used for the determination of elemental compositions, and the mass measurements of LPE and LPC $[M+H]^+$ ions also directly assigned the fatty acyl chain composition.

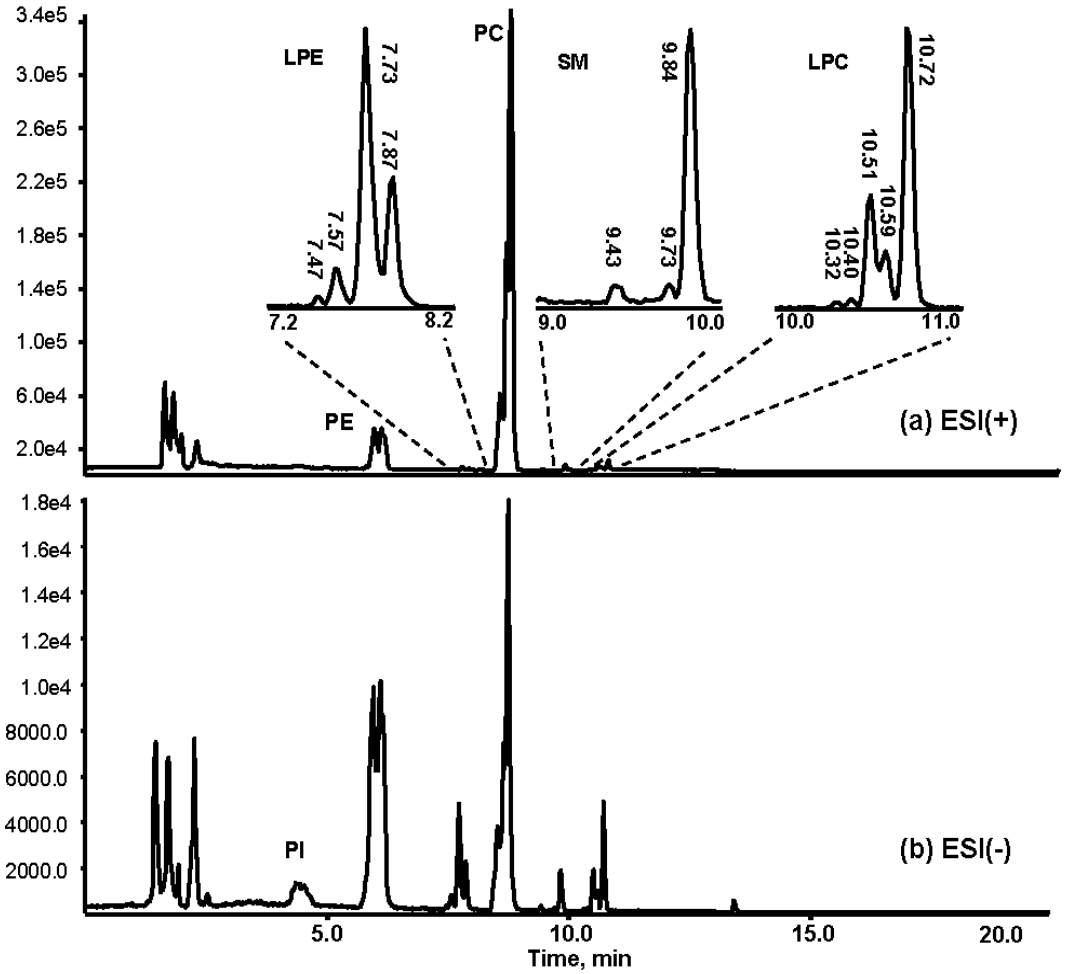

Figure 6-3. TIC of HILIC/MS analysis of egg yolk PL extract: (a) detected under ESI (+); (b) detected under ESI (-).

In order to obtain the information of fatty acyl chain composition in PI, PE, PC and SM, information dependent acquisition (IDA) was used during HILIC/MS/MS analysis in negative ion mode. During IDA, CID with CE of -35 and -42 eV were applied to ions with intensity higher than 10 cps. The product ions $[R_1COO]^-$ and $[R_2COO]^-$ from the CID of $[M-H]^-$ ions of PE, PI and $[M+HCOO]^-$ ions of PC were used for the determination of fatty acyl chain composition. For SM, the mass difference between $[M-CH_3]^-$ and $[M-CH_3-R_1CO]^-$ ions was used to determine the composition of N-acyl chain, then the composition of LCB chain in SM could also be deduced from this information. In this way, the chain length and number of double bonds in PI, PE, PC and SM were assigned even for the isomeric species such as PE(18:0/18:3) and PE(18:1/18:2), which were listed in **Table 6-1**.

Table 6-1. PL species identified in egg yolk PL extract.

Ions	Formula	Mass Accuracy (ppm)	Molelular Species		t_R (min)	Double Bond Position *n*-	Ozonolysis Product Aldehyde Ions (*m/z*)
PI $[M-H]^-$							
833.5182	$C_{43}H_{78}O_{13}P$	-0.5	34:2(ECN=30)	16:0/18:2	7.37	*n*-6,9	765,725
857.5182	$C_{45}H_{78}O_{13}P$	-0.5	36:4(ECN=28)	16:0/20:4	7.16	N/A	N/A[a]
859.5307	$C_{45}H_{80}O_{13}P$	-4.1	36:3(ECN=30)	16:0/20:3	7.60	*n*-6,9,12	791,751,711
861.5537	$C_{45}H_{82}O_{13}P$	4.4	36:2(ECN=32)	18:0/18:2	8.30	*n*-6,9	793,753
863.5684	$C_{45}H_{84}O_{13}P$	3.4	36:1(ECN=34)	18:0/18:1	9.43	*n*-9	753
885.5486	$C_{47}H_{82}O_{13}P$	-1.5	38:4(ECN=30)	18:0/20:4	8.11	*n*-6,9,12,15	817,777,737,697
887.5657	$C_{47}H_{84}O_{13}P$	0.2	38:3(ECN=32)	18:0/20:3	8.60	*n*-6,9,12	819,779,739
PE $[M+H]^+$							
716.5223	$C_{39}H_{75}NO_8P$	-0.3	34:2(ECN=30)	16:0/18:2	10.14	*n*-6,9	648,608
718.5356	$C_{39}H_{77}NO_8P$	-3.5	34:1(ECN=32)	16:0/18:1	11.36	*n*-9	608
740.5231	$C_{41}H_{75}NO_8P$	0.8	36:4(ECN=28)	16:0/20:4	9.91	*n*-6,9,12,15	672,632,592,552
				18:2/18:2	9.39	N/A	N/A[a]
742.5376	$C_{41}H_{77}NO_8P$	-0.6	36:3(ECN=30)	18:0/18:3	10.53	*n*-6,9,12	674,634,594
				18:1/18:2	10.21	N/A	N/A[a]
744.5536	$C_{41}H_{79}NO_8P$	-0.3	36:2(ECN=32)	18:0/18:2	11.73	*n*-6,9	676,636
746.5703	$C_{41}H_{81}NO_8P$	1.2	36:1(ECN=34)	18:0/18:1	13.58	*n*-9	636
764.5262	$C_{43}H_{75}NO_8P$	4.8	38:6(ECN=26)	16:0/22:6	9.56	*n*-3,6,9,12,15,18	738,698,658,618,578,538
768.5552	$C_{43}H_{79}NO_8P$	1.8	38:4(ECN=30)	18:0/20:4	11.38	*n*-6,9,12,15	700,660,620,580
792.5534	$C_{45}H_{79}NO_8P$	-0.5	40:6(ECN=28)	18:0/22:6	10.89	*n*-3,6,9,12,15,18	766,726,686,646,606,566
PC $[M+H]^+$							
732.5537	$C_{40}H_{79}NO_8P$	-0.1	32:1(ECN=30)	16:0/16:1	11.86	*n*-9	622
734.5672	$C_{40}H_{81}NO_8P$	-3.0	32:0(ECN=32)	16:0/16:0	12.86	Saturate	Saturate
756.5550	$C_{42}H_{79}NO_8P$	1.6	34:3(ECN=28)	16:0/18:3	11.43	*n*-3,6,9	730,690,650
758.5683	$C_{42}H_{81}NO_8P$	-1.5	34:2(ECN=30)	16:0/18:2	12.02	*n*-6,9	690,650
760.5860	$C_{42}H_{83}NO_8P$	1.2	34:1(ECN=32)	16:0/18:1	12.93	*n*-9	650
762.5998	$C_{42}H_{85}NO_8P$	-1.2	34:0(ECN=34)	16:0/18:0	14.52	Saturate	Saturate
780.5535	$C_{44}H79NO_8P$	-0.4	36:5(ECN=26)	16:0/20:5	10.95	N/A	N/A[a]
782.5693	$C_{44}H_{81}NO_8P$	-0.1	36:4(ECN=28)	16:0/20:4	11.84	*n*-6,9,12,15	714,674,634,594
784.5832	$C_{44}H_{83}NO_8P$	-2.4	36:3(ECN=30)	16:0/20:3	12.27	*n*-6,9,12	636,676,716
				18:1/18:2	12.07	*n*-9/*n*-9,12	674/ 606,566
786.5987	$C_{44}H_{85}NO_8P$	-2.5	36:2(ECN=32)	18:1/18:1	13.01	*n*-9/*n*-9	676/566
				18:0/18:2	13.26	*n*-6,9	718,678

Table 6-1. Continued: PL species identified in egg yolk PL extract.

Ions	Formula	Mass Accuracy (ppm)	Molelular Species		t_R (min)	Double Bond Position *n*-	Ozonolysis Prodcut Aldehyde Ions (*m/z*)
788.6195	$C_{44}H_{87}NO_8P$	3.9	36:1(ECN=34)	18:0/18:1	14.68	*n*-9	678
806.5696	$C_{46}H_{81}NO_8P$	0.2	38:6(ECN=26)	16:0/22:6	11.57	*n*-3,6,9,12,15,18	780,740,700,660,620,580
808.5830	$C_{46}H_{83}NO_8P$	-2.6	38:5(ECN=28)	18:0/20:5	12.21	N/A	N/A[a]
				18:1/20:4	11.88	N/A	N/A[a]
810.6009	$C_{46}H_{85}NO_8P$	0.2	38:4(ECN=30)	18:0/20:4	12.98	*n*-6,9,12,15	742,702,662,622
812.6151	$C_{46}H_{87}NO_8P$	-1.6	38:3(ECN=32)	18:0/20:3	13.67	*n*-6,9,12	744,704,664
834.5990	$C_{48}H_{85}NO_8P$	-2.0	40:6(ECN=28)	18:0/22:6	12.59	*n*-3,6,9,12,15,18	808,768,728,688,648,608
LPE $[M+H]^+$							
454.2930	$C_{21}H_{45}NO_7P$	0.4	*sn*-2-16:0		7.72	Saturated	Saturated
			sn-1-16:0		7.87	Saturated	Saturated
466.3295	$C_{23}H_{49}NO_6P$	0.6	18:1-eLPE		7.47	*n*-9	356
480.3079	$C_{23}H_{47}NO_7P$	-1.2	18:1		7.78	*n*-9	370
482.3239	$C_{23}H_{49}NO_7P$	-0.4	*sn*-2-18:0		7.57	Saturated	Saturated
			sn-1-18:0		7.73	Saturated	Saturated
SM $[M+H]^+$							
703.5737	$C_{39}H_{80}N_2O_6P$	-1.7	d18:1/16:0		9.84	Saturated	Saturated
705.5927	$C_{39}H_{82}N_2O_6P$	3.1	d18:0/16:0		9.73	Saturated	Saturated
731.6078	$C_{41}H_{84}N_2O_6P$	2.1	d18:1/18:0		9.72	Saturated	Saturated
813.6846	$C_{47}H_{94}N_2O_6P$	0.2	d18:1/24:1		9.43	*n*-9	703
LPC $[M+H]^+$							
496.3400	$C_{24}H_{51}NO_7P$	0.4	*sn*-2-16:0		10.54	Saturated	Saturated
			sn-1-16:0		10.72	Saturated	Saturated
522.3541	$C_{26}H_{53}NO_7P$	-0.5	*sn*-2-18:1		10.40	*n*-9	412
			sn-1-18:1		10.60	*n*-9	412
524.3705	$C_{26}H_{55}NO_7P$	-1.1	*sn*-2-18:0		10.32	Saturated	Saturated
			sn-1-18:0		10.50	Saturated	Saturated

[a] The intensity of ozonolysis product aldehyde ions is too low to observe.

6.3.3.2. 2D-LC/MS and 2D-LC/O_3-MS analysis of PI, PE and PC class

In Chapter 5, HILIC×C18 LC was successfully developed for on-line molecular species separation of PC from rat liver using a 10-port 2-position switching valve as the interface. In this study, a C18 column with the same type of solid phase but only half the length (75 mm) was used in order to shorten the second dimensional separation time from 30 min to 20 min, since separation capacity and resolution was not much compromised by using this shorter column. Accordingly, the gradient of HILIC was modified in order to achieve class separation within 20 min, which has been described in details in Experimental Section. Here, 2D-LC/MS analysis was applied for the molecular species separation of PI, PE and PC class from egg yolk PL extract. In-line ozonolysis was also performed for the detailed structure inspection of each eluting molecule in PI, PE and PC class.

For 2D-LC separation of PI molecular species, the fraction eluting from the HILIC column was transferred and injected on the C18 column by switching the valve to Position B at 4.0 min and back to Position A at 4.8 min. ESI(-)-MS was used for the detection of PI species, since molecular ions can only be observed as $[M-H]^-$ ions. Compared to the HILIC separation (**Figure 6-3b**), the molecular species of PI were much better separated on C18 column (**Figure 6-4a**). The observed molecular species and their corresponding t_R have been listed in **Table 6-1**. The elution order of these PI species was consistent with their ECN, meaning the PI molecules with higher ECN were retained longer on the C18 column. In order to assign the specific fatty acyl chains in these PI species,

2D-LC was coupled to O_3-MS in the negative ion mode. As an example, the O_3-MS spectrum of PI(18:0/18:2) in this egg yolk PL extract is shown in **Figure 6-4b**. In addition to the intact $[M-H]^-$ ions at *m/z* 861, ozonolysis product ions appeared at *m/z* 753, 787, 793 and 827. The ions at *m/z* 787 and 827 have 34 Da higher masses than the ions at *m/z* 753 and 793 respectively, indicating that they correspond to the H_2O adducts of the corresponding Criegee intermediates, consistent with the product ions generated by in-line ozonolysis of PI(18:0/20:4) standard (**Figure 6-2e**). The ions at *m/z* 793 and 753 are deprotonated ions of ozonolysis product aldehydes from the oxidative cleavage of double bonds at *n*-6 and -9 along the 18:2 acyl chain. For the other PI molecular species in this sample, the ozonolysis product aldehydes along with the products of 34 Da higher masses are also observed and used for the determination of double bond positions (**Table 6-1**).

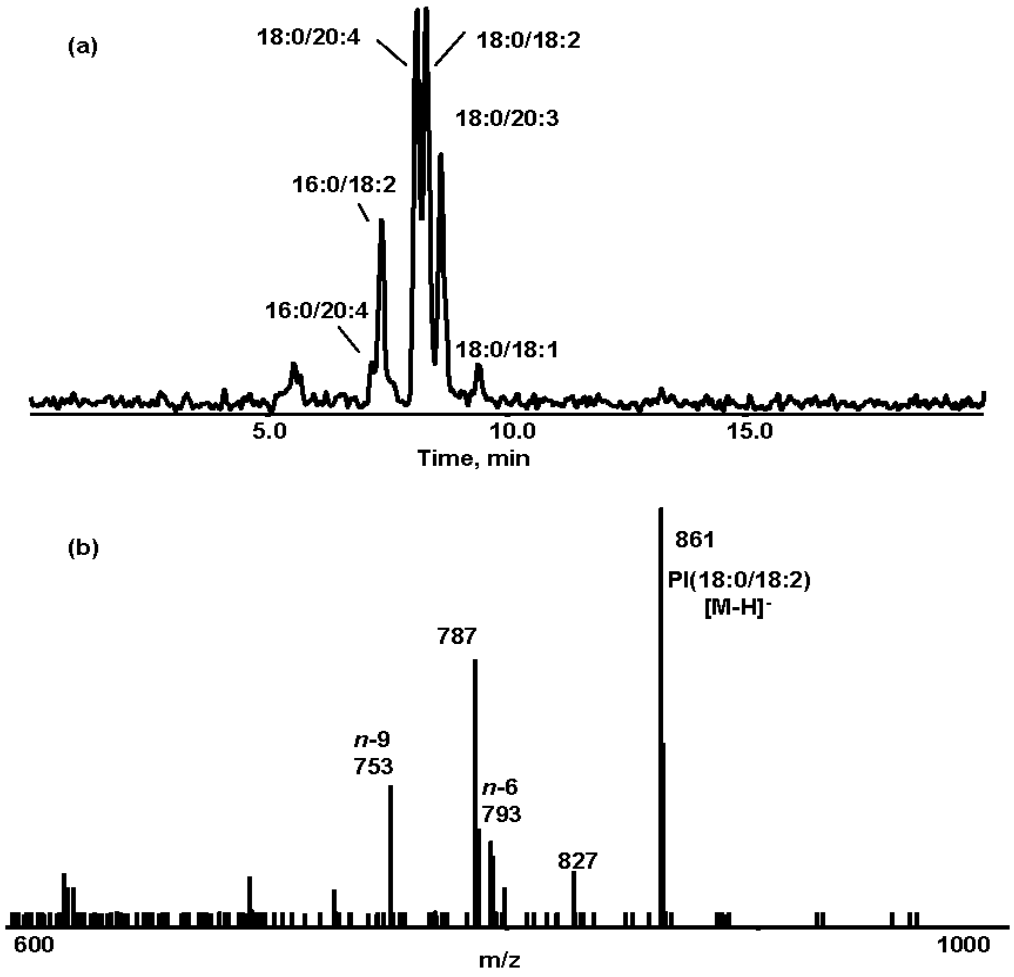

Figure 6-4. (a) TIC of 2D-LC/MS analysis of PI class in egg yolk PL extract in negative ion mode; (b) O_3-MS spectrum of PI(18:0/18:2) in the egg yolk sample.

For molecular species separation of PE class, the fraction eluting between 5.6 and 6.4 min from the HILIC column was re-injected onto the C18 column during a separate injection. While certain degree of PE species separation could be obtained by the HILIC column (**Figure 6-3a**), the diversity of PE molecular species was much better observed after 2D-LC separation (**Figure 6-5a**). PE were easily ionized as $[M+H]^+$ molecular ions under ESI (+) and had higher intensity than $[M-H]^-$ ions under ESI (-), thus 2D-LC/MS analysis was carried out

under positive ion mode. Due to the valve switching at 5.6 and 6.4 min, a baseline fluctuation was observed around 6 min. The first eluting species was PE(16:0/22:6) (ECN =26) at 9.56 min and the rest PE molecular species eluted generally according to their ECN ranging from 26 to 34. One exception was observed for PE(18:0/22:6) with ECN of 28 eluting at 10.89 min, which retained longer even than PE(16:0/18:2) (t_R 10.14 min) with ECN of 30. A similar retention order exception was also observed during 2D-LC separation of PC in rat liver in Chapter 5, which is probably related to the existence of PUFA chain in these PE and PC molecules. Even though PE species containing PUFA such as PE(16:0/22:6), PE(18:0/22:6), PE(16:0/20:4) and PE(18:0/ 20:4) were relatively well separated from other species, no more detailed structure information could be derived from just the 2D-LC/MS analysis to identify them as *n*-3 or *n*-6 PUFA. Therefore, 2D-LC/O_3-MS analysis was also performed on PE species. As an example, the O_3-MS spectrum of PE(18:0/22:6) in the sample is shown in **Figure 6-5b**. The mass difference of 26 Da between the intact PE(18:0/22:6) $[M+H]^+$ ion at *m/z* 792 and the ozonolysis product ion at *m/z* 766 directly assigned the first double bond at the *n*-3 position. The successive ozonolysis product ions at *m/z* 726, 686, 646, 606 and 566, with 40 Da mass differences between each other, provided the evidences that these double bonds were connected by methylene groups. Thus, PE(18:0/22:6) in egg yolk contains the *n*-3 fatty acid docosahexaenoic acid (DHA).

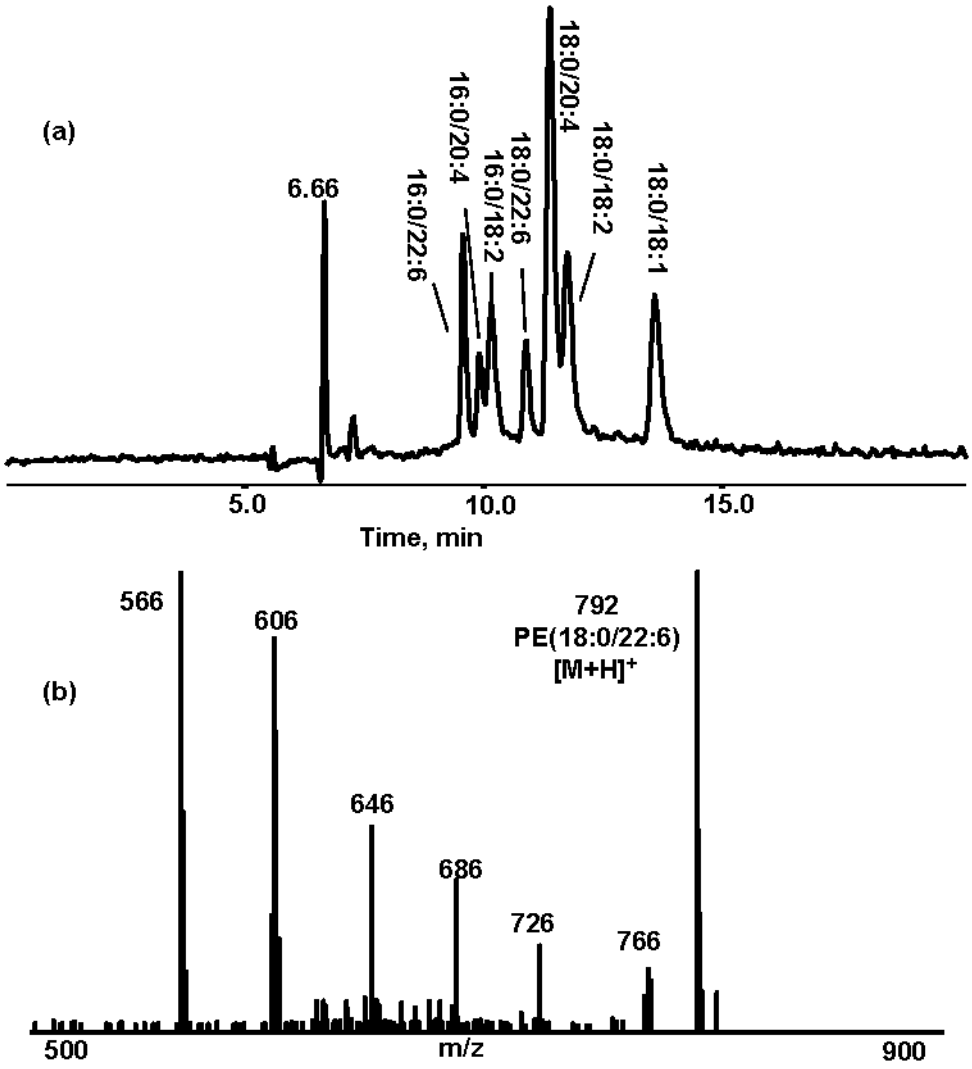

Figure 6-5. (a) TIC of 2D-LC/MS analysis of PE class in egg yolk PL extract in positive ion mode; (b) O3-MS spectrum of PE(18:0/22:6) in the egg yolk sample.

PC class eluting between 8.2 and 9.0 min from the HILIC column was also re-injected to C18 column for the further separation of molecular species. The major PC species were listed in **Figure 6-6a**; other minor PC species are shown in **Table 6-1** due to their partial co-elution with major species. Compared to PI and PE, PC class had even higher level of species diversity with ECN ranged from 26 to 34. PC molecular species still eluted based on their ECN, with the

exception that PC molecules with PUFA such as PC(16:0/22:6) and PC(18:0/22:6) had longer retention than the PC species with higher ECN. In-line ozonolysis was also performed on PC species and the ozonolysis product aldehydes that are characteristic of double bond positions were detected as $[M+H]^+$ ions. The isomers of PC36:2 in the egg yolk were used as an example to illustrate how the double bond positions were assigned by using in-line ozonolysis. In the extracted ion chromatogram (XIC) of the ion at *m/z* 786 (**Figure 6-6b**), two peaks appeared at 13.01 and 13.26 min, indicating they were PC(18:1/18:1) and PC(18:0/18:2) isomers. In the O_3-MS spectrum of the peak at 13.01 min (**Figure 6-6c**), ozonolysis product ions were observed at *m/z* 676 besides the intact molecular ion at *m/z* 786, which directly assigned the double bond at *n*-9 in one of 18:1 acyl chains; the other ozonolysis product ion at *m/z* 566 was generated from the further ozonolysis of the double bond in the other chain, and the mass loss of 110 Da from *m/z* 676 also located the second double bond at *n*-9 position in the other 18:1 acyl chain. The ion at *m/z* 760 of PC(16:0/18:1) also appeared with its ozonolysis product ion at *m/z* 650 due to the partial co-elution, but it did not affect the ozonolysis of PC(18:1/18:1) at 13.01 min. In **Figure 6-6d**, the ozonolysis product ions at *m/z* 718 and 678 facilitate the assignment of the double bond positions at *n*-6 and 9 in PC(18:0/18:2).

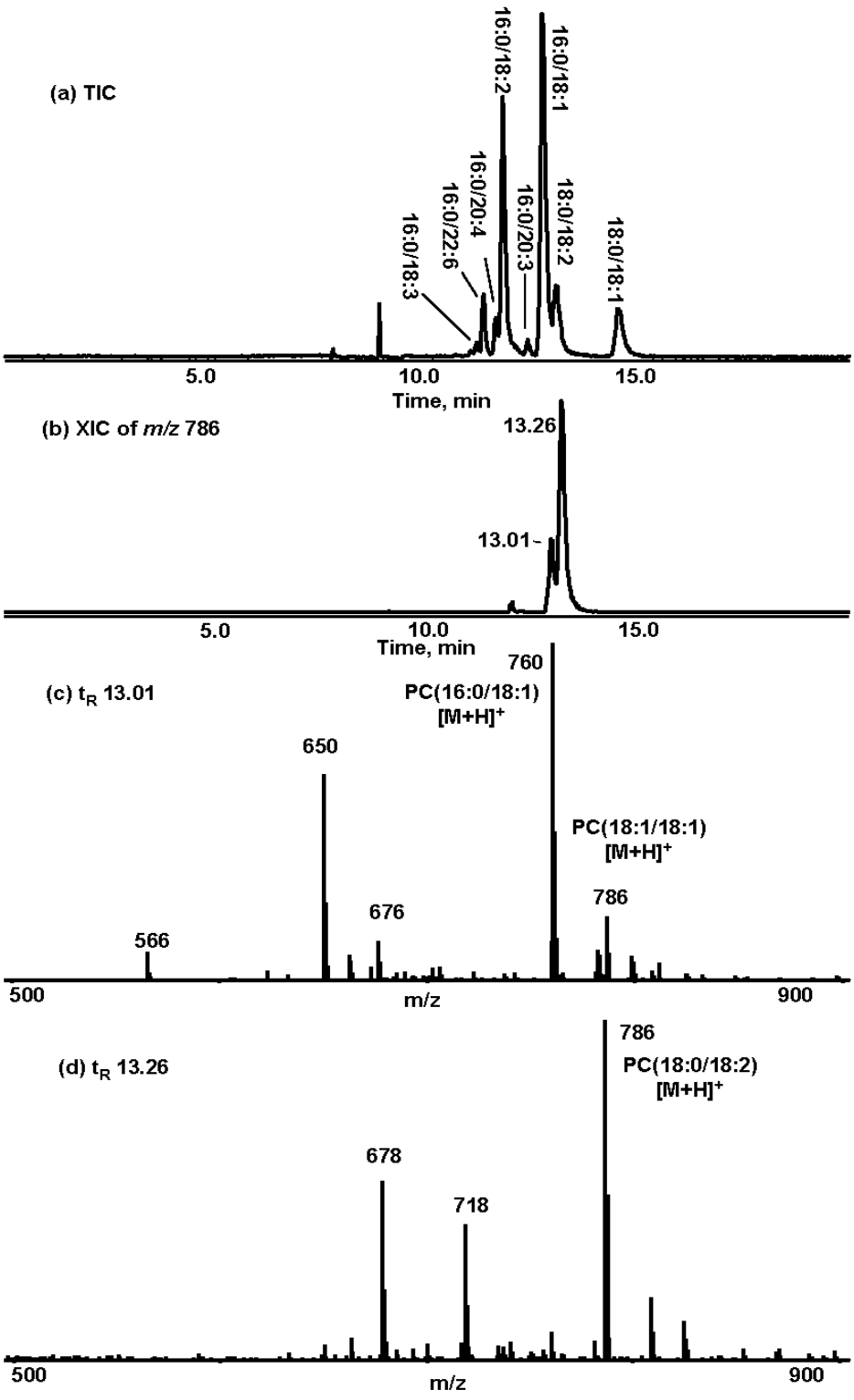

Figure 6-6. (a) TIC of 2D-LC/MS analysis of PC class in egg yolk PL extract in positive ion mode; (b) XIC of *m/z* 786 from (a); (c) O_3-MS spectrum of peak at 13.01 min; (d) O_3-MS spectrum of peak at 13.26 min.

6.3.3.3. HILIC/O_3-MS analysis of LPE, LPC and SM class

Initially, as in the 2D-LC/MS analysis of PI, PE and PC, LPE class eluting between 7.2-8.0 min and LPC class eluting between 10.2-11.0 min from HILIC column were also injected on C18 column and eluted using the same isocratic condition. However, all the species in both LPE and LPC class had very little retention and almost eluted within one single peak on C18 column. The low retention of LPE and LPC class on C18 column was also observed in the off-line 2D-LC study, in which LPE and LPC classes from HILIC column were collected and injected onto a C18 column separately for molecular species separation. All the species of both LPE and LPC classes eluted within 6 min with partial or complete co-elution even though the separation condition of C18 column has been optimized [155].

On the contrary, partial molecular species separation of LPE and LPC was already achieved on the HILIC column as seen in the insets of **Figure 6-3a**. The mass measurement of the ion at *m/z* 454 identified it as LPE(16:0). In the XIC of the ion at *m/z* 454 from **Figure 6-3a**, two peaks at 7.73 and 7.87 min appeared, representing regio-isomers of the LPE with 16:0 acyl chain at either *sn*-1 or *sn*-2 position. The regio-isomers of LPE(18:0) at *m/z* 482 were also observed at 7.57 and 7.73 min. The accurate assignment of the regio-isomers cannot be achieved by our study. It has been shown that *sn*-1 LPE and LPC retained longer than the corresponding *sn*-2 isomers on HILIC column [155]. Thus, the assignment of *sn*-isomers was solely based on the retention time on the HILIC column in our study (**Table 6-1**). LPE(18:1) at *m/z* 480 were observed at 7.78 min, co-eluting with

LPE(16:0). We also observed the ions at *m/z* 466 from a LPE species existing in low intensity with t_R at 7.47 min. The exact mass measurement at *m/z* 466.3295 was used to determine the elemental composition as $C_{23}H_{47}NO_7P^+$, which excluded the possibility that this ion represented LPE(17:1). Thus, this ion is identified as the 18:1 *e*LPE with the chain bonded by 1-O-alkyl ether (plasmanyl) or 18:0 *p*LPE with chain boned by 1-O-alk-1'-enyl (plasmenyl). At this point, we can not determine the exact structure as either 18:1 *e*LPE or 18:0 *p*LPE, since the MS/MS spectrum in both positive and negative polarity failed to provide product ions that could be used for the specific assignment. The acidic hydrolysis treatment has been performed on the ether PL before MS analysis, since the double bond in 1-O-alk-1'-enyl linkage is unstable under the acid treatment [156]. It has also been shown that product ions from the loss of R_1OH could only be observed from MS/MS analysis of the *p*LPC $[M+Li]^+$ ions, not from the MS/MS analysis of *e*LPC $[M+Li]^+$ ions [157].

For LPC, the regio-isomers were also observed from LPC(16:0), LPC(18:0) and LPC(18:1) in their XIC of *m/z* 496, 524 and 522, respectively. Like LPE, the identification of regio-isomers only relied on their retention time on HILIC column (**Table 6-1**).

For SM, even though there are two substituents in the molecules besides the polar head group, the SM fraction eluting between 9.2 and 10.0 min from HILIC column had poor retention and resolution under current C18 column separation condition. On the other hand, the SM molecular species were separated on HILIC column just like LPE and LPC (inset of **Figure 6-3a**).

SM(d18:1/24:1) eluted at 9.43 min and was well separated from SM(d18:1/16:0) (t_R 9.84 min) and SM(d18:1/18:0) (t_R 9.72 min); only SM(d18:0/16:0) co-eluted with SM(d18:1/18:0) at 9.73 min.

Although the separation of molecular species of LPE, LPC and SM class was already achieved on the HILIC column, the double bond positions in unsaturated species such as LPE(18:1), LPC(18:1) and SM(d18:1/24:1) could not be assigned. Therefore, the in-line ozonolysis device was coupled with HILIC column (HILIC/O_3-MS), in this way each eluting molecules from LPE, LPC and SM class would go through the in-line ozonolysis device, and the ozonolysis products were detected by ESI (+)-MS. For example, in **Figure 6-7a** the ion at *m/z* 370 appeared in the O_3-MS spectrum of LPE(18:1) besides the intact $[M+H]^+$ ions at *m/z* 480, the mass loss of 110 Da immediately assigned the only double bond in this LPE at *n*-9 position. The ion at *m/z* 454 representing LPE(16:0)was also observed due to the co-elution, but did not compromise using characteristic ozonolysis product aldehydes for the determination of double bond position. In the O_3-MS spectrum averaged at between 7.45 and 7.50 min, the ion at *m/z* 466 was still observed, and the ozonolysis product ion appeared at *m/z* 356, which indicated the double bond locates at *n*-9 position. The observation of this ozonolysis product ion supports the suggestion that the ion at *m/z* 466 corresponds to *e*LPE(18:1(*n*-9)), not 18:0 *p*LPE (the double bond located next to the ether group at the end of the chain). In this case, the in-line O_3-MS experiment appears to distinguish plasmanyl and plasmenyl LPE isomers such as *e*LPE(18:1(*n*-9))and

*p*LPE(18:0). Further development of O_3-MS method is needed for this specific identification purpose.

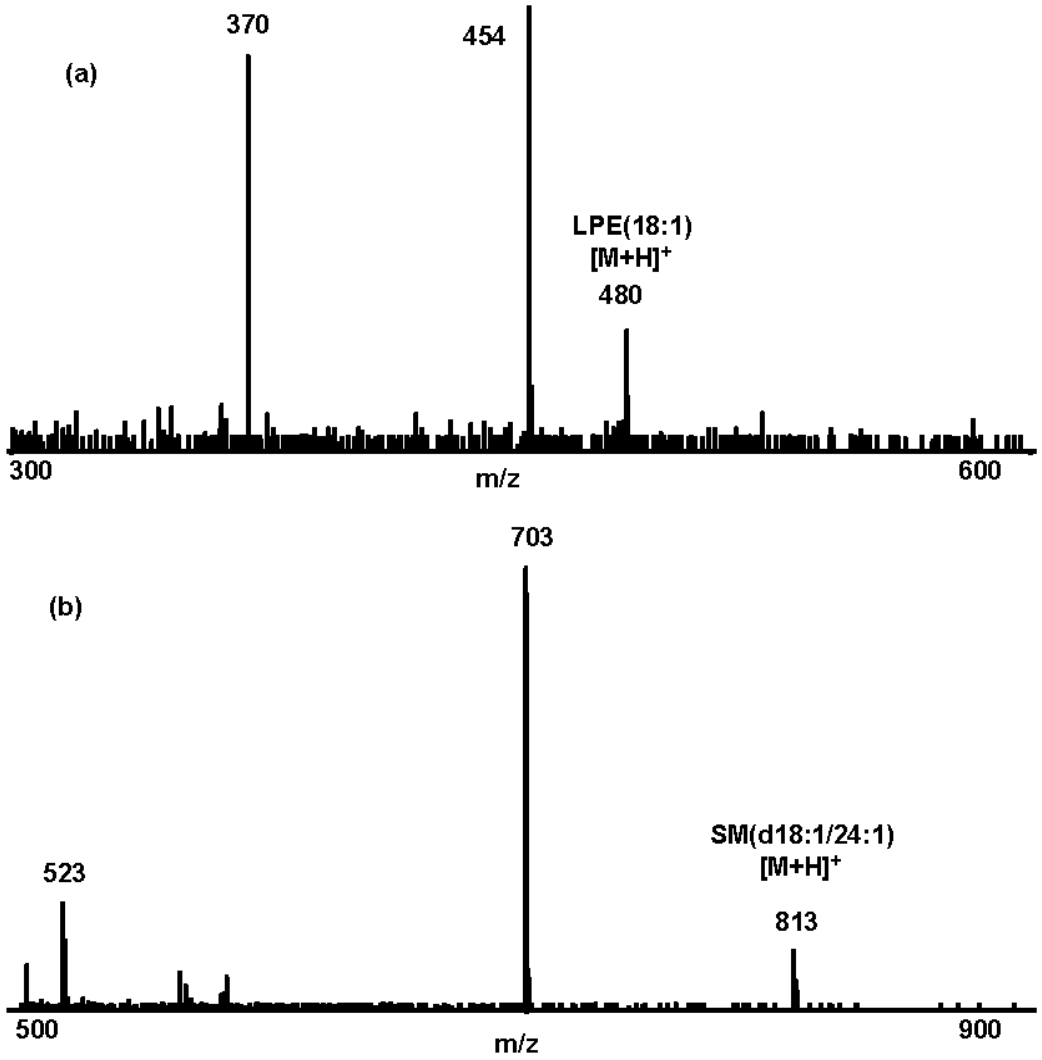

Figure 6-7. (a) O_3-MS spectrum of LPE(18:1);(b) O_3-MS spectrum of SM(d18:1/24:1) in the egg yolk sample.

For SM(d18:1/24:1) in the sample, the ozonolysis product aldehydes were observed at *m/z* 703 and 523 besides the intact $[M+H]^+$ at *m/z* 813 (**Figure 6-7b**). The double bond along the N-24:1 chain was localized at *n*-9 position based on the observation of the ion at *m/z* 703 that had 110 Da lower masses than *m/z* 813.

The ion at *m/z* 523 represented another ozonolysis product aldehyde generated by further oxidative cleavage of the double bond in d18:1 chain besides the N-24:1 chain. The similar pattern of ozonolysis product ions was seen in the O_3-MS spectrum of SM(d18:1/18:1(*n*-9)) standard (**Figure 6-2d**).

Therefore, in the egg yolk PL extract all the molecular species in PI, PE and PC were unambiguously identified by using HILIC/MS and MS/MS analysis followed by 2D-LC/ O_3-MS; LPE, LPC and SM molecular species were accurately assigned by using HILIC/MS and HILIC/O_3-MS analysis. All these identified species including 7 PI, 11PE, 19 PC, 3 LPE, 1 *e*LPE, 4 SM and 6 LPC have been listed in **Table 6-1**. Our findings have revealed even more diversity of PL species in egg yolk compared with previous reports [124,139]. The results are comparable to egg yolk profiling using the off-line 2D-LC/MS method developed by Lisa et al [155]. Besides, our method has demonstrated the unambiguous identification of each species with the position of double bond directly assigned.

6.4. Conclusions

In this study, we have successfully developed a comprehensive method for PL profiling by using the combination of HILIC/MS(/MS) and on-line 2D-LC/MS analysis. The use of in-line ozonolysis coupled with HILIC column and 2D-LC column has been shown to be necessary for the elucidation of the exact structure of the chains within the molecules. While shotgun lipidomics reveals a great lipid diversity within relatively short analysis time, the minor species and most isomers can only be observed with chromatographic separation prior to MS detection, and

other analytical techniques are also required to confirm the species identification. Compared with shotgun lipidomics, although the method demonstrated here requires longer analysis time, it can be used for the separation and identification of individual molecular species, especially the minor species. The experimental setup is also very flexible, which is especially helpful for the profiling of PL that is a group of chemically diverse compounds. This approach has shown great promised for PL profiling including detailed molecular structures, which can be applied complementary with shotgun lipidomics.

CHAPTER 7

General Discussions and Conclusions

In this study, the unambiguous determination of double bond positions in lipids has been successfully achieved by using in-line ozonolysis mass spectrometry (O_3-MS). The gas-permeable and liquid- impermeable Teflon tube was used as the in-line ozonolysis device placed prior to the ionization source of mass spectrometer. In this experiment, as the lipid molecules in mobile phase were passing through the semi-permeable tube, ozone that penetrated through the wall of the tube could immediately react with double bonds, resulting in oxidative cleavage products. Then, these ozonolysis products carried by the mobile phase were directed to ionization source and analyzed in real time by the mass spectrometer. The *m/z* values of these diagnostic ozonolysis product ions were then used for the double bond localization. The configuration of this in-line ozonolysis device was also found to be compatible with liquid chromatography (LC) (LC/O_3-MS), which is very important for the double bond position assignment for unsaturated lipids existing in complex samples. The applications of the LC/O_3-MS method for the direct assignments of double bond positions in natural lipid samples were demonstrated by the analyses of fatty acid methyl ester (FAME) (Chapter 3 and 4) and phospholipids (PL) mixtures (Chapter 5 and 6).

Many of the previous methods for the determination of double bond positions in lipids are based on the principle of charge remote fragmentation, such as gas chromatography coupled with electron ionization mass spectrometry

(GC/EI-MS) analysis of fatty acid dimethyloxazolines (DMOX) derivatives [17], tandem mass spectrometry (MS/MS) analysis of lithiated adduct ions of fatty acid [22] and triacylglycerols (TAG) [65], and N-(4-aminomethylphenyl) pyridinium (AMPP) detrivatives of fatty acids [24,25]. Theoretically, the information of double bond positions could be derived from the fragment ions in these mass spectra. However, ambiguities still exists due to the low intensity of the diagnostic ions due to extensive fragmentation, which is especially problematic for the species present in low abundance and also for polyunsaturated species. Compared to these previous methods, the mass spectra from in-line O_3-MS analyses are much simpler, as has been well demonstrated in this work (Chapter 3, 4, 5 and 6). Ozonolysis reactions have high specificity, meaning ozone vapor dominantly reacts with carbon-carbon double bonds in unsaturated lipids [37]. Therefore, only ions corresponding to ozonolysis products from oxidative cleavage right at the double bonds are observed during in-line O_3-MS analyses. These ozonolysis product ions have characteristic *m/z* valves that can be directly used for unambiguous assignment of double bond positions.

While ozonolysis reactions have been used for assignment of double bond positions in unsaturated lipids before, the in-line O_3-MS method described in this work possessed obvious advantages for its practical and easy use. Unlike off-line ozonolysis experiments [30], during in-line O_3-MS analysis the ozonolysis reaction occurs in the semi-permeable tube that is placed in-line with ionization source. This configuration greatly simplifies the procedure and also avoids the possible sample loss problem that is associated with off-line reactions. Since the

ozonolysis reaction occurs totally outside of the mass spectrometer, no instrumental modifications are needed for the introduction of ozone vapor into the mass spectrometer unlike ozone electrospray ionization mass spectrometry (OzESI-MS) [38] and ozone-induced dissociation (OzID-MS) [39] approaches. In OzID-MS experiments, ozone vapor was introduced into either an ion trap [39] or liner ion trap mass spectrometer [40] for gas-phase reaction between lipid ions and ozone vapor. The lipid ions of interests were trapped for certain time in order to generate enough ozonolysis product ions. Thus, the OzID-MS approach could only be performed on ion trap mass spectrometers and also might suffer from the low sensitivity. On the other hand, there is no specific requirement of certain type of mass spectrometer for in-line O_3-MS analysis, and the in-line ozonolysis device is compatible with all mass spectrometers equipped with a spray ionization source.

Another advantage of the in-line O_3-MS method is its compatibility with LC, which makes the analysis of complex lipid mixtures possible. The ends of the Teflon tube can be easily connected to the LC column using the tubing sleeves and nuts of standard dimensions. In this way, each eluting fraction from the LC column can pass through the in-line ozonolysis device according to their retention times. Thus, coupling with LC separation greatly reduces the ion suppression that can be a problem for detecting minor lipid species, at the same time the O_3-MS spectrum becomes simple for interpretation. As has been described in Chapter 5 and 6, the in-line ozonolysis device is also compatible with two dimension LC (2D-LC) using hydrophilic interaction liquid chromatography column as the first

dimensional LC for PL class separation and C18 column as the second dimensional LC for molecular species separation. This is a huge advantage for the structural elucidation of the fatty acyl chains in PL which consists of diverse molecular species. While co-elution still exists due to the limited LC column efficiency and the large number of isomers, double bond positions of these co-eluting species can still be assigned based on the observation of diagnostic ozonolysis product ions with different *m/z* values. This was demonstrated by the double bond localization of 18:1 FAME positional isomers in bovine fat sample (Chapter 3) [101], conjugated linoleic acid isomers from different sources (Chapter 4) [137] and also phosphotidycholine species in rat liver (Chapter 5) and egg yolk samples (Chapter 6).

It is not possible to determine whether the double bonds are in the *cis* or *trans* configuration by in-line O_3-MS method itself. However, this structural information can be derived from the retention order on the LC column, especially when using a silver ion LC (Ag^+-LC) column, where an isomer with a *trans* double bond elutes earlier than the corresponding isomer with *cis* double bond [77]. By coupling Ag^+-LC column with O_3-MS, in a 30 min analysis all of the 18:1 FAME isomers in a bovine fat sample were identified including the position and the configuration of double bonds assigned (Chapter 3). In contrast to the previous studies using 2D-GC and Ag^+-LC/MS [78], no standards were needed and nor was excessive resolution between the 18:1 FAME isomers necessary during Ag^+-LC/O_3-MS analysis, since the assignment of double bond position only depended on the observation of the characteristic ozonolysis product ions.

The configuration of the double bond was then easily determined by the relative retention time. Ag^+-LC/O_3-MS analyses were also applied for the identification of CLA isomers from different sources. For CLA isomers, a pair of diagnostic ozonolysis products ions indicating the position of the conjugated double bonds was observed and the *m/z* values are these diagnostic ions are fully predictable. Thus, CLA positional isomers were identified *de novo* and confirmed by examining the extracted ion chromatograms (XIC) of these diagnostic ions. The retention times of CLA isomers on Ag^+-LC column were then used to determine whether the conjugated double bonds were in *cis,cis*- or *trans,trans*-configuration. The Ag^+-LC/O_3-MS method greatly simplifies the CLA analysis procedures and also avoids the identification ambiguity.

The degree of ozonolysis reaction can be easily controlled by adjusting the length of the semi-permeable tube that is inserted into the chamber filled with ozone vapor. Therefore, sufficient ozonolysis of double bonds can be achieved for lipid species covering a wide range of abundances and also under LC flow rates of between 0.2 and 1 mL/min. Current lipidomic analyses using various LC/MS and MS/MS methods can now reveal abundant structural information of lipids in complex mixtures. However, many isomeric species that may possess important biological functions remain unidentified [7,63,64]. The in-line O_3-MS method can provide insight into the specific structure of these isomers and further reveal the complexity of the lipidome. Furthermore, the in-line ozonolysis experiment can be easily incorporated into many existing LC/MS methods due to its compatibility with LC and most of mass spectrometers. It is also possible for

most analytical laboratories to adapt the in-line O_3-MS method for direct double bond localization by the addition of an inexpensive low-flow ozone generator.

In conclusion, this work has demonstrated a novel approach to coupling the ozonolysis reaction with modern mass spectrometers for unambiguous assignment of double bond positions in lipids. Combining LC with in-line O_3-MS has shown great success in the analyses of FAME and PL species existing in complex samples. The in-line O_3-MS method has been proved to be a very practical and relatively easy solution to the analytical challenge of identifying subtle structure differences between lipid species. Future work will include applying the O_3-MS method to TAG species. Since TAG moleculs contain three fatty acyl chains, they will give O_3-MS spectra that are more complicated to interpret. The in-line O_3-MS experiment can provide insight into the specific structure of unsaturated lipid molecules and at the same time can be easily incorporated into LC/MS analyses. It would also be possible to develop algorithms to automatically identify the diagnostic ozonolysis product ions and hence identify specific lipid isomers. This could be complementary to the current shotgun lipidomic approach.

REFERENCES

1. Vance, D.E.; Vance, J.E. *Biochemistry of lipids, lipoproteins and membranes.* Elsevier Science B.V.: Amsterdam, 2008.

2. Santos, C.R.; Schulze, A. Lipid metabolism in cancer. *FEBS J.* 2012, *279,* 2610-2623.

3. Sagin, F.G.; Sozmen, E.Y. Lipids as key players in Alzheimer disease: alterations in metabolism and genetics. *Curr. Alzheimer Res.* 2008, *5,* 4-14.

4. Arsenault, B.J.; Boekholdt, S.M.; Kastelein, J.J.P. Lipid parameters for measuring risk of cardiovascular disease. *Nat. Rev. Cardiol.* 2011, *8,* 197-206.

5. Milne, S.; Ivanova, P.; Forrester, J.; Alex, B.H. Lipidomics: an analysis of cellular lipids by ESI–MS. *Methods* 2006, *39,* 92-103.

6. Quehenberger, O.; Armando, A.M.; Brown, A.H.; Milne, S.B.; Myers, D.S.; Merrill, A.H. Lipidomics reveals a remarkable diversity of lipids in human plasma. *J. Lipid Res.* 2010, *51,* 3299-3305.

7. Shevchenko, A.; Simons, K. Lipidomics: coming to grips with lipid diversity. *Nat. Rev. Mol. Cell Biol.* 2010, *11,* 593-598.

8. Fahy, E.; Subramaniam, S.; Brown, A.,H.; Christopher, G.K.; Merrill, J.,Alfred H.; Murphy, R.C.; Raetz, C.R.H.; Russell, D.W.; Seyama, Y.; Shaw, W.; Shimizu, T.; Spener, F.; van Meer, G.; VanNieuwenhze, M.S.; White, S.H.; Witztum, J.L.; Dennis, E.A. A comprehensive classification system for lipids. *J. Lipid Res.* 2005, *46,* 839-861.

9. LIPID MAPS http://www.lipidmaps.org/.

10. Wall, R.; Ross, R.P.; Fitzgerald, G.F.; Stanton, C. Fatty acids from fish: the anti-inflammatory potential of long-chain omega-3 fatty acids. *Nutr. Rev.* 2010, *68,* 280-289.

11. Evans, M.E.; Brown, J.M.; McIntosh, M.K. Isomer-specific effects of conjugated linoleic acid (CLA) on adiposity and lipid metabolism. *J. Nutr. Biochem.* 2002, *13,* 508-516.

12. Pariza, M.W.; Park, Y.; Cook, M.E. The biologically active isomers of conjugated linoleic acid. *Prog. Lipid Res.* 2001, *40,* 283-298.

13. Hou, W.; Zhou, H.; Elisma, F.; Bennett, S.A.L.; Figeys, D. Technological developments in lipidomics. *Brief Funct Genomic Proteomic.* 2008, *7,* 395-409.

14. Brouwers, J.F. Liquid chromatographic –mass spectrometric analysis of phospholipids.Chromatography, ionization and quantification. *Biochim. Biophys. Acta* 2011, *1811,* 763-775.

15. Mitchell, T.W.; Pham, H.; Thomas, M.C.; Blanksby, S.J. Indentification of double bonds position in lipids: From GC to OzID. *J. Chromatogr. B* 2009, *877,* 2722-2735.

16. Christie, W.W. Gas chromatography-mass spectrometry methods for structural analysis of fatty acids. *Lipids* 1998, *33,* 343-353.

17. Spitzer, V. Structure analysis of fatty acids by gas chromatography - low resolution electron impact mass spectrometry of their 4,4-dimethyloxazoline derivatives - a review. *Prog. Lipid Res.* 1997, *35,* 387-408.

18. Michaud, A.L.; Diau, G.; Abril, R.; Brennaa, J.T. Double bond localization in minor homoallylic fatty acid methyl esters using acetonitrile chemical ionization tandem mass spectrometry. *Anal. Biochem.* 2002, *307,* 348-360.

19. Michaud, A.L.; Yurawecz, M.P.; Delmonte, P.; Corl, B.A.; Bauman, D.E.; Brenna, J.T. Identification and characterization of conjugated fatty acid methyl esters of mixed double bond geometry by acetonitrile chemical ionization tandem mass spectrometry. *Anal. Chem.* 2003, *75,* 4925-4930.

20. Lawrence, P.; Brenna, J.T. Acetonitrile covalent adduct chemical ionization mass spectrometry for double bond localization in non-methylene-interrupted polyene fatty acid methyl esters. *Anal. Chem.* 2006, *78,* 1312-1317.

21. Tomer, K.B.; Crow, F.W.; Gross, M.L. Location of double-bond position in unsaturated fatty acids by negative ion MS/MS. *J. Am. Chem. Soc.* 1983, *105,* 5487-5488.

22. Hsu, F.; Turk, J. Distinction among isomeric unsaturated fatty acids as lithiated adducts by electrospray ionization mass spectrometry using low energy collisionally activated dissociation on a triple stage quadrupole instrument. *J. Am. Soc. Mass Spectrom.* 1999, *10,* 600-612.

23. Hus, F.; Turk, J. Elucidation of the double-bond position of long-chain unsaturated fatty acids by multiple-stage linear ion-trap mass spectrometry with electrospray ionization. *J. Am. Soc. Mass Spectrom.* 2008, *19,* 1673-1680.

24. Yang, K.; Dilthey, B.G.; Gross, R.W. Identification and quantitation of fatty acid double bond positional isomers: A shotgun lipidomics approach using charge-switch derivatization. *Anal. Chem.* 2013, *85,* 9742-9750.

25. Wang, M.; Han, R.H.; Han, X. Fatty acidomics: Global analysis of lipid species containing a carboxyl group with a charge-remote fragmentation-assisted approach. *Anal. Chem.* 2013, *85,* 9312-9320.

26. Moe, M.K.; Anderssen, T.; Strøm, M.B.; Jensen, E. Total Structure Characterization of Unsaturated Acidic Phospholipids Provided by Vicinal Di-Hydroxylation of Fatty Acid Double Bonds and Negative Electrospray Ionization Mass Spectrometry. *J. Am. Soc. Mass. Spectrom.* 2005, *16,* 46-59.

27. Dupau, P.; Epple, R.; Thomas, A.A.; Fokin, V.V.; Sharpless, B. Osmiumcatalyzed dihydroxylation of olefins in acidic media: Old process, new tricks. *Adv. Synth. Cat.* 2002, *344,* 421-433.

28. Xu, Y.; Brenna, J.T. Atmospheric pressure covalent adduct chemical ionization tandem mass spectrometry for double bond localization in monoene- and diene-containing triacylglycerols. *Anal Chem* 2007, *79,* 2525-2536.

29. Privett, O.S.; Nickell, E.C. Determination of structure of unsaturated fatty acids via reductive ozonolysis. *J. Am. Oil. Chem. Soc.* 1962, *39,* 414-419.

30. Harrison, K.A.; Murphy, R.C. Direct mass spectrometric analysis of ozonides: Application to unsaturated glycerophosphocholine lipids. *Anal. Chem.* 1996, *68,* 3224-3230.

31. Streng, A.G. Tables of ozone properties. *J. Chem. Eng. Data* 1961, *6,* 431-436.

32. Baily, P.S. *Ozonation in organic chemistry.* Academic Press: New York, 1978; Vol. 1, Olefinic Compounds.,

33. Dodd, M.; Buffle, M.; Gunten, U.v. Oxidation of antibacterial molecules by aqueous ozone: Moiety-specific reaction kinetics and application to ozone-based wastewater treatment. *Environ. Sci. Technol.* 2006, *40,* 1969-1977.

34. Kim, J.; Yousef, A.E.; Dave, S. Application of ozone for enhancing the microbiological safety and quality of foods: A review. *J. Food Prot.* 1999, *9,* 975-1096.

35. Kockritz, A.; Martin, A. Synthesis of azelaic acid from vegetable oil-based feedstocks. *Eur. J. Lipid Sci. Technol.* 2011, *113,* 83-91.

36. Bailey, P.S. The reaction of ozone with organic compounds. . *Chem. Rev.* 1958, *58,* 925-1010.

37. Criegee, R. Mechanism of ozonolysis. *Angew. Chem. internal. Edit* 1975, *14,* 745-752.

38. Thomas, M.C.; Mitchell, T.W.; Harman, D.G.; Deeley, J.M.; Murphy, R.C.; Blanksby, S.J. Elucidation of double bond position in unsaturated lipids by ozone electrospray ionization mass spectrometry. *Anal. Chem.* 2007, *79,* 5013-5022.

39. Thomas, M.C.; Mitchell, T.W.; Harman, D.G.; Deeley, J.M.; Nealon, J.R.; Blanksby, S.J. Ozone-induced dissociation: Elucidation of double bond position within mass-selected lipid ions. *Anal. Chem.* 2008, *80,* 303-311.

40. Poad, B.L.J.; Pham, H.T.; Thomas, M.C.; Nealon, J.R.; Campbell, J.L.; Mitchell, T.W.; Blanksby, S.J. Ozone-induced dissociation on a modified tandem linear ion-trap: Observations of different reactivity for isomeric lipids. *J. Am. Soc. Mass Spectrom.* 2010, *21,* 1989-1999.

41. Behr, A.; Gomes, J.P. The refinement of renewable resources: New important derivatives of fatty acids and glycerol. *Eur. J. Lipid Sci. Technol.* 2010, *112,* 31-50.

42. Yue, J.; Narine, S.S. Separation and quantification of vegetable oil based polyols by high performance liquid chromatography with evaporative light scattering detection. *J. Am. Oil Chem. Soc.* 2007, *84,* 803-807.

43. Tran, P.; Graiver, D.; Narayan, R. Ozone-mediated polyol synthesis from soybean oil. *J. Am. Oil Chem. Soc.* 2005, *82,* 653-659.

44. Omonov, T.S.; Kharraz, E.; Curtis, J.M. Ozonolysis of canola oil: A study of product yields and ozonolysis knetics in different solvent systems. *J. Am. Oil Chem. Soc.* 2011, *88,* 689-705.

45. Soriano, N.U.; Migob, V.P.; Matsumuraa, M. Ozonation of sunflower oil: Spectroscopic monitoring of the degree of unsaturation. *J. Am. Oil Chem. Soc.* 2003, *80,* 997-1001.

46. Sega, A.; Zanardia, I.; Chiasserinia, L.; Gabbriellia, A.; Boccib, V.; Travaglia, V. Properties of sesame oil by detailed ^{1}H and ^{13}C NMR assignments before and after ozonation and their correlation with iodine value, peroxide value, and viscosity measurements. *Chem. Phys. Lipids* 2010, *163,* 148-156.

47. Sadowska, J.; Johansson, B.; Johannessen, E.; Friman, R.; Broniarz-Press, L.; Rosenholm, J.B. Characterization of ozonated vegetable oils by spectroscopic and chromatographic methods. *Chem. Phys. Lipids* 2008, *151,* 85-91.

48. Pryor, W.A.; Das, B.; Church, D.F. The ozonation of unsaturated fatty acids: Aldehydes and hydrogen peroxide as products and possible mediators of ozone toxicity. *Chem. Res. Toxicol* 1991, *4,* 341-348.

49. Burris, N. Three-, six- and nine-carbon ozonolysis products from cottonseed oil and crude *Chlorella* Lipids. *J. Am. Oil Chem. Soc.* 1983, *60,* 806-811.

50. Wu, M.; Church, D.F.; Mahier, T.J.; Barker, S.A.; Pryor, W.A. Separation and spectral data of the six isomeric ozonides from methyl oleate. *Lipids* 1992, *27,* 129-135.

51. Thornberry, T.; Abbatt, J.P.D. Heterogeneous reaction of ozone with liquid unsaturated fatty acids: Detailed kinetics and gas-phase product studies. *Phys. Chem. Chem. Phys* 2004, *6,* 84-93.

52. Woo, H.; Go, E.P.; Hoang, L.; Trauger, S.A.; Bowen, B. Phosphonium labeling for increasing metabolomic coverage of neutral lipids using electrospray ionization mass spectrometry. *Rapid Commun. Mass Spectrom.* 2009, *23,* 1849-1855.

53. Zahardis, J.; LaFranchi, B.W.; Petrucci, G.A. Photoelectron resonance capture ionization-aerosol mass spectrometry of the ozonolysis products of oleic acid particles: Direct measure of higher molecular weight oxygenates. *J. Geophys. Res.* 2005, *110,* 1-10.

54. Zahardis, J.; LaFranchi, B.W.; Petrucci, G.A. Direct observation of polymerization in the oleic acid–ozone heterogeneous reaction system by photoelectron resonance capture ionization aerosol mass spectrometry. *Atmos. Environ.* 2006, *40,* 1661-1670.

55. Reynolds, J.C.; Last, D.J.; Mcgillen.M; Nijs, A.; Horn, A.B.; Percival, C.; Carpenter, L.J.; Lewis, A.C. Structural analysis of oligomeric molecules formed from the reaction products of oleic acid ozonolysis. *Environ. Sci. Technol.* 2006, *40,* 6674-6681.

56. Hung, H.; Katrib, Y.; Martin, S.T. Products and mechanisms of the reaction of oleic acid with ozone and nitrate radical. *J. Phys. Chem. A* 2005, *109,* 4517-4530.

57. Ziemann, P.J. Aerosol products, mechanisms, and kinetics of heterogeneous reactions of ozone with oleic acid in pure and mixed particles. *Faraday Discuss.* 2005, *130,* 469-490.

58. Zhang, J.I.; Tao, W.A.; Cooks, R.G. Facile determation of double bond position in unsatured fatty acids and esters by low temperature plasma ionizaiton mass spectrometry. *Anal. Chem.* 2011, *83,* 4738-4744.

59. Byrdwell, W.C.; Neff, W.E. Dual parallel electrospray ionization and atmospheric pressure chemical ionization mass spectrometry (MS), MS/MS and MS/MS/MS for the analysis of triacyglycerols and triacyglycerol oxidation products. *Rapid Commun. Mass Spectrom.* 2002, *16,* 300-319.

60. Bauld, N.L.; Thompson, J.A.; Hudson, C.E.; Bailey, P.S. Stereospecificity in ozonide and cross-ozonide formation. *J. Am. Chem. Soc.* 1968, *90,* 1822-1830.

61. Unger, R.H. Lipotoxic Diseases. *Annu. Rev. Med.* 2002, *53,* 319-336.

62. Blanksby, S.J.; Mitchell, T.W. Advances in mass spectrometry for lipidomics. *Annu. Rev. Anal. Chem.* 2010, *3,* 433-465.

63. Murphy, R.C.; Gaskell, S.J. New applications of mass spectrometry in lipid analysis. *J. Biol. Chem.* 2011, *286,* 25427-25433.

64. Wenk, M.R. Lipidomics: New Tools and Applications. *Cell* 2010, *143,* 888-895.

65. Hsu, F.; Turk, J. Structural characterization of triacylglycerols as lithiated adducts by electrospray ionization mass spectrometry using low- energy collisionally activated dissociation on a triple stage quadrupole instrument. *J. Am. Soc. Mass. Spectrom.* 1999, *10,* 587-599.

66. Yang, K.; Zhao, Z.; Gross, R.W.; Han, X. Identification and quantitation of unsaturated fatty acid isomers by electrospray ionization tandem mass spectrometry: A shotgun lipidomics approach. *Anal. Chem.* 2011, *83,* 4243-4250.

67. Pavlaskova, K.; Strnadova, M.; Strohalm, M.; Havlicek, V.; Sulc, M.; Volny, M. Time-dependent oxidation during nano-assisted laser desorption ionization mass spectrometry: A useful tool for structure determination or a source of possible confusion? *Anal. Chem.* 2011, *83,* 5661-5665.

68. Ellis, S.R.; Hughes, J.R.; Mitchell, T.W.; Panhuis, M.i.h.; Blanksby, S.J. Using ambient ozone for assignment of double bond position in unsaturated lipids. *Analyst* 2012, *137,* 1100-1110.

69. Pinnau, I.; Toy, L.G. Gas and vapor transport properties of amorphous perfluorinated copolymer membranes based on 2,2-bistrifluoromethyl-4,5-difluoro-l,3-dioxole/tetrafluoroethylene. *J. Membr. Sci.* 1996, *109,* 125-133.

70. O'Brien, M.; Baxendale, I.R.; Ley, S.V. Flow ozonolysis using a semipermeable Teflon AF-2400 membrane to effect gas-liquid contact. *Org. Lett.* 2010, *12,* 1596-1598.

71. Folch, J.; Lees, M.; Stanley, G.H.S. A simple method for the isolation and purification of total lipides from animal tissues. *J. Biol. Chem.* 1957, *226,* 497-509.

72. Juáreza, M.; Polvilloa, O.; Contòb, M.; Ficcob, A.; Ballicob, S.; Failla, S. Comparison of four extraction/methylation analytical methods to measure fatty

acid composition by gas chromatography in meat. *J. Chromatogr. A* 2008, *1190,* 327-332.

73. Marchi, I.; Rudaz, S.; Veuthey, J. Atmospheric pressure photoionization for coupling liquid-chromatography to mass spectrometry: A review. *Talanta* 2009, *78,* 1-18.

74. Anonymous The properties of ozone can be checked at http://www.ozoneapplications.com/info/ozone_properties.htm (Accessed August 24, 2012).

75. Sun, C.; Zhao, Y.; Curtis, J.M. A study of the ozonolysis of model lipids by electrospray ionization mass spectrometry. *Rapid Commun. Mass Spectrom.* 2012, *26,* 921-930.

76. Karr, J.E.; Alexander, J.E.; Winningham, R.G. Omega-3 polyunsaturated fatty acids and cognition throughout the lifespan: A review. *Nutr. Neurosci.* 2011, *14,* 216-225.

77. Momchilova, S.; Nikolova-Damyanova, B.; Christie, W.W. Silver ion high-performance liquid chromatography of isomeric *cis* and *trans*-octadecenoic acids Effect of the ester moiety and mobile phase composition. *J. Chromatogr. A* 1998, *793,* 275-282.

78. Villegas, C.; Zhao, Y.; Curtis, J.M. Two methods for the separation of monounsaturated octadecenoic acid isomers. *J. Chromatogr. A* 2010, *1217,* 775-784.

79. Banni, S.; Angioni, E.; Murru, E.; Carta, G.; Melis, M.P.; Bauman, D.; Dong, Y.; Ip, C. Vaccenic acid feeding increases tissue levels of conjugated linoleic acid and suppresses development of premalignant lesions in rat mammary gland. *Nutr. Cancer* 2001, *41,* 91-97.

80. Corl, B.A.; Barbano, D.M.; Bauman, D.E.; Ip, C. *Cis*-9, *trans*-11 CLA derived endogenously from *trans*-11 18:1 reduces cancer risk in rats. *J. Nutr.* 2003, *133,* 2893-2900.

81. Fritschea, J.; Fritsche, S.; Solomon, M.B.; Mossoba, M.M.; Yurawecz, M.P.; Morehouse, K. Quantitative determination of conjugated linoleic acid isomers in beef fat. *Eur. J. Lipid Sci. Technol.* 2000, *102,* 667-672.

82. Mendis, S.; Cruz-Hernandez, C.; Ratnayake, W.M.N. Fatty acid profile of Canadian dairy products with special attention to the *trans*-octadecenoic acid and conjugated linoleic acid isomers. *J. AOAC Int.* 2008, *91,* 811-819.

83. Ip, C.; Scimeca, J.A.; Thompson, H.J. Conjugated linoleic acid. A powerful anticarcinogen from animal fat sources. *Cancer* 1994, *74,* 1050-1054.

84. Lee, J.H.; Cho, K.H.; Lee, K.T.; Kim, M.R. Antiatherogenic effects of structured lipid containing conjugated linoleic acid in C57BL/6J mice. *J. Agric. Food Chem.* 2005, *53,* 7295-7301.

85. Park, Y.; Albright, K.J.; Storkson, J.M.; Liu, W.; Cook, M.E.; Pariza, M.W. Changes in body composition in mice during feeding and withdrawal of conjugated linoleic acid. *Lipids* 1999, *34,* 243-248.

86. Kelley, N.S.; Hubbard, N.E.; Erickson, K.L. Conjugated linoleic acid isomers and cancer. *J. Nutr.* 2007, *137,* 2599-2607.

87. Belury, M.A.; Mahon, A.; Banni, S. The conjugated linoleic acid (CLA) isomer, t10c12-CLA, is inversely associated with changes in body weight and serum leptin in subjects with type 2 diabetes mellitus. *J. Nutr.* 2003, *133,* 257-260.

88. Kramer, J.K.G.; Cruz-Hernandez, C.; Zhou, J. Conjugated linoleic acids and octadecenoic acids: Analysis by GC. *Eur. J. Lipid Sci. Technol.* 2001, *103,* 600-609.

89. Prandini, A.; Sigolo, S.; Piva, G. Comparative study of fatty acid composition and CLA concentration in commercial cheeses. *J. Food Compost. Anal.* 2011, *24,* 55-61.

90. Roach, J.A.G.; Yurawecza, M.P.; Kramer, J.K.G.; Mossoba, M.M.; Eulitza, K.; Ku, Y. Gas chromatography-high resolution selected-ion mass spectrometric identification of trace 21:0 and 20:2 fatty acids eluting with conjugated linoleic acid isomers. *Lipids* 2000, *35,* 797-802.

91. Christie, W.W.; Dobson, G.; Adlof, R.O. A practical guide to the isolation, analysis and identification of conjugated linoleic acid. *Lipids* 2007, *42,* 1073-1084.

92. Sehat, N.; Kramer, J.K.G.; Mossoba, M.M.; Yurawecz, M.P.; Roach, J.A.G.; Eulitz, K.; Morehouse, K.M.; Ku, Y. Identification of conjugated linoleic acid isomers in cheese by gas chromatography, silver ion high performance liquid chromatography and mass spectral reconstructed ion profiles. Comparison of chromatographic elution sequences. *Lipids* 1998, *33,* 963-970.

93. Liu, X.; Li, H.; Chen, Y.; Cao, Y. Method for screening of bacterial strains biosynthesizing specific conjugated linoleic acid isomers. *J. Agric. Food Chem.* 2012, *60,* 9705-9710.

94. Sehat, N.; Yurawecz, M.P.; Roach, J.A.G.; Mossoba, M.M.; Kramer, J.K.G.; Ku, Y. Silver-ion high-performance liquid chromatographic separation and identification of conjugated linoleic acid isomers. *Lipids* 1998, *33,* 217-221.

95. Yurawecz, M.P.; Roach, J.A.G.; Sehat, N.; Mossoba, M.M.; Kramer, J.K.G.; Fritsche, J.; Steinhart, H.; Ku, Y. A new conjugated linoleic acid isomer, 7*trans*, 9*cis*-octadecadienoic acid, in cow milk, cheese, beef and human milk and adipose tissue. *Lipids* 1998, *33,* 803-809.

96. Delmonte, P.; Kataoka, A.; Corl, B.A.; Bauman, D.E.; Yurawecz, M.P. Relative retention order of all isomers of *cis/trans c*onjugated linoleic acid FAME from the 6,8- to 13,15-positions using silver ion HPLC with two elution systems. *Lipids* 2005, *40,* 509-514.

97. Eulitz, K.; Yurawecz, M.P.; Sehat, N.; Fritsche, J.; Roach, J.A.G.; Mossoba, M.M.; Kramer, J.K.G.; Adlof, R.O.; Ku, Y. Preparation, separation, and confirmation of the eight geometrical *cis/trans c*onjugated linoleic acid isomers 8,10- through 11,13-18:2.
. *Lipids* 1999, *34,* 873-877.

98. Kramer, J.K.G.; Sehat, N.; Dugan, M.E.R.; Mossoba, M.M.; Yurawecz, M.P.; Roach, J.A.G.; Eulitz, K.; Aalhus, J.L.; Schaefer, A.L.; Ku, Y. Distributions of conjugated linoleic acid (CLA) isomers in tissue lipid classes of pigs fed a commercial CLA mixture determined by gas chromatography and silver ion-high performance liquid chromatography. *Lipids* 1998, *33,* 549-558.

99. Muller, A.; Mickel, M.; Geyer, R.; Ringseis, R.; Eder, K.; Steinhart, H. Identification of conjugated linoleic acid elongation and β-oxidation products by coupled silver-ion HPLC APPI-MS. *J. Chromatogr. B* 2006, *837,* 147-152.

100. Pham, H.T.; Maccarone, A.T.; Campbell, J.L.; Mitchell, T.W.; Blanksby, S.J. Ozone-induced dissociation of conjugated lipids reveals significant reaction rate enhancements and characteristic odd-electron product ions. *J. Am. Soc. Mass Spectrom.* 2013, *24,* 286-296.

101. Sun, C.; Zhao, Y.; Curtis, J.M. The direct determination of double bond positions in lipid mixtures by liquid chromatography/in-line ozonolysis/mass spectrometry. *Anal. Chim. Acta* 2013, *762,* 68-75.

102. Christie, W.W. *Gas chromatography and lipids : a practical guide.* The Oily Press: Bidgwater, Somerset, 1989; Vol. 1,

103. Bligh, E.G.; Dyer, W.J. A rapid method of toal lipid extraction and purification. *Can. J. Biochem. Physiol.* 1959, *37,* 911-917.

104. Black, B.A.; Zannini, E.; Curtis, J.M.; Gänzle, M.G. Antifungal hydroxy fatty acids produced during sourdough fermentation: Microbial and enzymatic pathways, and antifungal activity in bread. *Appl. Environ. Microbiol.* 2013, *79,* 1866-1873.

105. Kramer, J.K.G.; Hernandez, M.; Cruz-Hernndez, C.; Kraft, J.; Dugan, M.E.R. Combining results of two GC separations partly achieves determination of all *cis* and *trans* 16:1, 18:1, 18:2 and 18:3 except CLA isomers of milk fat as demonstrated using Ag-ion SPE fractionation. *Lipids* 2008, *43,* 259-273.

106. Gammill, W.; Proctor, A.; Jain, V. Comparative study of high-linoleic acid vegetable oils for the production of conjugated linoleic acid. *J. Agric. Food Chem.* 2010, *58,* 2952-2957.

107. Ma, D.W.L.; Wierzbicki, A.A.; Field, C.J.; Clandinin, M.T. Preparation of conjugated linoleic acid from safflower oil. *J. Am. Oil Chem. Soc.* 1999, *76,* 729-730.

108. Dhiman, T.R.; Nam, S.H.; Ure, A.L. Factors affecting conjugated linoleic acid content in milk and meat. *Crit Rev Food Sci Nutr.* 2005, *45,* 463-482.

109. Dhiman, T.,R.; Satter, L.D.; Pariza, M.,W.; Galli, M,P,; Albright, K.; Tolosa, M.X. Conjugated linoleic acid (CLA) content of milk from cows offered diets rich in linoleic and linolenic acid. *J Dairy Sci.* 2000, *83,* 1016-1027.

110. Yurawecz, M.P.; Sehat, N.; Mossoba, M.M.; Roach, J.A.G.; Kramer, J.K.G.; Ku, Y. Variations in isomer distribution in commercially available conjugated linoleic acid. *Eur. J. Lipid Sci. Technol.* 1999, *101,* 277-282.

111. Deng, Z.; Dugan, M.E.R.; Santercole, V.; Kramer, J.K.G.; Or-Rashid, M.; Cruz-Hernandez, C.; Delmonte, P.; Yurawecz, M.P.; Kraft, J. Systematic analysis of *trans* and conjugated linoleic acids in the milk and meat of ruminants. In *Advances in Conjugated Linoleic Acid Research.* Banni , S., Kramer , John K . G ., Gudmundsen , O., Pariza , Michael W . and Yurawecz , M.P., Eds.; AOCS Press: Champaign, IL, 2003; Vol.3 pp. 45-93.

112. Kelsy, J.A.; Corl, B.A.; Collier, R.J.; Bauman, D.E. The effect of breed, parity, and stage of lactation on conjugated linoleic acid (CLA) in milk fat from dairy cows. *J. Dairy Sci.* 2003, *86,* 2588-2597.

113. Jiang, J.; Bjoerck, L.; Fondén, R.; Emanuelson, M. Occurrence of conjugated *cis*-9,*trans*-11-octadecadienoic acid in bovine milk: effects of feed and dietary regimen. *J. Dairy Sci.* 1996, *79,* 438-445.

114. McCrorie, T.A.; Keaveney, E.M.; Wallace, J.M.W.; Binns, N.; Livingstone, M.B.E. Human health effects of conjugated linoleic acid from milk and supplements. *Nutr. Res. Rev.* 2011, *24,* 206-227.

115. Andrade, J.C.; Ascenção, K.; Gullón, P.; Henriques, S.M.S.; Pinto, J.M.S.; Rocha-Santos, T.A.P.; Freitas, A.C.; Gomes, A.M. Production of conjugated linoleic acid by food-grade bacteria: a review. . *Int. J. Dairy Technol.* 2012, *65,* 467-481.

116. Ogawa, J.; Matsumura, K.; Kishino, S.; Omura, Y.; Shimizu, S. Conjugated linoleic acid accumulation via 10-hydroxy-12-octadecaenoic acid during microaerobic transformation of linoleic acid by *Lactobacillus acidophilus.*. *Appl. Environ. Microbiol.* 2001, *67,* 1246-1252.

117. Kishino, S.; Park, S.; Takeuchi, M.; Yokozeki, K.; Shimizu, S.; Ogawa, J. Novel multi-component enzyme machinery in lactic acid bacteria catalyzing C=C double bond migration useful for conjugated fatty acid synthesis. *Biochem. Biophys. Res. Commun.* 2011, *416,* 188-193.

118. Martinez-Seara, H.; Rog, T.; Pasenkiewicz-Gierula, M.; Vattulainen, I.; Karttunen, M.; Reigada, R. Interplay of unsaturated phospholipids and cholesterol in membranes: Effect of the double bond position. *Biophys. J.* 2008, *95,* 3295-3305.

119. Retra, K.; Bleijerveld, O.B.; van Gestel, R.A.; Tielens, A.G.M.; van Hellemond, J.J.; Brouwers, J.F. A simple and universal method for the separation and identification of phospholipid molecular species. *Rapid Commun. Mass Spectrom.* 2008, *22,* 1853-1862.

120. Han, X.; Gross, R.W. Structural determination of picomole amounts of phospholipids via electrospray ionizaion tandem mass spectrometry. *J. Am. Soc. Mass Spectrom.* 1995, *6,* 1202-1210.

121. Kim, H.; Wang, T.L.; Ma, Y. Liquid chromatography/mass Spectrometry of phospholipids using electrospray ionization. *Anal. Chem.* 1994, *66,* 3977-3982.

122. Pang, L.; Liang, Q.; Wang, Y.; Ping, L.; Luo, G. Simultaneous determination and quantification of seven major phospholipid classes in human blood using normal-phase liquid chromatography coupled with electrospray mass spectrometry and the application in diabetes nephropathy. *J. Chromatogr. B* 2008, *869,* 118-125.

123. Berdeaux, O.; Juaneda, P.; Martine, L.; Cabaret, S.; Bretillon, L.; Acar, N. Identification and quantification of phosphatidylcholines containing very-long-chain polyunsaturated fatty acid in bovine and human retina using liquid

chromatography/tandem mass spectrometry. *J. Chromatogr. A* 2010, *1217,* 7738-7748.

124. Pacetti, D.; Boselli, E.; Hulan, H.W.; Frega, N.G. High performance liquid chromatography-tandem mass spectrometry of phospholipid molecular species in eggs from hens fed diets enriched in seal blubber oil. *J. Chromatogr. A* 2005, *1097,* 66-73.

125. Smith, M.; Jungalwala, F.B. Reversed- phase high performance liquid chromatography of phosphatidylcholine: a simple
method for determining relative hydrophobic interaction of various molecular species. *J. Lipid Res.* 1981, *22,* 697-704.

126. Patton, G.M.; Fasulo, J.M.; Robins, S.J. Separation of phospholipids and individual molecular species of phospholipids by high-performance liquid chromatography. *J. Lipid Res.* 1982, *23,* 190-196.

127. Brouwers, J.F.; Gadella, B.M.; van Golde, L.M.; Tielens, A.G. Quantitative analysis of phosphatidylcholine molecular species using HPLC and light scattering detection. *J. Lipid Res.* 1998, *39,* 344-353.

128. McHowat, J.; Jones, J.H.; Creer, M.H. Gradient elution reversed-phase chromatographic isolation of individual glycerophospholipid molecular species. *J. Chromatogr. B* 1997, *702,* 21-32.

129. Pulfer, M.; Murphy, R.C. Electrospay mass spectrometry of phospholipids. *Mass Spectrom. Rev.* 2003, *22,* 332-364.

130. Houjou, T.; Yamatani, K.; Imagawa, M.; Shimizu, T.; Taguchi, R. A shotgun tandem mass spectrometric analysis of phospholipids with normal-phase and/or reverse-phase liquid chromatography/electrospray ionization mass spectrometry. *Rapid Commun. Mass Spectrom.* 2005, *19,* 654-666.

131. Nie, H.; Liu, R.; Yang, Y.; Bai, Y.; Guan, Y.; Qian, D.; Wang, T.; Liu, H. Lipid profi ling of rat peritoneal surface layers by online normal- and reversed-phase 2D LC QToF-MS. *J. Lipid Res.* 2010, *51,* 2833-2844.

132. Dugo, P.; Fawzy, N.; Cichello, F.; Cacciola, F.; Donato, P.; Mondello, L. Stop-flow comprehensive two-dimensional liquid chromatography combined with mass spectrometric detection for phospholipid analysis. *J. Chromatogr. A* 2013, *1278,* 46-53.

133. Montealegre, C.; Verardo, V.; Gómez-Caravaca, A.M.; García-Ruiz, C.; Marina, M.L.; Caboni, M.F. Molecular characterization of phospholipids by high-performance liquid chromatography combined with an evaporative light scattering detector, high-performance liquid chromatography combined with mass

spectrometry, and gas chromatography combined with a flame ionization detector in different oat varieties. *J. Agric. Food Chem.* 2012, *60,* 10963-10969.

134. Grandois, J.L.; Marchiono, E.; Zhao, M.; Giuffrida, F.; Ennahar, S.; Bindler, F. Investigation of natural phosphatidylcholine sources: Separation and identification by liquid
chromatography -electrospray ionization- tandem mass spectrometry (LC -ESI-MS^2) of molecular species. *J. Agric. Food Chem.* 2009, *57,* 6014-6020.

135. Narváez-Rivas, M.; Gallardo, E.; Ríos, J.J.; León-Camacho, M. A new high-performance liquid chromatographic method with evaporative light scattering detector for the analysis of phospholipids. Application to Iberian pig subcutaneous fat. *J. Chromatogr. A* 2011, *1218,* 3453-3458.

136. Hsu, F.; Turk, J. Structural characterization of unsaturated glycerophospholipids by multiple-stage linear ion-trap mass spectrometry with electrospray ionization. *J. Am. Soc. Mass Spectrom.* 2008, *19,* 1681-1691.

137. Sun, C.; Black, B.A.; Zhao, Y.; Ganzle, M.G.; Curtis, J.M. The identification of conjugated linoleic acid (CLA) isomers by silver ion- liquid chromatography/ in-line ozonolysis/ mass spectrometry (Ag^+-LC/O_3-MS). *Anal. Chem.* 2013, *85,* 7345-7352.

138. Xiong, Y.; Zhao, Y.; Goruk, S.; Oilund, K.; Field, C.J.; Jacobs, R.L.; Curtis, J.M. Validation of an LC–MS/MS method for the quantification of choline-related compounds and phospholipids in foods and tissues. *J. Chromatogr. B* 2012, *911,* 170-179.

139. Zhao, Y.; Xiong, Y.; Curtis, J.M. Measurement of phospholipids by hydrophilic interaction liquid chromatography coupled to tandem mass spectrometry: The determination of choline containing compounds in foods. *J. Chromatogr. A* 2011, *1218,* 5470-5479.

140. Dugo, P.; Cacciola, F.; Kumm, T.; Dugo, G.; Mondello, L. Comprehensive multidimensional liquid chromatography: Theory and applications. *J. Chromatogr. A* 2008, *1184,* 353-368.

141. Abrahim, A.; Al-Sayah, M.; Skrdla, P.; Bereznitski, Y.; Chen, Y.; Wu, N. Practical comparison of 2.7 μm fused-core silica particles and porous sub-2 μm particles for fast separations in pharmaceutical process development. *J. Pharm. Biomed. Anal.* 2010, *51,* 131-137.

142. Cole, L.K.; Vance, J.E.; Vance, D.E. Phosphatidylcholine biosynthesis and lipoprotein metabolism. . *Biochim. Biophys. Acta* 2012, *1821,* 754-761.

143. Vernooij, E.A.; Brouwers, J.F.; Kettenes-van den Bosch, J.J.; Crommelin, D.J. RP-HPLC/ESI MS determination of acyl chain positions in phospholipids. . *J. Sep. Sci.* 2002, *25,* 285-289.

144. Hvattum, E.; Hagelin, G.; Larsen, A. Study of mechanisms involved in the collisioninduced dissociation of carboxylate anions from glycerophospholipids using negative ion electrospray tandem quadrupole mass spectrometry. *Rapid Commun. Mass Spectrom.* 1998, *12,* 1405-1409.

145. Brouwers, J.F.; Vernooij, E.A.; Tielens, A.G.; van Golde, L.M. Rapid separationand identification of phosphatidylethanolamine molecular species. *J. Lipid Res.* 1999, *40,* 164-169.

146. Nakanishi, H.; Lida, Y.; Shimizu, T.; Taguchi, R. Separation and quantification of sn-1 and sn-2 fatty acid positional isomers in phosphatidylcholine by RPLC-ESI MS/MS. *J. Biochem.* 2010, *147,* 245-256.

147. Amate, L.; Gil, A.; Ramirez, M. Feeding infant piglets formula with long-chain polyunsaturated fatty acids as triacylglycerols or phospholipids influences the distribution of these fatty acids in plasma lipoprotein fractions. *J. Nutr.* 2001, *131,* 1250-1255.

148. Küllenberg, D.; Taylor, L.A.; Schneider, M.; Massing, U. Health effects of dietary phospholipids. *Lipids Health Dis* 2012, *11,* 1-16.

149. Bunea, R.; El, F.K.; Deutsch, L. Evaluation of the effects of Neptune Krill Oil on the clinical course of hyperlipidemia. *Altern. Med. Rev.* 2004, *9,* 420-428.

150. Ekroos, K.; Chernushevich, I.V.; Simons, K.; Shevchenko, A. Quantitative profiling of phospholipids by multiple precursor ion scanning on a hybrid quadrupole time-of-flight mass spectrometer. *Anal. Chem.* 2002, *74,* 941-949.

151. Houjou, T.; Yamatani, K.; Nakanishi, H.; Imagawa, M.; Shimizu, T.; Taguchi, R. Rapid and selective identification of molecular species in phosphatidylcholine and sphingomyelin by conditional neutral loss scanning and MS^3. *Rapid Commun. Mass Spectrom.* 2004, *18,* 3123-3130.

152. Shen, Q.; Wang, Y.; Gong, L.; Guo, R.; Dong, W.; Cheung, H. Shotgun lipidomics strategy for fast analysis of phospholipids in fisheries waste and its potential in species differentiation. *J. Agric. Food Chem.* 2012, *60,* 9384-9393.

153. Norris, C.; Fong, B.; MacGibbon, A.; McJarrow, P. Analysis of phospholipids in rat brain using liquid chromatography-mass spectrometry. *Lipids* 2009, *44,* 1047-1054.

154. Hus, F.; Turk, J. Characterization of phosphatidylinositol, phosphatidylinositol-4-phosphate, and phosphatidylinositol-4,5-bisphosphate by electrospray ionization tandem mass spectrometry: A mechanistic study. *J. Am. Soc. Mass Spectrom.* 2000, *11,* 986-999.

155. Lísa, M.; Cífková, E.; Holcapek, M. Lipidomic profiling of biological tissues using off-line two dimensional high-performance liquid chromatography–mass spectrometry. *J. Chromatogr. A* 2011, *1218,* 5146-5156.

156. Chen, S.; Li, K.W. Mass Spectrometric Identification of molecular species of phosphatidylcholine and
lysophosphatidylcholine extracted from shark liver. *J. Agric. Food Chem.* 2007, *55,* 9670-9677.

157. Hus, F.; Turk, J.; Thukkani, A.K.; Messner, M.C.; Wildsmith, K.R.; Ford, D.A. Characterization of alkylacyl, alk-1-enylacyl and lyso subclasses of glycerophosphocholine by tandem quadrupole mass spectrometry with electrospray ionization. *J. Mass Spectrom.* 2003, *38,* 752-763.

APPENDIX

Title: Locating double bonds in lipids – New approaches to the use of ozonolysis
Author: Chenxing Sun,Jonathan M. Curtis
Publication: Lipid Technology
Publisher: John Wiley and Sons
Date: Dec 4, 2013

Logged in as:
Chenxing Sun
Account #:
3000736638
LOGOUT

Order Completed

Thank you very much for your order.

This is a License Agreement between Chenxing Sun ("You") and John Wiley and Sons ("John Wiley and Sons"). The license consists of your order details, the terms and conditions provided by John Wiley and Sons, and the payment terms and conditions.

Get the printable license.

License Number	3313410312334
License date	Jan 20, 2014
Licensed content publisher	John Wiley and Sons
Licensed content publication	Lipid Technology
Licensed content title	Locating double bonds in lipids – New approaches to the use of ozonolysis
Licensed copyright line	Copyright © 2013 WILEY-VCH Verlag GmbH & Co. KGaA, Weinheim
Licensed content author	Chenxing Sun,Jonathan M. Curtis
Licensed content date	Dec 4, 2013
Start page	279
End page	282
Type of use	Dissertation/Thesis
Requestor type	Author of this Wiley article
Format	Electronic
Portion	Full article
Will you be translating?	No
Total	0.00 USD

APPENDIX

Rightslink® by Copyright Clearance Center

PERMISSION/LICENSE IS GRANTED FOR YOUR ORDER AT NO CHARGE

This type of permission/license, instead of the standard Terms & Conditions, is sent to you because no fee is being charged for your order. Please note the following:

- Permission is granted for your request in both print and electronic formats, and translations.
- If figures and/or tables were requested, they may be adapted or used in part.
- Please print this page for your records and send a copy of it to your publisher/graduate school.
- Appropriate credit for the requested material should be given as follows: "Reprinted (adapted) with permission from (COMPLETE REFERENCE CITATION). Copyright (YEAR) American Chemical Society." Insert appropriate information in place of the capitalized words.
- One-time permission is granted only for the use specified in your request. No additional uses are granted (such as derivative works or other editions). For any other uses, please submit a new request.

If credit is given to another source for the material you requested, permission must be obtained from that source.

BACK CLOSE WINDOW

APPENDIX

Order Completed

Thank you very much for your order.

This is a License Agreement between Chenxing Sun ("You") and John Wiley and Sons ("John Wiley and Sons"). The license consists of your order details, the terms and conditions provided by John Wiley and Sons, and the payment terms and conditions.

Get the printable license.

License Number	3313400420369
License date	Jan 20, 2014
Licensed content publisher	John Wiley and Sons
Licensed content publication	Rapid Communications in Mass Spectrometry
Licensed content title	A study of the ozonolysis of model lipids by electrospray ionization mass spectrometry
Licensed copyright line	Copyright © 2012 John Wiley & Sons, Ltd.
Licensed content author	Chenxing Sun,Yuan-Yuan Zhao,Jonathan M. Curtis
Licensed content date	Feb 28, 2012
Start page	921
End page	930
Type of use	Dissertation/Thesis
Requestor type	Author of this Wiley article
Format	Electronic
Portion	Full article
Will you be translating?	No
Total	0.00 USD

APPENDIX

APPENDIX

Copyright Clearance Center RightsLink®

Home | Account Info | Help

ACS Publications High quality. High impact.

Title: Identification of Conjugated Linoleic Acid (CLA) Isomers by Silver Ion-Liquid Chromatography/In-line Ozonolysis/Mass Spectrometry (Ag+-LC/O3-MS)

Author: Chenxing Sun, Brenna A. Black, Yuan-Yuan Zhao, Michael G. Gänzle, and Jonathan M. Curtis

Publication: Analytical Chemistry

Publisher: American Chemical Society

Date: Aug 1, 2013

Copyright © 2013, American Chemical Society

Logged in as: Chenxing Sun
Account #: 3000736638

LOGOUT

PERMISSION/LICENSE IS GRANTED FOR YOUR ORDER AT NO CHARGE

This type of permission/license, instead of the standard Terms & Conditions, is sent to you because no fee is being charged for your order. Please note the following:

- Permission is granted for your request in both print and electronic formats, and translations.
- If figures and/or tables were requested, they may be adapted or used in part.
- Please print this page for your records and send a copy of it to your publisher/graduate school.
- Appropriate credit for the requested material should be given as follows: "Reprinted (adapted) with permission from (COMPLETE REFERENCE CITATION). Copyright (YEAR) American Chemical Society." Insert appropriate information in place of the capitalized words.
- One-time permission is granted only for the use specified in your request. No additional uses are granted (such as derivative works or other editions). For any other uses, please submit a new request.

APPENDIX

ELSEVIER LICENSE
TERMS AND CONDITIONS

Jun 14, 2014

This is a License Agreement between Chenxing Sun ("You") and Elsevier ("Elsevier") provided by Copyright Clearance Center ("CCC"). The license consists of your order details, the terms and conditions provided by Elsevier, and the payment terms and conditions.

All payments must be made in full to CCC. For payment instructions, please see information listed at the bottom of this form.

Supplier	Elsevier Limited The Boulevard,Langford Lane Kidlington,Oxford,OX5 1GB,UK
Registered Company Number	1982084
Customer name	Chenxing Sun
Customer address	11135 80th Ave Edmonton, AB T6G 0R4
License number	3407290056792
License date	Jun 13, 2014
Licensed content publisher	Elsevier
Licensed content publication	Journal of Chromatography A
Licensed content title	Elucidation of phosphatidylcholine isomers using two dimensional liquid chromatography coupled in-line with ozonolysis mass spectrometry
Licensed content author	Chenxing Sun,Yuan-Yuan Zhao,Jonathan M. Curtis
Licensed content date	18 July 2014
Licensed content volume number	1351
Licensed content issue number	None
Number of pages	9
Start Page	37
End Page	45
Type of Use	reuse in a thesis/dissertation
Intended publisher of new work	other
Portion	full article
Format	both print and electronic
Are you the author of this Elsevier article?	Yes
Will you be translating?	No